STUDIES ON THE HYDRO-THERMAL AND VISCOELASTIC PROPERTIES OF LEATHER

A thesis submitted for the degree of

Doctor of Philosophy

University of Leicester

Sujeevini Jeyapalina

BSc, MSc

August 2004

ProQuest LLC
789 East Eisenhower Parkway
P.O. Box 1346
Ann Arbor, MI 48106-1346

Disclaimer

The content of this dissertation describes the original work by the candidate, except where specific reference is made to the work of others. No part of this dissertation has been submitted for a higher degree to any other university.

Sujeevini Jeyapalina

British School of Leather Technology

University College Northampton.

Acknowledgements

I am grateful to Prof. G.E Attenburrow and Prof. A.D Covington for their academic support, productive advice and systematic guidance throughout my PhD studies. I am also grateful to Mrs. P. Potter, who at times has given great help when setting up experiments. My sincere gratitude also goes to all the BSLT staff members, especially Mr. K. Flowers for his guidance in the tannery.

I would also like to express my heartfelt appreciation to Mr. Roy Thomson at the Leather Conservation Centre for his advice and assistance and also in providing me with various types of leathers.

Finally I would like to give my gratitude to all my friends and family members, who gave me great strength, encouragement and financial support throughout my studies.

ABSTRACT

The temperature dependent viscoelastic behaviour of synthetic polymers has been shown to be of high importance for their properties and applications. However for leather this aspect of viscoelasticity has not been studied. In order to further the understanding of structure-property relationships, the viscoelastic transitions of leather were investigated in this research work.

This thesis reports the dynamic mechanical behaviour of leather within the temperature region of –100 to 300°C, where three major viscoelastic transitions were identified, termed α, β and γ. The β transition peak represents the glass transition temperature of the amorphous region of collagen molecules.

It is also shown that tanning agents act as plasticisers and depress the glass transition temperature to a lower temperature. Thus the tanning process itself may be viewed as a plasticisation of the collagen molecule. In this event, tanning molecules interpose themselves between the collagen chains, thus reducing the forces holding the chain together. Different tanning agents show differing degrees of plasticisation.

The effect of water on the viscoelastic transitions of leather was also investigated. It was shown that leather remains in a transitional viscoelastic region between -50 and 70°C regardless of the moisture content of a sample. This imparts unique properties to leather. Initially, the absorbed water molecules act as a plasticiser and depress viscoelastic transitions to a lower temperature region. Depending on the leather type, above a certain percentage of absorbed water, splitting of the glass transition peak is observed. This may be due to a preferential hydration of certain hydrophilic amino acid residues, leading to the separation of the transitions due to hydrophobic and hydrophilic amino acid residues.

It is demonstrated that the rate of stress relaxation is temperature dependent and the stress relaxation property of leather above and below the glass transition differs greatly. Two critical temperatures related to heat setting were identified, which may be termed the critical and the optimum temperature. The critical temperature is the temperature above, which the set increases markedly and has been positively identified as the glass transition temperature. Finally, changes in the dynamic modulus during the drying of leather revealed information concerning the nature of the moisture-leather relationship at the critical stages accompanying drying. It is concluded that leather undergoes three different phases during drying, when only the final phase is related to the final stiffness of the leather.

NOMENCLATURE

Symbol	Definition
σ	- Stress
$\sigma(t)$	- Time dependent stress
ε	- Strain
ε_0	- Initial applied strain
ω	- Angular frequency
η	- Viscosity
η_x	- Internal viscosity
τ	- Relaxation time
ρ	- Polymer density
ΔE	- Activation energy
C_p	- Heat capacity
E(t)	- Time dependent relaxation modulus
E'	- Storage modulus
E"	- Loss modulus
E*	- Complex modulus
F	- Force
ℓ_s	- Length after straining
ℓ_o	- Length before straining
ℓ_d	- Length after drying under controlled humidity
M_e	- Molecular weight
R	- Universal gas constant
Tan δ	- Loss tangent
T_g	- Glass transition temperature
T_m	- Melting point
T_s	- Shrinkage temperature
V_f	- Free volume

Abbreviation	Definition
DMTA	- Dynamic Mechanical Thermal Analysis
DSC	- Differential Scanning Calorimetry
DTA	- Differential Thermal Analysis
RH	- Relative Humidity
TMA	- Thermo Mechanical Analysis
WLF	- Williams-Landel-Ferry

LEATHER GLOSSARY

Bating
Removal of residual unhairing chemicals and non-leather making substances by enzyme treatment to clean inside of skin.

Corium layer
Corium or dermis is the central layer of the hide or skin remaining after the removal of epidermis, hair and flesh, and which is converted into leather. This layer amounts to approximately 95 t0 98% of the total thickness of the hide or skin.

Crust
Term used to describe leather, which has been tanned, but not finished.

Curing
Preserving skins by salting and/or drying.

Degreasing
Removing grease by scraping or slicking, or using solvents.

Deliming
The process of neutralising alkali with the weak acid to prevent it from interfering with the tanning process.

Fatliquoring
The process of adding oil and related fatty substances as one of the last wet operations in the processing of leather. This procedure regulates the final pliability and increases the tensile strength of the leather.

Flesh side
The inner surface of the hide or skin, which was in contact with the animal body.

Grain layer
The portion of a hide or skin extending from the surface exposed by removal of the hair or wool and epidermis down to about the level of the hair or wool roots.

Lasting
Operation of shaping the shoe upper.

Liming
Treatment of hides and skin, originally essentially with a lime solution, but today also with other alkalis, or alkalis together with reducing agents, in order to loosen, or destroy, the hair or wool, remove unwanted proteins, saponify fatty matter, open-up fibre structure, etc.

Opening up
Loosening of the corium structural network and of the fibre bundles and fibres and a chemical modification of the collagen, without actual rupture of the polypeptide chains.

Pickling
Treatment of pelts with an acid liquor, such as a solution of sulphuric acid and sodium chloride, to preserve them or to prepare them for tanning.

Samming
Mechanical operation of bring leather to uniform semi-dry state (approximately 50% to 60% water content on wet weight basis) by passing it through the samming machine or by pressing.

Tannin
General term for the vegetable tanning materials.

Tanning
The chemical and mechanical process of converting raw hides into leather

Toggle drying
A method of drying leather where the hide is kept in a stretched position by means of clips called "toggles" in order to maintain their shape and size.

Unhairing
Removal of hair or wool from hides or skins.

Wet blue
Leather, which after chrome tanning has not been further processed and is sold in the wet condition.

TABLE OF CONTENTS

Chapter 1

INTRODUCTION

As the principal constituent of animal skins, collagen is modified and preserved to give leather by a process known as tanning. Both skins and leathers show non-linear viscoelastic behaviour and as a result the mechanical response to loading involves both a viscous component associated with energy dissipation and an elastic component associated with energy storage[1].

The viscoelastic properties of a polymer differ depending on the temperature. As the temperature increases from cold, at a specific temperature, additional molecular chain relaxations can occur, which markedly change the flexibility of the polymer and hence its viscoelastic properties[2]. This distinct temperature, when a material's properties change profoundly, is said to be a viscoelastic transition temperature. The existence of these viscoelastic transitions becomes apparent when the modulus, representing the stiffness of a given material, is plotted as a function of temperature. The major viscoelastic transition of an amorphous polymer is known as the glass transition (T_g) whereas the major transition of a crystalline polymer is melting (T_m).

The main component of leather, collagen, is responsible for its mechanical strength, viscoelastic properties and thermal stability. Collagen has been considered to be a crystalline material (i.e. highly structured) with well-defined sequences of amino acid residues[3-4]. This ordered structure is necessary for its thermal stability and biological function. Sometimes collagen may be referred to as a semi-crystalline material due to the presence of the disordered regions, revealed by the X-ray diffraction pattern[5-6]. For this reason, leather may be expected to show thermal properties associated with both crystalline and amorphous materials. Some researchers regard the shrinkage temperature (T_s) as the melting of the crystalline regions and this transition is well studied in leather research[7-9]. Whereas the T_g, associated with amorphous region of leather fibres, has not been studied extensively[10-11].

The rheological and thermal properties of any polymer have dependency on its molecular structure[2]. Therefore, it is vital to have an understanding of the molecular structure of a material in order to gain complete understanding of its thermal and mechanical properties. In polymer science, structure-property relationships of synthetic polymers are relatively well understood[2,12]. However, such relationships are less well understood in leather science. Furthermore, it is

surprising to find how little research work has been published on the subject of the influence of temperature on the mechanical behaviour of leather. The research work that is reported in this thesis is therefore dedicated to underpin the relationship between molecular structure and the temperature/time dependent rheological properties of leather.

Understanding the thermo-rheological properties of leather is vital in order to understand its mechanical performance at a given temperature. Moreover, by understanding the nature of any viscoelastic transitions occurring in leather, well informed choices regarding leather making processes can be made, allowing the tanner to achieve a tailor-made product that will be fit for a given purpose.

1.1 Viscoelasticity

In order to understand viscoelasticity, it is necessary to consider the rheological behaviour of simple solids and liquids. For perfectly elastic solids, the applied strain is proportional to the stress, as described by Hooke's law. The classic example is the loaded spring. The extension of the spring is directly proportional to the applied force. Such a system does not exhibit any time dependent rheological behaviour. A perfectly viscous liquid obeys Newton's law, where the applied stress is proportional to the rate of strain, the constant of proportionality being the viscosity, η. A viscoelastic material shows both elastic and viscous behaviour and has a time dependent stress-strain rheological behaviour[13-15].

The interwoven network of collagen fibres is responsible for the unique rheological properties of skin. The elastin fibres, which form an interpenetrating network between the collagen fibres, are responsible for shape recovery after a deforming stress has been removed. Thus, the elastic behaviour of skin is mainly attributed to the presence of elastin[1]. Skin behaves in a totally elastic way only at very low stress levels. Beyond such stress levels, the collagen network becomes load bearing and the skin shows viscoelastic behaviour. At high stress levels viscoplastic behaviour occurs[1].

As stated earlier, skin exhibits non-linear viscoelastic behaviour, which is similar to that found in other biomaterials and some textile fibres[16-17]. Thus, the relationship between stress and strain is non-linear and is in the form of a so-called "J" curve[17]. That is the stress-strain curve is concave towards the strain axis at low strain. This behaviour is attributed to the presence of the fibrous network[18]. Such a stress-strain relationship is critical for the biological function of skin and ensures large extensibility, when needed[19-20].

The viscoelastic properties of materials are determined by imposing either a constant stress or constant strain to produce creep or stress relaxation data[12-14,21]. The basic theories of stress relaxation and creep recovery are given in Appendices 1 and 2. In addition to stress relaxation and creep experiments, another type of measurement, the dynamic mechanical test is frequently used to characterise viscoelastic behaviour. Here, stress or strain is an oscillatory function, where either a controlled stress (force) or a controlled strain (displacement) is used. By using a temperature scan, the dynamic mechanical method can be used to assess the temperature dependent structure and properties of viscoelastic materials via their dynamic moduli and damping.

There are two approaches that are used in the interpretation of viscoelasticity: the continuum mechanical approach and the molecular approach[2]. The former attempts to express the viscoelastic behaviour of a body by means of a mathematical scheme, while the latter attempts to explain the bulk viscoelastic properties from a molecular structure standpoint. In this research work, the viscoelastic properties of leather will be discussed in terms of the molecular approach. In order to familiarise the reader with the structural order, the basic structure of collagen molecule will be discussed in Section 1.2.

1.1.1 The four regions of viscoelastic behaviour

As noted earlier, polymer properties differ depending on the temperature. Amorphous polymers show four distinct regions of viscoelastic relaxation behaviour depending on the temperature, as presented in Figure 1.1. They are termed glassy, transition, rubbery and flow. The tensile modulus is often used to identify these different regions of viscoelastic behaviour[2,12-14]. When stress relaxation is monitored as a function of time at a defined strain, the modulus at an arbitrary time (ten seconds) can be obtained by using equation 1.1, when t = 10 seconds then the modulus is termed the ten-second tensile relaxation modulus.

$$E(t) = \sigma(t)/\varepsilon_0 \qquad (1.1)$$

Where E(t) is the time dependent modulus, $\sigma(t)$ is the time dependent stress and ε_0 is the initial applied strain.

At low temperature when the modulus is high, the polymer is hard and usually brittle; this is the so-called glassy region. In this region, molecular segmental motions are not possible in the time scale of the experiments. With increasing temperature, when thermal energy becomes comparable to the potential energy barriers of the segmental rotation, then a glassy polymer

becomes a "leather[i]" like flexible material, accompanied by a sharp decrease in modulus, when a glass transition is observed. This is termed the transitional region. As the temperature is further increased, the modulus reaches a plateau, which is known as the rubbery region. Here, the molecular vibrational motions, which give rise to the so-called leathery behaviour, occur faster than the measurement time of ten seconds. In this region, chain segments orientate relative to each other but large-scale translational motion does not take place. When the temperature is further increased, translational movements of polymer chains may occur. The modulus will begin to decrease again and this region is said to be the flow region[2,13].

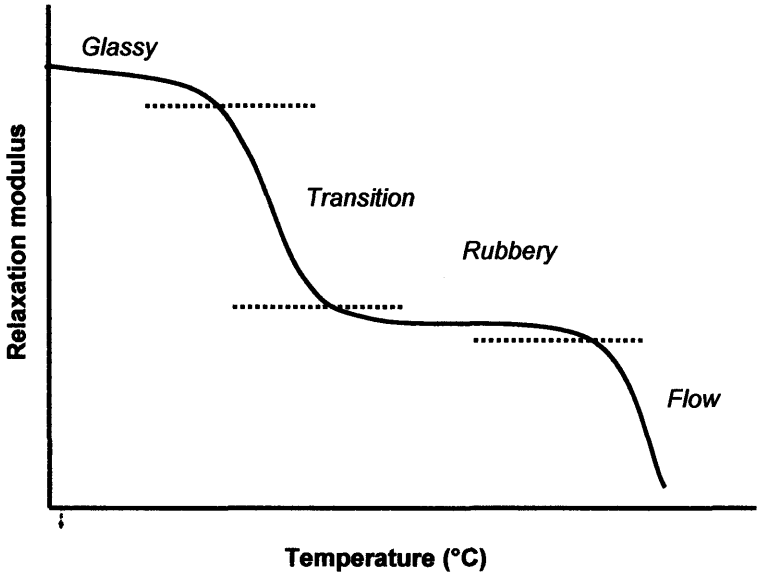

Figure 1.1: Schematic modulus-temperature curve showing various regions of viscoelastic behaviour for a glassy polymer[2].

The general characteristics attributed to amorphous polymers are not greatly modified in semi-crystalline polymers. There is still a glass to rubber transition, a rubbery plateau and flow region. However, the glass to rubber relaxation range is broadened in semi-crystalline materials, and in the flow region, in addition to the large-scale translation of polymer chains, there is a transition from ordered crystals to a disordered liquid state (i.e. melting)[2,22]. Figure 1.2 shows the ten-second tensile modulus temperature curve for the semi-crystalline polymers polyethylene and polyvinyl chloride, showing similar behaviour as the totally amorphous polymer, polystyrene. As with many polymers, leather cannot be viewed as totally crystalline, but rather partly crystalline and partly amorphous. Thus, it may be expected to show behavioural characteristics of both types of material; the rheological characteristics of the crystalline region are superimposed upon the rheological characteristics of the amorphous regions.

[i] This is a description given by polymer scientists and implies that the polymer has a leather-like feel.

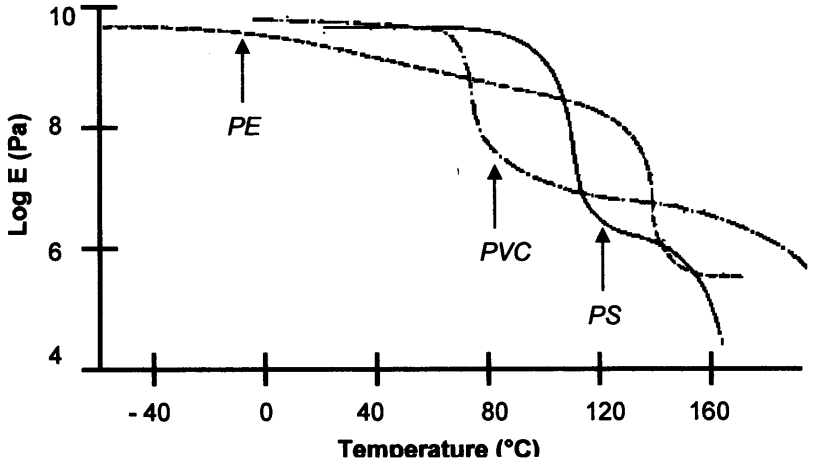

Figure 1.2: Comparison of the ten-second modulus versus temperature curves for the semi-crystalline polymers, polyethylene (PE) and polyvinyl chloride (PVC), contrasted with the amorphous polymer, polystyrene (PS)[2].

(a) Molecular interpretation of transitions and relaxation in polymers

Stress relaxation

When an instantaneous stress is applied to a polymer at a constant temperature, the molecular structure reacts to this stress by disordering itself (bond stretching)[2]. This results in a high modulus. Over longer time periods, reorientation of chain segments is possible. Therefore, the relaxation modulus decreases, resulting in the stress relaxation phenomenon[13].

Stress relaxation can be realistically modelled by considering the relaxation of co-operative segmental units[23]. Co-operative relaxation is needed when these units are densely packed and each unit can relax only if its neighbours also relax. In this interpretation, in order for a larger segmental unit to relax, smaller units must relax first. Therefore, longer relaxation time is associated with the relaxation of the larger segmental units, whereas the shortest relaxation time is associated with the molecular conformational relaxation[24].

The rate of such relaxations increases with temperature, due to the greater availability of thermal energy to overcome activation energy barriers[2]. The re-orientation of chain segments can occur at elevated temperature, thus resulting in a lower value of modulus. The relaxation modulus of a material has dependency on both time as well as temperature and the time-temperature superposition principle can be used to construct a master curve of modulus–time behaviour at a given temperature[25].

Glass transition (T_g)

As the temperature of a polymer increases, it passes through the solid state transitions. At specific temperatures, various chain segmental movements can occur and the polymer softens. Such thermal transitions in polymers are explained in terms of the free volume, thermodynamic or kinetic theories. A detailed description of these theories can be found in any viscoelasticity textbook[2, 13-14]. An overview of the free volume theory will now be presented.

Free volume is defined as the localised space a molecule has for its internal motion[2,15] and the Williams-Landel-Ferry (WLF) equation, which predicts the glass transition temperature of a given polymer, was derived on the basis of free volume concept[26]. Unless enough free volume exists, significant molecular motion cannot occur. As the material warms up and expands, the free volume of the polymer increases and consequently the ability of its molecular segments to move in various directions also increases. The increased mobility can be either for its side chains or for small adjacent groups of the backbone, either way such movement results in a lower modulus.

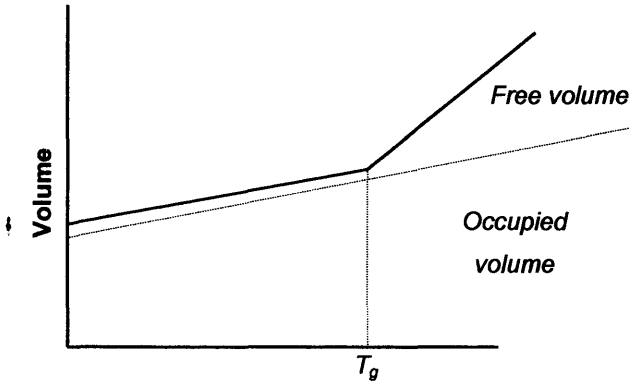

Figure 1.3: The proposed relationship of free volume to the glass transition temperature[12].

Polymer molecules can undergo conformational changes to dissipate applied thermal energy. The gauche conformation, being a high-energy state, requires a larger average volume than the trans conformation[23]. As the volume continues to increase with increasing temperature, a polymer may dissipate the thermal energy by increasing the population of the high-energy state, gauche conformation. Above a certain temperature, i.e. T_g, molecular segments cannot occupy the volume created by the thermal expansion and hence large-scale relaxation motions may take place, due to the free volume (Figure 1.3).

A polymeric material can exhibit other relaxation processes in the glassy state. Since large-scale motions such as those accompanying the T_g are impossible, one approach to understanding low temperature transitions is the proposed crankshaft mechanism[13]. In this model, molecules are treated as a series of joined segments that have some degree of movement and where uncoordinated partial vibration is possible. In polymer science, such a relaxation process has often been attributed to a local motion resembling a rotating crankshaft (Figure 1.4). Other models also exist that allow for more precision in describing behaviour and Aklonis and McKnight give a good summary of the available models[2].

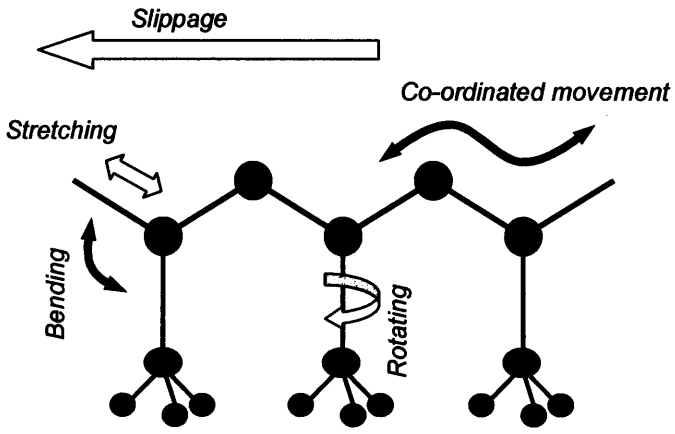

Figure 1.4: Crankshaft model showing the segmental motions within a polymer chain[12].

As described, the physical properties of polymers change drastically as the material goes from a hard glassy to a rubbery state[2]. Thus, T_g defines one end of the temperature range over which the polymer can be used, often called the operating temperature range. It is the upper temperature limit for a polymer when strength and stiffness is needed, but it is the lower temperature limit when flexibility is needed for the polymer's performance[12].

Changes in free volume are often monitored directly, as volumetric changes in the polymer, or indirectly by associated absorption or release of heat, loss of stiffness, increased flow or by changes in relaxation time. Calorimetry or thermo-mechanical or dynamic methods are often used to detect the thermal transition of polymers. A brief overview of the thermo-mechanical methods is discussed in the proceeding sections.

1.1.2 Thermo-mechanical methods

Thermo-mechanical methods have the common feature of a mechanical parameter being measured as temperature is scanned[27]. These methods are ideal for solid materials. The simplest method belonging to this group of tests is thermo-dilatometry, where length changes with temperature are followed. If the expansion of length is hindered by application of a load, then the technique is called Thermo Mechanical Analysis (TMA) and here, the modulus changes are recorded. Impressing a sinusoidal stress onto a sample in a well-defined geometry provides more information about transitions. Such a technique is termed Dynamic Mechanical Thermal Analysis (DMTA).

(a) Thermo-dilatometry

Dilatometry is a technique whereby changes in the volume of a polymer are measured as a function of temperature. Here, a sample under investigation is immersed in a fluid and expansion is measured as a function of temperature. Inflection occurs at the transition point, as shown in Figure 1.5. This method is suitable for measuring the T_g of any solid polymers, but will be unsuitable for measuring the melting transition. Dilatometry methods are simple in principle, but complex in practice. The success of the method depends on the selection of a fluid that is neither absorbed by the polymer nor has phase transitions in the temperature range of interest.

(b) Thermo Mechanical Analysis (TMA)

The primary application of TMA is in the detection of changes in the modulus of a material at major transitions, such as T_g, T_s and T_m. Instrumentation allows a predetermined load to be applied to the sample by a quartz rod, while temperature is altered. The probe penetration, ΔL, is used to detect the transition temperature. The probe penetration changes when a material passes through a transition and is illustrated schematically in Figure 1.5.

(c) Dynamic Mechanical Thermal Analysis (DMTA)

DMTA can be simply described as the application of an oscillating force to a sample, with analysis of the material's response to that force whilst the temperature is altered[12]. The tendency to flow, as indicated by the phase lag and the modulus, is often determined by this technique. Figure 1.5 shows the schematic behaviour of a glassy polymeric solid investigated by these three thermo-mechanical methods.

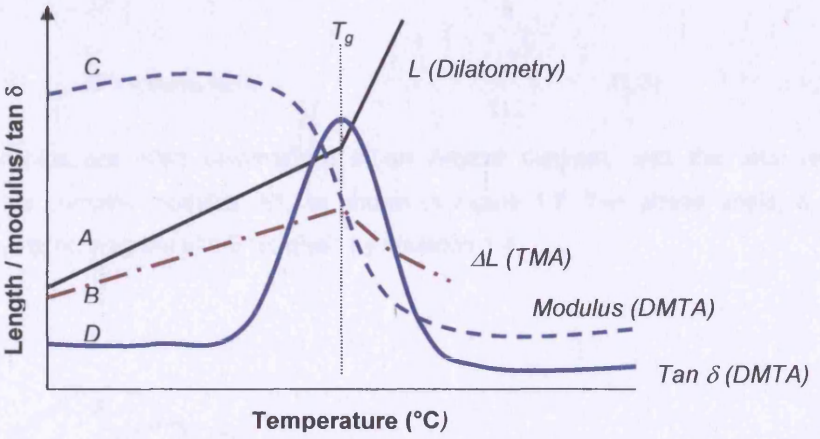

Figure 1.5: Glass transition temperature measured by different thermo-mechanical methods. (A) Dilatometry, (B) TMA, (C) DMTA (modulus) and (D) DMTA (tan δ)[27].

Principle of the DMTA technique

When a sinusoidally varying stress is applied to a sample, then its response will be to deform sinusoidally. This sinusoidal strain lags behind the applied stress because of the time-dependent relaxation processes taking place within the material. This will be reproducible, if the material is kept within its linear viscoelastic limit[12]. The basic theory underlying this method is discussed in various publications[12,27-32]. The time dependent strain resulting from an imposed sinusoidal stress is shown in Figure 1.6. When a sinusoidal stress is applied to a perfectly elastic solid the deformation occurs exactly in phase with this applied stress (phase lag (δ) will be 0°). For a purely viscous material, the deformation will lag by 90° behind the applied stress. For a viscoelastic material, behaviour will be neither perfectly elastic nor perfectly viscous and the resultant strain will lag behind the stress by a phase lag (δ). This phase lag results from the time required for molecular rearrangements to occur and is associated with the relaxation mechanism in the material.

The viscoelastic response may be resolved into an in-phase elastic component, defined as the storage modulus (E′) and an out-of-phase viscous component, defined as the loss modulus (E″). The storage modulus, E′, is calculated as follows,

$$E' = \sigma_0/\varepsilon_0 \cos \delta \qquad (1.2)$$

Where δ is the phase angle, σ_0 the amplitude of the applied stress and ε_0 is the amplitude of the resultant strain. The amount of irrecoverable energy, lost to internal molecular motion, is related to the loss modulus, E″, also called the imaginary modulus. It is also calculated from the phase lag between the two sine waves:

$$E'' = \sigma_0/\varepsilon_0 \sin \delta \qquad (1.3)$$

These relationships are often summarised in an Argand diagram, with the total response governed by the complex modulus, E*, as shown in Figure 1.7. The phase angle, δ, is also defined in the Argand diagram and E* is given by equation 1.4.

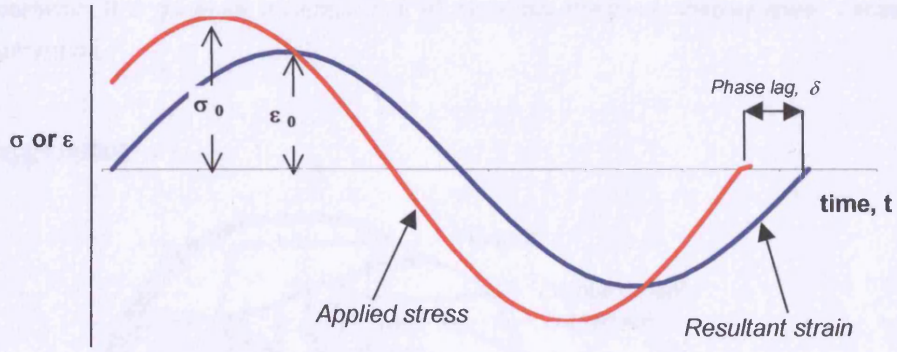

Figure 1.6: Sinusoidally varying stress and strain in a dynamic mechanical experiment, showing the phase lag (δ), the amplitude of the applied stress (σ_0) and the amplitude of the resultant deformation of the material (ε_0).

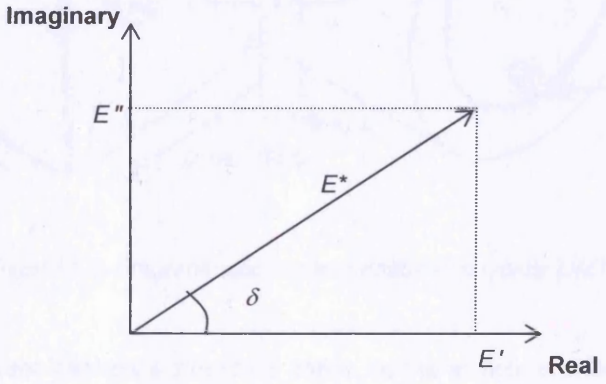

Figure 1.7: Argand diagram showing the relation between dynamic moduli[27].

$$E^* = E' + iE'' \qquad (1.4)$$

The tangent of the phase angle is the most fundamental property measured in such experiments. This property is also related to mechanical damping and is the ratio of energy lost to energy

stored per deformation cycle. Tan δ is the ratio of loss modulus to storage modulus as given in equation 1.5. Tan δ indicates the extent to which material loses energy to molecular rearrangements (internal friction).

$$\text{Tan } \delta = E''/E' \qquad (1.5)$$

It should be noted that dynamic moduli are defined by assuming that the material is linear viscoelastic. It is generally accepted that all materials effectively display linear viscoelasticity at small strains.

Instrumentation

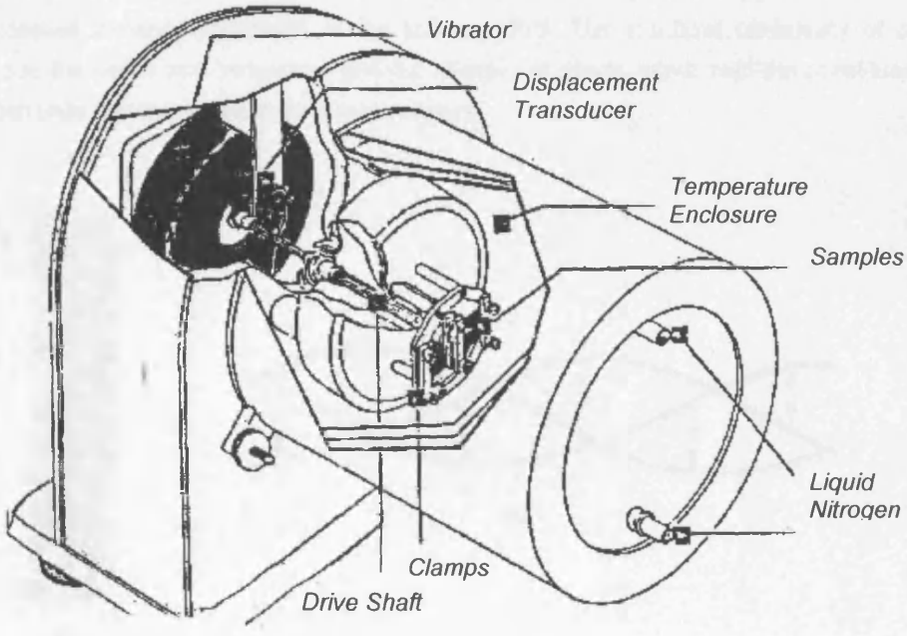

Figure 1.8: Diagrammatic representation of a typical DMTA head.

The DMTA analyser imposes a sinusoidal stress on the sample in a bending, shear or tensile mode and the sample moduli (E′ and E″) and tan δ are determined as a function of temperature and frequency. In the dual cantilever-bending mode, the sample is usually in the form of a rectangular bar clamped rigidly at both ends and with its central point vibrated sinusoidally by the drive shaft. The environment within the temperature enclosure is controllable. The coolant (liquid nitrogen) circulates in a separate jacket. Temperature is sensed and controlled via a platinum resistor lying immediately behind the sample. Figure 1.8 shows the layout of the head of a typical DMTA.

1.2 Structure of collagen

Soft connective tissue, such as skin, is designed to serve specific functions in the body of an animal. The main component, collagen, may be regarded as a most advanced polymeric material and is made up of macromolecular building blocks[33]. The main features of the collagen triple helix (Figure 1.9) were defined in the late 1950s.' However, the complete amino acid residual sequences of the collagen molecule only become known in the 1980s[34]. At present, 27 different types of collagen have been identified in vertebrates. The most abundant collagen is type I, which consists of three left handed helical chains (two $\alpha 1$ and one $\alpha 2$) of 300 nm in length, twisting around each other in a characteristic right-handed triple helix[34-38]. Due to the lateral interactions, these rod like triple helices pack together side by side, with adjacent ones being displaced from one another by about one-quarter of their length, 67 nm. This quarter staggered array results in the classical banded appearance of the collagen fibril. The structural complexity of collagen relates to the amino acid sequences and the diversity of bonds, which hold the constituent tropo collagen units together in the hierarchical structure.

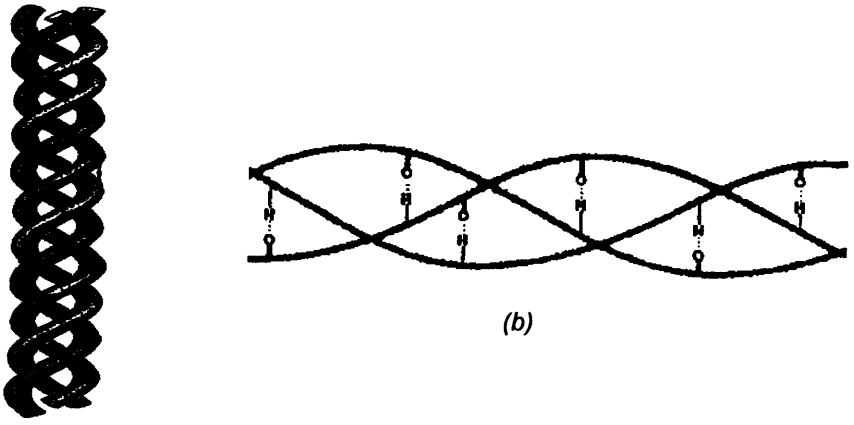

(a)

(b)

Figure 1.9: (a) Schematic of the triple-stranded collagen[39], (b) Diagrammatic representation of the triple helix showing hydrogen bonds[38].

In order to understand its unique thermo-mechanical properties, it is important to review the known structure of collagen. Thus, this section of the introduction reviews the current understanding of collagen structure at its molecular level.

1.2.1 Levels of order in collagen

(a) Primary structure

Collagen is mainly made up of 18 amino acid residues, which are present in different amounts, and the primary structure denotes the complete sequence of amino acid residues. Glycyl residues make up one third of the total amino acid residues. These residues are reported to be spaced evenly almost throughout the chain structure[40-43]. Collagen also contains the amino acid hydroxyproline, which is not commonly found in other proteins, except elastin[44].

The basic structure of the collagen molecule is relatively simple. The primary sequence is a tripeptide repeating unit of $(Gly\text{-}X\text{-}Y)_n$, where X and Y are variable amino acids but not completely random. Hence, collagen can be considered as a poly-tripeptide with glycine at every third position. Another important feature is the high content of the imino-acids proline and hydroxyproline in the X and Y positions. These imino acid residues together constitute almost a quarter of the total number of residues. This implies that, in almost one in four residues, rotation around the bond denoted by a red arrow in Figure 1.10, would not take place. This restriction of rotation and the intramolecular hydrogen bonding within the chain leads to the unique secondary structure[37].

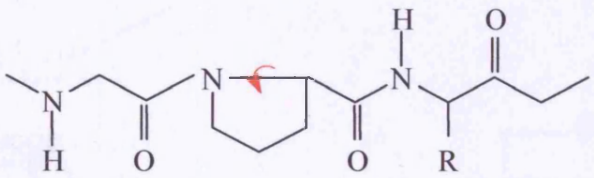

Figure 1.10: A tripeptide unit (sequence of Gly-Pro-Y), indicating the restriction to free rotation caused by the imino acid on the polypeptide backbone[37].

(b) Secondary structure

The secondary structure of collagen is a left-handed polyproline helix with a strong affinity for inter-chain, rather than intra-chain, hydrogen bonds[37]. The configuration of polypeptide chains is resolved to a larger extent by the stereochemical features of the constituent amino acid residues. The abundance of the prolyl and hydroxyprolyl residues prevents the formation of a α-helical chain segments; instead they form the long sequences of the individual chains of collagen which resemble the left-handed version of the poly-L-proline-II-helix[45]. The peptide chains usually have a molecular weight of about 100,000 and contain roughly 1,000 amino acid residues. The small side

chain of glycine allows these polyproline helices to pack in close contact to form a super-coiled triple helix. This arrangement restricts the intra-chain hydrogen bonding and consequently creates the inter-chain hydrogen bonds required for a stable tertiary structure.

(c) Tertiary structure

Tertiary structure refers to the large scale folding of the fundamental structural unit of collagen, tropocollagen. This is a right-handed super helix with a repeat distance of about 100 Å, made up of three left-handed strands[41]. Each of the three polypeptides is known as an α-chain and two of them have an almost identical amino acid composition[37]. Initially, two α-chains are dimerised by covalent crosslinking to form a β-chain while a third strand is crosslinked to form the γ-chain; the so called tropocollagen molecule. This triple helix is stabilised by hydrogen bonds from the glycine to the peptide backbone of an adjacent chain (Figure 1.9(b)). In this structure, larger side chains are arranged in such a way that they provide a certain charge profile along this super helical structure (i.e the larger polar amino acid residue side chains face outward from the cylindrical helix). The end regions of the tropocollagen are known to be non-helical (Figure 1.11) and contain lysyl residues[46]. These non-helical (telopeptide regions) are essential for *in vivo* fibril formation and are the specific sites for lysine-based crosslink formation between collagen molecules[47].

Figure 1.11: Diagrammatic representation of collagen triple helix indicating the non-helical telopeptide end region.

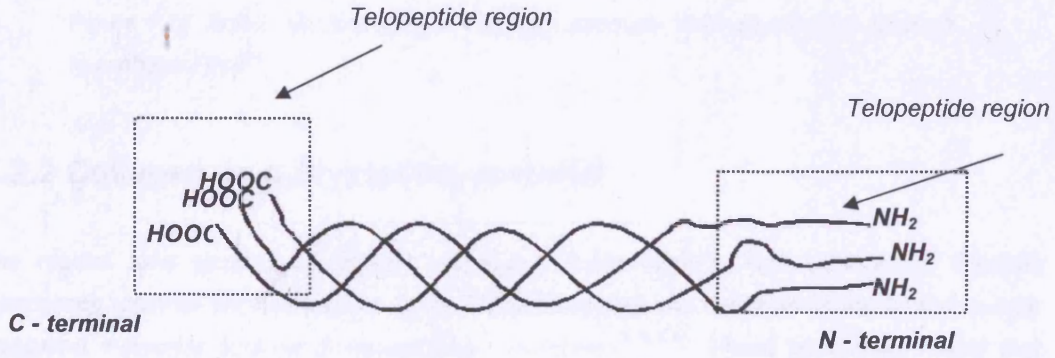

(d) Hierarchical structure

Hierarchical structure refers to small orderly aggregates of tropocollagen. The charge profile on the tropocollagen molecule spontaneously drives the self-assembly of the five tropocollagen molecules into a quarter-staggered alignment to form a microfibril as indicated by Figure 1.12[48]. This structure is further stabilised by water molecules as well as covalent bonding at lysyl residues and forms fibrils of 50 to 200 nm in diameter. Collagen fibrils from mature animals are

insoluble in water, because of this covalent crosslinking[40]. Fibrils then assemble in parallel bundles and consequently form collagen fibres.

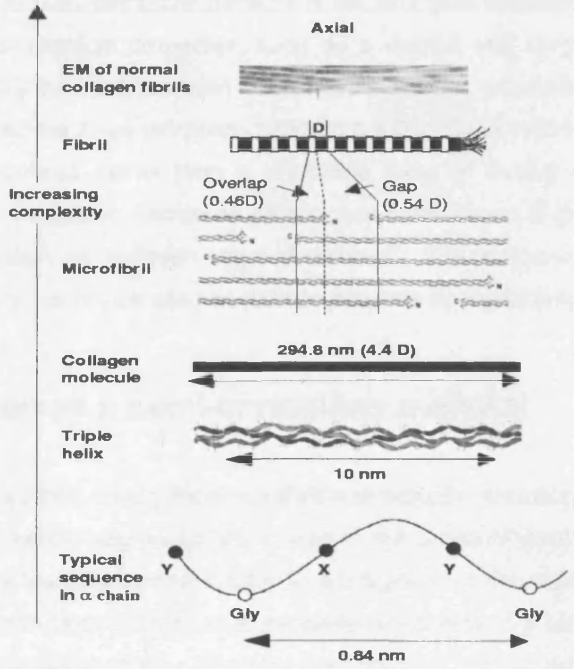

Figure 1.12: Schematic hierarchy of collagen structure, from alpha chain through to collagen Fibril[33].

1.2.2 Collagen as a crystalline material

The regular axial packing of collagen molecules within fibrils is well established. Electron microscopy together with wide-angle X-ray diffraction allows the definition of the lateral quarter staggered molecular packing of tropocollagen molecules[3-4,33-37]. These techniques reveal that collagen molecules are aligned and packed together in a regular fashion. Therefore the structure of collagen has long been considered as a fibrillar crystallite[48-50]. Although two-dimensional structure is well established, the absolute three-dimensional packing of collagen is not well understood, even though it has been subjected to intensive research.

Evidence for the existence of the orderly arrangement of tropocollagen was initially proposed from the observation of discrete peaks on the equatorial X-ray diffraction patterns[51]. Recently, improvement in the quality of the diffraction data has allowed several researchers to propose different molecular packing models. Fraser *et al.*[52] have proposed a triclinic unit cell arrangement

and this was later supported by Wess and his co-workers[5,53-54]. These findings provide further evidence for the regular packing of collagen molecules.

The appearance of X-ray diffraction patterns is the strongest evidence of the crystalline structure of collagen. Other physical properties, such as a distinct and reversible melting point, which distinguishes crystalline materials from amorphous materials, are not exhibited by collagen. It may even be argued that the X-ray diffraction patterns are due to the orderly arrangement of the amino acid residue sequences, rather than a crystalline array of rodlike molecules. The completely amorphous form of collagen, known as gelatin, has been shown to give the same wide-angle X-ray diffraction pattern as collagen upon stretching[55]. This suggests that the X-ray diffraction pattern of a material cannot be used as definite proof for its crystallinity.

1.2.3 Collagen as a semi-crystalline material

It is well established that, during the biosynthesis of helical tropocollagen, regions of globular type structure (i.e. non-helical segments) are formed at the C and N terminals[46]. The globular regions or telopeptides are partially removed prior to aggregation of the molecule in the quarter-stagger alignment but overall tropocollagen is a molecule comprised of a triple helix with small globular terminal regions consisting of 10 – 20 amino acid residues[56]. Even though the amorphous regions of the tropocollagen molecule are small, it can still be viewed as a semi-crystalline polymer. Furthermore, the X-ray diffraction pattern of collagen has been shown to consist of a significant amount of diffuse scatter, indicative of static or thermal disorder within the fibrils[5]. Thus, collagen can be viewed as a semi-crystalline polymer.

1.2.4 Collagen as a block copolymer

In polymer science terms, copolymers are those which show chemical heterogeneity. The question that needs to be answered here is whether collagen can be considered as a copolymer. Bear and co-workers suggested that the axially repeating pattern in native collagen, revealed by electron microscopy and small-angle X-ray diffraction, might be due to a regular alternating of groups of amino acids[4,57]. They also postulated that the "band" regions contain a concentration of "polar" amino acid residues and that the "interband" regions contain mostly "nonpolar" amino acid residues. Research carried out by Kuhn and co-workers supported this view, and suggested that the stained regions in the fibrils, while staining with phosphotungstic acid, correspond to sequences of mainly polar amino acids[45]. Hannig and Nordwig concluded, when reviewing work on the sequencing of collagen, that the primary structure of collagen is discontinuous and is composed of sequences of neutral amino acids and sequences of polar amino acids[36]. This leads

to the concept of collagen as a block copolymer. Taking all the literature evidence into account, Yannis suggested that, to a rough approximation, collagen might be modelled as follows[37]:

$$(Gly\text{-}A\text{-}B)_M - (Gly\text{-}Pro\text{-}Hyp)_N$$

"polar nonpolar" model[37].

Where A and B are almost exclusively any of the α-amino acids.

Dölz and Heidemann[59] studied the sequence of tripeptides in collagen type 1 and proposed a "cluster model" which corresponds to the model proposed by Bear[4]. They listed the most frequently occurring tripeptides as follows;

Gly-Pro-Hyp	≈16%
Gly-Pro-Ala	≈12%
Gly-Ala-Hyp	≈9%
Gly-Leu-Hyp	≈4.5%
Gly-Glu-Hyp	≈4.5%
Gly-Glu-Arg	≈4.5%
Gly-Pro-Ser	≈4%
Gly-Ala-Arg	≈4%

The persistent reoccurrence of Gly-Pro-Z (almost 28%) gives further evidence supporting the block copolymer theory. From this analysis, a second better approximation can be attained from knowledge of the sequence of amino acid residues. This is indicated as follows:

$$-(Gly\text{-}X\text{-}Y)_M\text{-}(Gly\text{-}Pro\text{-}Z)_N$$

" cluster" model[59].

Where Z is Hypro, Ala or Ser.

In this approximation, the "nonpolar" regions frequently contain polar amino acid residues and there is, in fact, a less sharp distinction between polar and nonpolar regions[37]. However, in spite of all the uncertainties, it is useful to consider collagen in the solid state as a block copolymer. Recently, Fraga and Williams provided further evidence to support this block copolymer theory, through their research on the thermal properties of gelatin: differential scanning calorimetry of gelatin revealed two distinct T_g values, indicating two different blocks[58].

Both of these models are schematically presented in Figure 1.13. When two pyrrolidine rings are in sequence, then they determine the position of nine bonds in the collagen backbone, which is a complete turn of the polyproline helix[58]. Fraga and Williams proposed a block copolymer theory

based on these restriction in the rotation imposed by imino acid residues, which views collagen is composed of segments of "hard" and "soft" block[58]. A restriction on rotation of segments in the hard block is imposed by the presence of imino acids that will influences the flexibility.

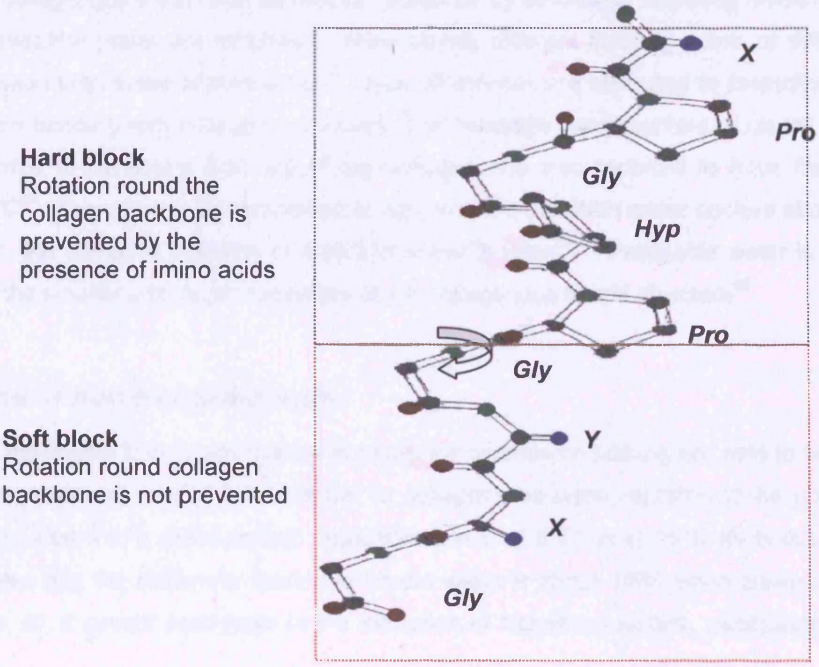

Figure 1.13: A representation of the Gly-X-Y-Gly-Pro-Hyp-Gly-Pro-X segment of the collagen molecule. Filled red circles (●) represent oxygen atoms, filled green circles (●) represent nitrogen atoms, filled blue circles (●) represent α-amino acid residues.

1.2.5 The collagen-water system

To this point, the structure of collagen has been reviewed in terms of amino acid sequences and their ability to form ordered and defined structure. However, the triple helical structure of collagen is held together not only by the inter/intra chain hydrogen bonds but also by the hydrogen bonds from the water bridges[60-62]. In fact, water is an important and integral part of collagen structure. The mechanical and thermal properties of collagen have a high dependency on the water content (often referred as moisture content). Removing water molecules from the collagen structure alters the flexibility of the chain. Thus, anhydrous collagen is brittle and hard, but hydrated collagen is soft and flexible. There are two main states of water that are reported to be found in collagen; free/freezable and bound/non-freezable water[63-68].

(a) Freezable water

In a hydrated collagen, not all the water molecules behave like bulk water and form crystals upon cooling. Water molecules that resemble the bulk water are said to be the freezable water content of collagenous tissues and have been studied extensively[63-68]. The amount of freezable water within the collagenous matrix can be readily measured by differential scanning colorimetry. Some states of freezable water are reported to show slightly different freezing points or different latent heats of fusion than those of pure water[64]. Such differences are attributed to restrictions imposed by hydrogen bonding with collagen molecules. The freezable water content of rat tail tendon has been reported to be above 0.50 g/g of dry collagen and also reported to have freezing point around -7°C[64]. This value is also expected to vary with the pH. With water content above 0.60 g/g of collagen, the same ice enthalpy of pure/bulk water is seen[63-65]. Freezable water is found to be present in the smaller and larger capillaries of the collagenous matrix structure[66].

(b) Bound or non-freezable water

The water molecules in collagen that do not form ice crystals on cooling are said to be the bound water. The relaxation time of bound water in collagen has been reported to be about 1 ns at 25°C[69] compared with a characteristic relaxation time,τ, of 8.27 ps at 25°C for bulk water[69]. This demonstrates that the molecular motion of bound water is about 1000 times slower than that of pure water, so, it cannot participate in the formation of flickering clusters, necessary to nucleate ice.

Pineri and co-workers[66] and Bienkiewicz[63] reviewed evidence for different types of bound water molecules in collagen and leather respectively. They have identified four types of bound water within collagen molecules. In the first state, the structural water molecules, cannot be extracted under normal conditions and they are firmly attached to the collagen structure. This state of water accounts for up to 0.01 g/g of dry collagen weight and is reported to form three hydrogen bonds with the collagen molecule[66]. The second state of bound water accounts for up to 0.07 g/g of dry collagen and is reported to be doubly bound. Both of these states of water molecules are essential for the stability of the triple helical structure. The third state of water is bound to collagen, 0.07 - 0.23 g/g of dry collagen, and is involved in the molecular packing of collagen molecules[68-69]. Absorption or removal of this state of water molecule from collagen results in a drastic change in the equatorial X-ray diffraction spacing and therefore it is concluded that these water molecules are located between the triple helices or within the fibrils. The fourth state of water molecule corresponds to 0.23 – 0.50 g/g of dry collagen and is reported to be fixed to collagen via one hydrogen bond[66]. Such water molecules are sometimes referred to as associated water. Bienkiewicz stated that these water molecules might be attached to functional groups on the side chains[63].

Water molecules have also been shown to have a profound influence on the structure of the crystalline regions of collagen. Heidemann and Keller demonstrated that collagen has maximum crystallinity when it contains 30% water (on a wet weight basis)[70]. Furthermore, Lees and co-workers have reported that the equatorial packing of collagen fibrils can vary from rectangular to hexagonal, depending on the crosslinking and the water content of the specific tissue[68-69]. It was proposed that the collagen molecules are forced apart with the accretion of water and thus equatorial spacing increases. When the water content exceeds some limit, there is no further expansion and thereafter water fills capillaries. These water molecules are not involved in the molecular packing of collagen molecules, they behave like bulk water and freeze upon cooling.

1.3 Skin

Skin is the outermost part of a living animal and the level of structure indicates its complex physiological functions. It is the basic starting material for leather production. Hence its structural knowledge is essential to understand the changes, which take place during the tanning process. Figure 1.14 indicates the basic structure of skin. Skin is composed of tree superimposed layers that are connected but very distinct in their architectural organisation. They are corium minor/gain, corium major/corium and flesh layers.

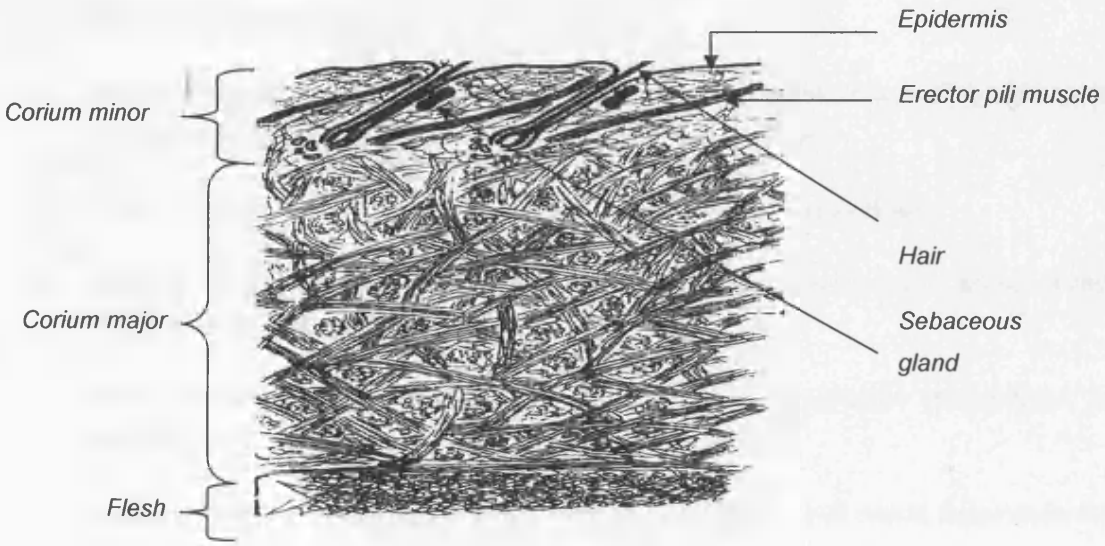

Figure 1.14: Cross section of cattle hide[76].

Corium minor is also known as grain layer consists of tightly packed individual fibres, whereas corium major is made up of a discrete fibre bundles with high angle of weave. The grain layer not only contains network of elastin but also sebaceous and sweat glands hair follicles etc. The epidermis covers the outer surface, which is a non-fibrous collagen. Towards the inner or flesh surface the fibre bundles become finer and run horizontal manner to separate the skin from the underlying muscles.

1.4 The aims and objectives of the research

It has been emphasised throughout this chapter that glass transition in polymers is accompanied by profound changes in their viscoelastic properties. Therefore, the temperature dependent viscoelastic behaviour of synthetic polymers has been studied extensively. However for leather this aspect of viscoelasticity has not been studied. In light of this, the primary aim of this research was to further the understanding of the viscoelastic behaviour of leather by investigating its temperature and moisture dependent dynamic mechanical properties. The secondary aim was to apply DMTA to study the modulus changes that occur during the leather processing, such as drying. The project had several objectives and they are;

1. To identify the presence of viscoelastic transitions in untanned and tanned skin.
2. To define the influence of water on such viscoelastic transitions.
3. To provide an explanation of observed viscoelastic transitions.
4. To define the practical implications of temperature dependent viscoelastic behaviour in leathers.
5. To improve understanding of the stress relaxation behaviour of leather in relation to the viscoelastic transition temperatures.

This thesis is divided into six Chapters.

- Chapter 2 outlines the viscoelastic transition temperatures of untanned skin using DMTA and gives the arguments for the presence of a glass transition in collagen.
- Chapter 3 shows on the effect of tanning agents on the glass transition of skin.
- Chapter 4 reports an investigation of stiffness changes accompanying leather drying, aimed at a better understanding of leather-water relationships.
- Chapter 5 investigates the relationship between viscoelastic transition temperatures, in particular, the T_g on the stress relaxation properties of leather.
- Chapter 6 summaries the main conclusions of this research work and makes suggestions for further work.

Chapter 2

INVESTIGATION OF THE TEMPERATURE DEPENDENT VISCOELASTIC PROPERTIES OF SKIN BY DYNAMIC MECHANICAL THERMAL ANALYSIS (DMTA)

2.1 Introduction

Animal skins have the same basic structure, fibrils of the protein collagen, held in bundles, which interweave in three dimensions through the skin[34]. A typical raw skin is comprised not only of collagen but also other soluble proteins, mucopolysaccharides, keratin, elastin, fat, water etc. During the early leather making process, most of the non-collagenous materials are removed from the skin, followed by the addition of tanning agents to confer stability and to give an aesthetic feel to the leather. Tanning agents are known to modify the hydrothermal stability of collagen fibres. Thus it was logical first to examine the thermal properties of untanned collagen prior to examining leather, in order to identify the temperature-linked changes occurring in untanned collagen. Helix-coil, glass, shrinking and melting transitions have been reported to be present in collagen[7-11,37,71-75]. However, some researchers have questioned the presence of a glass transition in collagen and to date it is not a fully established phenomenon[37].

As discussed in Chapter 1 (Section 1.2.2(c)), DMTA is an analytical technique which measures the rheological properties of a sample over a range of temperatures. Several researchers (refer to Table 2.1 on page 30) have used this technique to identify thermal transitions in collagenous materials. The DMTA method has several advantages in the study of temperature linked changes in collagen. The procedure is easy and simple to use. Because of its sensitivity in detecting subtle molecular changes, it appears to be the best tool for analysing higher order thermal transitions. For example, DMTA shows greater sensitivity to the glass transition in polymers, compared with other techniques, such as differential scanning calorimetry (DSC) or differential thermal analysis (DTA). DSC can sometimes detect secondary transitions, but the signal produced is often too weak or too broad for accurate determination of the transition temperatures[12].

Characterising and understanding secondary transitions in polymers and biopolymers are important, as these transitions have been associated with mechanical properties[2,12-14]. These

transitions are considerably affected by the extent of crosslinking and other structural variables, such as plasticisers[12]. Since both thermal and mechanical properties are associated with molecular structure, by studying the thermal properties of collagen based materials, a greater insight into their mechanical behaviour can be gained. It is believed that in fibrous collagen based materials, dehydration can introduce inter fibre sticking and hence the handling and physical properties, as well as the appearance of such materials may vary, depending on the degree of dehydration[76].

When the processed skin is dried in a stretched state at ambient conditions, the processed and separated fibre structure allows re-orientation and sticking of the fibres, to form a hard, translucent material resembling parchment. This is due to the high surface tension of water. As the skin dries, the free water vapour migrates from the capillaries to the skin surface, where it evaporates. As the water content falls in the internal capillaries, so the surface tension of the water begins to exert a pull on the walls of the capillaries, bringing them closer together until the fibril surfaces stick.

The physical properties and the appearance of leather are quite different from those of parchment. In order to have a meaningful comparison between tanned and untanned skin, it is essential to compare them in a similar physical state. In this study, processed skin was acetone-dried to produce a leather like feel and appearance; this is due to the low surface tension of the acetone, which prevents fibre sticking. In this chapter, the low temperature thermal transitions of acetone-dried skin and parchment-like skin are reported and the influence of moisture content upon the transition is examined in detail.

2.1.1 Transition temperatures in fibrous collagen

(a) First order phase transitions

Phase transitions for which the molar entropy and the molar volume are not equal to zero are said to be phase transitions of the first order[77]. They can be investigated using dilatometry, because the molar volume changes. Calorimetry can also be used to investigate this kind of transition, because the molar entropy changes. This implies that the molar enthalpy will also be changed and therefore the heat of transformation can be measured by calorimetric techniques[77]. During the shrinking or melting transition, the entropy and molar volume of leather changes: therefore, they are said to first order phase transitions.

Shrinking and melting transitions

Even a limited literature survey reveals that much effort has been made to understand the shrinking phenomenon of fibrous collagen immersed in liquid media. Shrinking is an irreversible

phase transition of the collagen macrostructure[7-9,71-73]. Some believe that shrinking is the collapsing of the fibrous structure due to extensive breakage of hydrogen bonds[7-9], while others view this process as a melting point of collagen crystallites[71-73,78].

Fibrous structural proteins such as collagen and keratin show structural stability, which is necessary for their biological activity. To maintain an optimum structural stability, they must also possess thermal stability. Thermal stability arises from interactions and bonds between molecules. They also generally show optimum thermal stability when arranged in crystal lattices, where interactions and bonding are optimised. Hence, crystals show a reversible and distinct melting point upon heating, when they undergo a solid to liquid phase transition.

In solution, tropocollagen molecules are aggregated to form complex crystallites (refer to Section 1.2), and are stable up to a critical temperature, above which a sudden collapse of the helix-coil into a disorganised random coil occurs. This transformation is only observed when collagen molecules are in dilute solution, discussed by Von Hippel[35]. However, when molecules of collagen are in a structurally organised fibrous form, they do not behave like a single crystal. In fibres, molecules are packed tightly and the inter-fibril hydrogen bonding and hydrophobic interactions restrict the degrees of freedom of the molecular collagen[7]. Collagen consists of an unusually high number of polar amino acids. These polar groups enable the formation not only of intra chain hydrogen bonds but also of inter chain hydrogen bonds between adjacent fibrils. These linkages further restrict free molecular movement of the individual collagen molecules. In fibres, the forces binding or stabilising the matrix structure are mainly hydrogen bonds and hydrophobic interactions[34-37]: these bonds will break at a certain critical temperature on heating and traditionally this is known as the shrinkage temperature (T_s). The shrinking or denaturation results directly from melting of the crystalline phase, but is not a true melting point of collagen fibrils, since these transitions are not completely reversible.

Flory and co-workers have shown that the normal measurement of T_s may involve superheating by as much as 10°C above the helix-coil transition temperature[78]. Later, a study by Rigby showed that the T_s of swollen fibres is higher than the helix-coil transition temperature by about 22°C[79]. This helix-coil transition may be regarded as the melting of the crystalline regions of collagen.

Weir investigated thermal shrinking of leather in terms of a rate process; treating shrinkage as a normal chemical reaction[80]. Covington described shrinking in terms of a kinetic process involving two steps as shown below[81].

$$\textit{Intact collagen} \underset{k_{-1}}{\overset{k_1}{\rightleftharpoons}} \textit{Dissociated collagen} \xrightarrow{k_2} \textit{Shrunk collagen}$$

According to his description, the first phase of the shrinkage reaction is completely reversible but once the collagen shrinkage enters the second phase, the reaction becomes irreversible.

If the rate process can be substituted by two known phase transitions of materials, i.e. melting and collapse transitions, then the irreversibility of shrinking could be explained. Flory was the first to introduce and quantify the collapse transition in polymers[82]. This transition arises from competition between the attractive interactions between monomer units, which acts to collapse the polymer onto itself, and the entropy of the polymer chain, which acts to expand the polymer. The same principle may well be applicable to collagen fibrils after they have undergone the helix-coil transition. The first stage of the transition is the true melting of fibrils into dissociated/random coil collagen. As expected by classical physics, the melting of the collagen crystallite is completely reversible. The second stage could be the collapse transition of dissociated collagen into shrunken collagen.

In fibrils, the dissociated collagen could be restricted from collapsing into a random coil by intermolecular crosslinking. Once the heat labile crosslinks are broken, then dissociated collagen molecules are free to collapse to the shrunken state. Because of the complicated nature of the shrinking phenomenon, researchers also describe the shrinking temperature as the melting point of collagen. In the literature, the words melting, denaturation and shrinking all refer to the same phase transition of collagen. The temperature at which this transformation occurs may also be affected by the presence of ionic solvents or plasticising agents and the extent of crosslinking. Covalent bridges increase the melting temperature and water depresses the melting temperature.

(b) Higher order transitions

Phase transitions, for which the molar entropy and the molar volume are equal to zero, are said to be phase transitions of higher order[77]. For a second order phase transition, the second derivatives of the Gibbs free energy with respect to temperature and/or pressure are not equal to zero. Thus, for this transition, there is no entropy or volume change. However, the heat capacity, the thermal expansion and the compressibility will change during this transition and hence it is widely analysed by calorimetry or thermal-mechanical analysis. The glass transition is said to be a pseudo second order transition. It is not a real second order transition, because the glassy state is not in thermodynamic equilibrium with the rubbery state. The value of the T_g is not only defined by thermodynamics, but also by a rate process.

Generally, as discussed in Chapter 1, the T_g can be interpreted as the temperature above which the segmental motion of macromolecules becomes thermally activated: this transition is also called the alpha transition, T_α. Normally the shorter the segment length, the more flexible the

macromolecular chain, and the T_g takes place in a lower temperature region. Conversely, the T_g of biopolymers increases with chain rigidity and the intensity of both inter and intra-molecular interactions, including hindrance to internal rotation along the macromolecular chain.

Besides the glass transition, there are several other higher order transitions that have been identified in polymers[12]. The existence of other higher order transitions becomes apparent when modulus/loss tangent is plotted over a wide range of temperatures. Figure 2.1 shows a typical plot for an amorphous polymer. Individual relaxation mechanisms can be distinguished by the stepwise reduction in modulus as the temperature increases. Higher order transition temperatures are also sensitive to plasticisers, such as water.

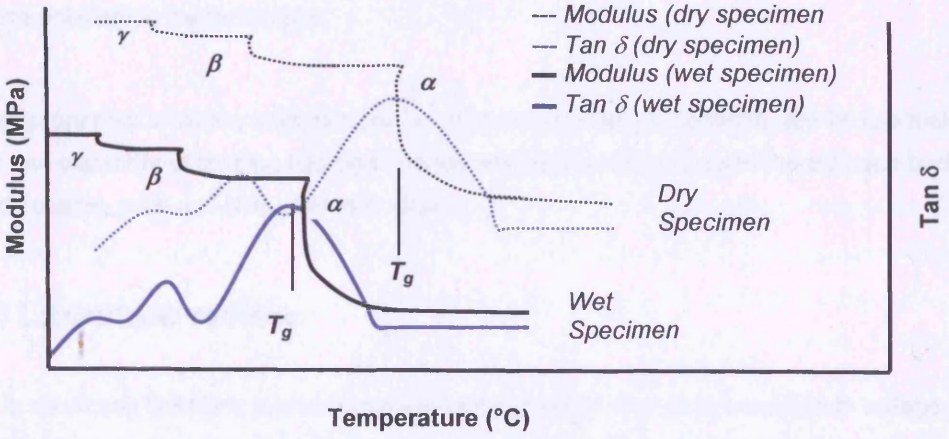

Figure 2.1: Temperature dependence of modulus and loss tangent for hydrophilic amorphous polymers in the wet and dry states[83].

For an amorphous polymer, the largest relaxation is the glass to rubber (α) transition, which is termed the "glass transition temperature". In this transition the modulus usually falls by a factor of 10^2-10^4. Other, secondary transitions occur at low temperatures and involve relatively small changes in modulus. These transitions may be attributed to the onset of more localised side chain mobility. These are termed β, γ relaxations etc. (refer to Figure 2.1).

2.1.2 Plasticising effect of water

An effective plasticiser should shield the inter- and intra-molecular interactions, facilitate segmental molecular motion and decrease internal friction in the polymeric materials[85]. The plasticising effect can be described in terms of the elastic modulus or viscosity of polymer-plasticiser mixtures. In order to shield molecular interactions, the plasticiser must be miscible with

the system it is plasticising. It must also be a small molecule with low viscosity. Good plasticisers are usually good solvents. Thermodynamically, a good solvent shields inter- and intra-molecular interactions and can dissolve some macromolecular associations and crystalline regions. In this way, solvation shells increase the distance between chain segments and decrease the activation energy for segmental motion. Many hydrophilic compounds of low molecular weight can act as plasticisers; however, none is as effective as water.

The thermal and viscoelastic properties of leather exhibit high dependency on water content. Water is known to act as a plasticiser in biological systems: leather is a modified biopolymer and hence water is expected to act as a plasticiser. However, the water–leather relationship is much more complicated than a simple solute-solvent system[63,84]. Water exists in several states within the hierarchical structure of collagen as discussed in Chapter 1 (Section 1.2.5) and even forms structural links within the molecules.

The key properties of water, important for its plasticising effect on collagen, are its low molecular weight and capability of forming hydrogen bonds with hydrophilic groups of the collagen backbone and side chains, such as $-NH_2$, -OH and -COOH.

2.1.3 Literature review

There is conflicting literature evidence regarding the concept of a glass transition in collagen. One difficulty is that a glass transition is characteristic of an amorphous material. Collagen is widely accepted as a crystalline material, since it shows an X-ray diffraction pattern. However, it may be argued that the X-ray diffraction pattern could result from an orderly arrangement of fibrils rather than the crystal structure of collagen molecules.

The glass transition is usually defined by reference to sharp changes in heat capacity, C_p, which occur when the system falls out of equilibrium during a thermal transition. Adiabatic calorimetric studies of collagen, in both dry and moist states, did not reveal a C_p jump at any temperature[77]. Therefore it was concluded that collagen is a fully crystalline polymer.

As early as 1958, Flory and Garrett reported the existence of an apparent T_g between 40-45°C in a beef achilles tendon–water system, containing approximately 40% of collagen by weight[78]. Furthermore, they also reported that this transition was completely reversible. They also attempted to prepare dry amorphous collagen by heating bovine achilles tendon at 175°C for several minutes, when they observed that the specimen shrank during heating. Precise dilatometric experiments on shrunken amorphous collagen revealed another glassy type transition

at 95°C, below its melting temperature. This transformation is partially reversible (because the latent volume change slowly recovered in part upon cooling). Furthermore, they concluded that the transformation at 95°C probably represents a phase transition of amorphous collagen/gelatin.

Rigby *et al.* found that the rate of stress relaxation of collagen fibres in saline solution increases rapidly at approximately 40°C[79]. Furthermore, the fibre lost its ability to return to its original length when the stress was removed. Therefore, they suggested this temperature of 40°C must be the T_g of collagen and the irreversibility of deformation may be due to the stress related conformational changes, which are expected to occur above the T_g. Further work by Rigby and Mason, a few years later, revealed further evidence for the presence of a T_g in collagen[86]. They investigated the specific volume changes as a function of temperature and showed the presence of a glass-like transition at 47.5°C. They also employed a force-temperature technique and reported a slight inflexion at 48°C. This further verifies the presence of a T_g in collagen.

Bear *el al.* examined the dynamic mechanical relaxation of human diaphragm tendon collagen by an inverted, free-oscillating, torsion pendulum[87]. They identified three relaxation processes and assigned them α, β and γ transitions. They also demonstrated how these transitions strongly depended on the water content. They explained their observations in terms of the absorbed water on the collagen, but failed to interpret these relaxation processes in terms of its structure. The α peak in their relaxation spectrum, located above 147°C at low moisture contents, progressively decreased as the moisture content increased. This suggests that this could be the molecular motion associated with shrinking transition of collagen. However their β transition, may well have been associated with a phase transition of water, since it remained constant at -13°C. The position of their γ peak increased from -123 to - 63°C with decreasing water content, indicating some kind of water sensitive transition of the side chains.

Nguyen and co-workers examined the dynamic mechanical properties of reconstituted collagen and reported the presence of three tan δ peaks[88]. Because of the frequency dependency of these tan δ peaks, they interpreted them as secondary transitions due to some molecular or sub-molecular motion.

Batzer and Kreibich later confirmed the existence of a glass transition, when investigating the influence of water on the thermal properties of collagen and gelatin[89]. They investigated the T_g as a function of water content and reported an exponentially falling relationship with water content. As expected, water depressed the T_g.

Kronick and co-workers investigated the dynamic mechanical properties of polymer-leather composites and revealed that moisture, lubricant oils and other polymer impregnants had an effect on the complex modulus of leather[90]. They reported that the grain layer of leather showed a maximum tan δ between -20 and +60°C. This falls within the transition temperature region reported by other workers.

Twombly, Cassel and Miller investigated the thermal transition of bovine collagen type 1 by DSC and DMA at 100% humidity[91]. They observed two transitions for hydrated collagen: a large decrease in storage modulus between 50 to 60°C, corresponding to shrinking, and a small tan δ peak at around 40°C, which was reported to correspond to the breakdown of heat labile crosslinks, but this was not termed a T_g.

Sarti and Scandola studied the viscoelastic and thermal properties of polyvinyl alcohol (PVA)–collagen blends by DSC and DMTA[92]. Although this study mainly addressed the biocompatibility of these blends in terms of their T_g, it clearly demonstrated the existence of a T_g in collagen. During the DSC scan at high heating rates, they observed an endothermic baseline shift for hydrated collagen at around 40°C and assigned this peak to the glass transition of the disordered fraction of collagen molecules. They also reported that the low temperature dynamic mechanical spectra of collagen show a secondary relaxation centred at about -80°C and they associated this relaxation with the local motions of the collagen chain.

Odlyha and co-workers investigated the effect of natural ageing on the thermal properties of wet leather and parchment using DMTA[93-94]. They observed the presence of a tan δ peak at around 65°C for dry parchment. The same authors proposed a model of collagen as a "block copolymer" and suggested that these blocks are thermally activated at various temperatures. They were the first researchers to introduce the block copolymer theory to leather, when explaining its thermal behaviour.

Table 2.1 shows the reported glass-like transition temperature of collagen. Variations in values may be due to variation of amino acid sequences and stability of structure of the collagen sources.

Authors	Source of collagen	Method	Experimental temperature range (°C)	Transition temperature (°C) and descriptions	Year	Reference
Flory and Garrett	Partially shrunken beef achilles tendon	Dilatometric	40 to 120	Glass-like transition at 45°C for native collagen	1958	78
Rigby and co-workers	Collagen fibre (Rat tail tendon)	Stress relaxation	20 to 60	Glass-like transition approximately at 40°C (wet)	1959	79
Rigby and Mason	Kangaroo tail tendon	Specific volume change	20 to 60	Glass-like transition at 47.5°C for native tendon	1963	86
Bear and co-workers	Human diaphragm tendon	Mechanical relaxation	196 to 147	3 transitions which are sensitive to moisture; α, β & γ. At 10% moisture content; -93, -3 and 48°C.	1972	87
Nguyen, Vu & Wilkes	Digested bovine tendon	DMTA	-100 to 100	3 loss tangent peaks 1,2 and 3 at -60, 20 and 60°C respectively (15% moisture content)	1974	88
Batzer and Kreibich	Corium layer of calf skin	DSC	-73 to 227	Presented a range of T_g values, which highly depend on the moisture content; T_g of 35°C reported for 10% moisture content.	1981	89
Kronick and co-workers	Chrome tanned cattle hide	DMTA	-80 to 60	Clearly resolved tan δ maximum at 25°C(55% RH)	1985	90
Twombly, Cassel & Miller	Type I bovine collagen	DSC and DMTA	0 to 100	Breaking of thermally labile crosslinks 42°C (wet)	1994	91
Sarti and Scandola	Acid soluble calf skin collagen	DSC and DMTA	-80 to 180	T_g at 35°C (51% RH)	1995	92
Odlyha and co-workers	Parchment (calf skin)	DMTA	-130 to 220	Motion of side chain of poly-peptides at -25°C and main chain polypeptides at 65°C (ambient conditions)	2003& 1999	93-94

Table 2.1: Reported transition temperatures for collagen below its denaturation temperature.

2.2 Experimental procedure

2.2.1 Materials

A calfskin was processed to the pickled condition by a conventional process, after which two rectangular pieces were cut from the leather as indicated by 1 and 2 in Figure 2.2. One of the samples was washed and air-dried under tension (toggled) into parchment-type material. The other piece was acetone-dried to give a leather-like feel to the processed skin. The processes for these operations are given in Appendix 3.

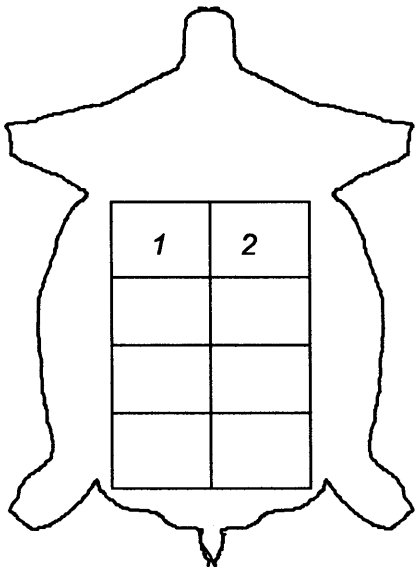

Figure 2.2: The position where samples were taken to make parchment-like (1) and leather-like (2) processed skin.

(a) Sample preparation

Prior to dynamic mechanical testing, samples were conditioned at controlled relative humidities of 0, 10, 35, 65, 80 and 98% for 48 hours achieved using saturated salt solutions (refer to Appendix 4) at 20°C. All the testing were performed on samples which were taken parallel to the backbone, unless otherwise specified.

2.2.2 Dynamic Mechanical Thermal Analysis

A dynamic mechanical thermal analyser, Mark II (Polymer Laboratories), was used in the dual-cantilever-bending mode, at frequencies of 1, 10 and 30 Hz and an amplitude of 64 μm. Thermal

transitions of the preconditioned samples were monitored by observing changes of storage modulus (E') and loss tangent (tan δ) with temperature. Each sample was inserted inside the DMTA head and clamped at room temperature. Then it was cooled to the predetermined starting temperature of -100°C and re-clamped to prevent slippage during the thermal scan. Transition temperature values reported are averages from three scans. Samples were weighed before and after the run and moisture content was determined by the official method (IUC 5^{95}).

2.2.3 Differential Scanning Calorimetry (DSC)

Calorimetry measurements were performed in a dry nitrogen atmosphere using a heat flux Mettler Toledo DSC 822^e differential scanning calorimeter. Approximately 60 mg of leather samples were weighed into medium pressure stainless steel pans, which were then heated at a rate of 20°C/min, with an empty pan as reference. The midpoint of the baseline shift was taken as the T_g.

2.2.4 Preparation of pepsinised soluble collagen

Bovine achilles tendon was cleaned, minced, and then washed three times with pH 7.5 phosphate buffer at 4°C. The minced tendons were suspended in 0.5M ethanoic acid at 4°C for 72 hours to extract soluble collagen. The insoluble residue was filtered and 50 g of this residue was re-suspended in 2500 ml of 0.5M ethanoic acid. 0.5 g of pepsin was added to the mixture and the temperature of the mixture was maintained at 4°C for 72h. Enzymatically solublised collagen solution was filtered out from the suspension and purified by repeated precipitation in 0.9M sodium chloride. The collagen precipitate was redissolved in 1.0M ethanoic acid and dialysed against 0.01M ethanoic acid. It was then freeze dried to obtain a foam, which was then compressed to get a uniform film of 1.0 mm thickness.

2.3 Results and discussions

Figure 2.3 shows tan δ and storage modulus, E′, as a function of temperature for a dehydrated air-dried skin sample (conditioned at 0% RH). The tan δ trace indicates three transition peaks within the studied temperature range of -100 to 260°C. These peaks have been assigned as α, β and γ, using the current system of labelling. This system of peak assignment can cause confusion because, here for example, the highest temperature peak, α, is not necessarily the glass transition, whereas, in polymer science the α peak is generally associated with the main chain glass transition.

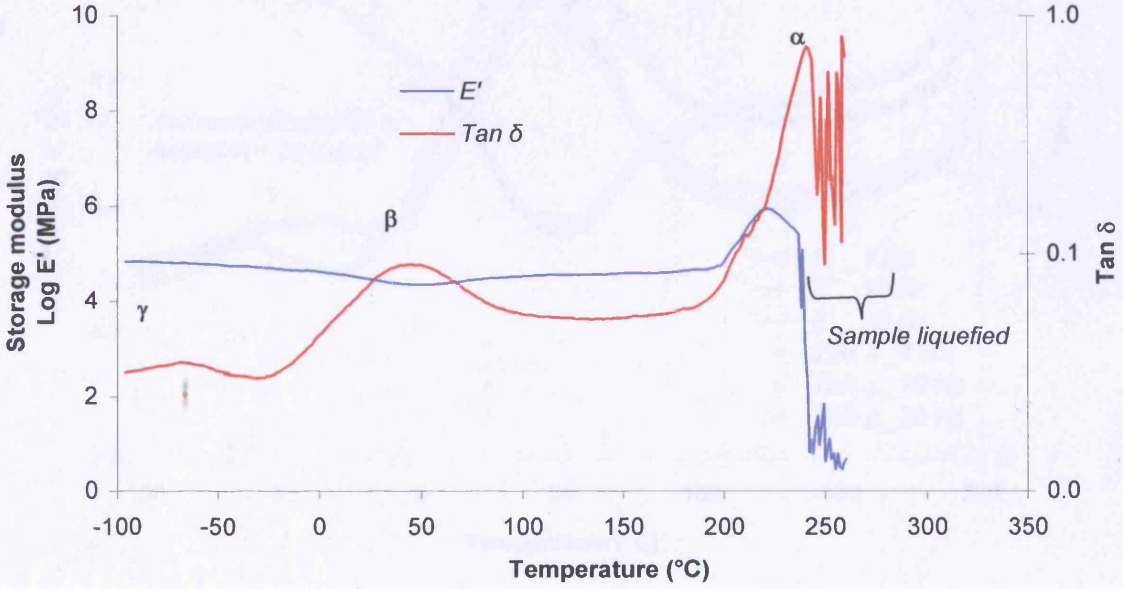

Figure 2.3: A typical DMTA thermogram of an air-dried skin sample preconditioned at 0% RH (moisture content was calculated to be 3.6% on a dry weight basis).

The interpretation of such results may not always be straightforward, particularly when studying a complicated system such as collagen. It is not always obvious whether the transition under observation is a main chain glass transition, a side chain transition or a thermal event associated with the crystalline regions of the sample. Therefore, a process of elimination and a consideration of past evidence from literature will be used to identify these peaks systematically.

When heated from -100°C, the sample initially shows a progressive decrease in E′ followed by a relatively steep decrease in E′ from 10 to 50°C, where the β transition was observed. This is then followed by an increase in modulus, resulting from the sample stiffening due to water loss. Finally,

at the onset of a liquefaction related transition at ~200°C, a large rapid decrease in modulus is observed due to the sample softening. The main peak, α, is assigned to the transition associated with liquefaction of the fibrils. This peak assignment is made for two reasons; (1) the visual observation of the sample having liquefied and (2) the inconsistency of data points at temperatures above the tan δ peak temperature.

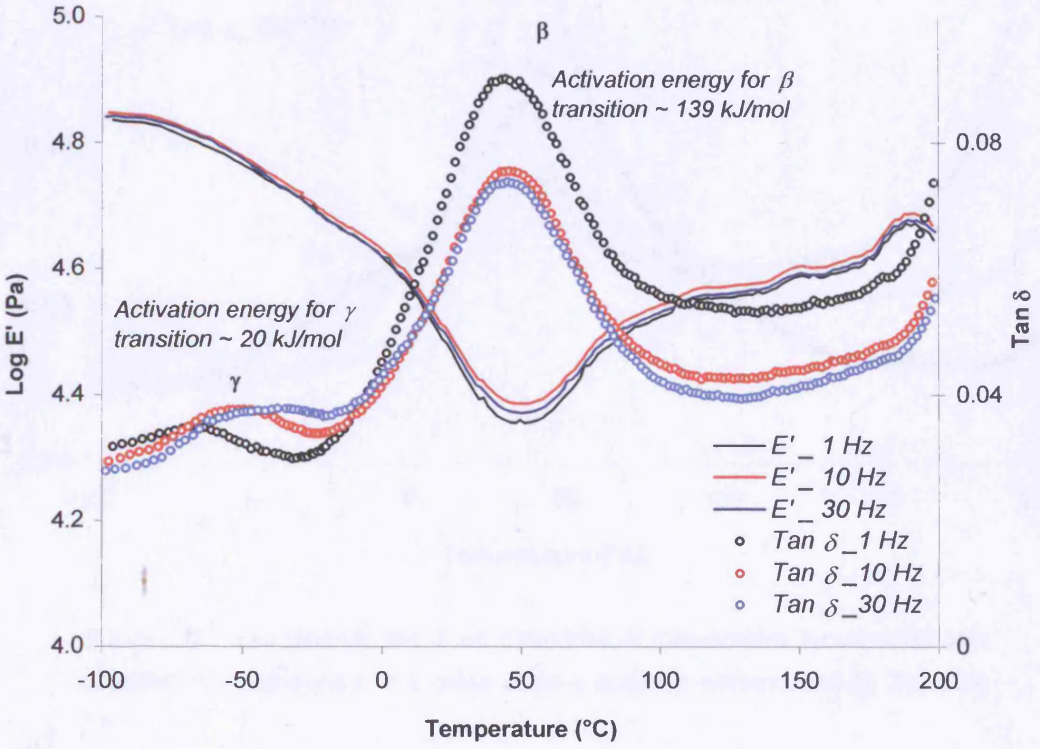

Figure 2.4: Storage modulus, E', and loss tangent, tan δ, as a function of temperature for three frequencies, 1, 10 and 30 Hz, of air-dried skin preconditioned at 0% RH (4.6% moisture content on dry weight basis).

The peak below room temperature, γ, is highly sensitive to the frequency of the oscillating applied stress (Figure 2.4) as well as the moisture content of the sample (Figure 2.5). The peak which is located at -67°C (1 Hz) for the dehydrated samples shifts towards higher temperatures as the hydration level increases and appears as a shoulder on the β transition peak (Figure 2.5). The magnitude of the peak also increases with moisture content. The fact that this peak appears at low temperature suggests that it may be due to a more localised side chain movement, rather than any motion of the main backbone chains. If this relaxation is the main glass transition, then it would be expected to move towards a lower temperature as the water content increased. Since this was not observed, the γ transition appears to be due to a molecular motion associated with

side chains, supported by an activation energy of 20 kJ/mol (refer to page 37). The sensitivity of this transition to moisture content suggests that these side chains are hydrophilic in nature

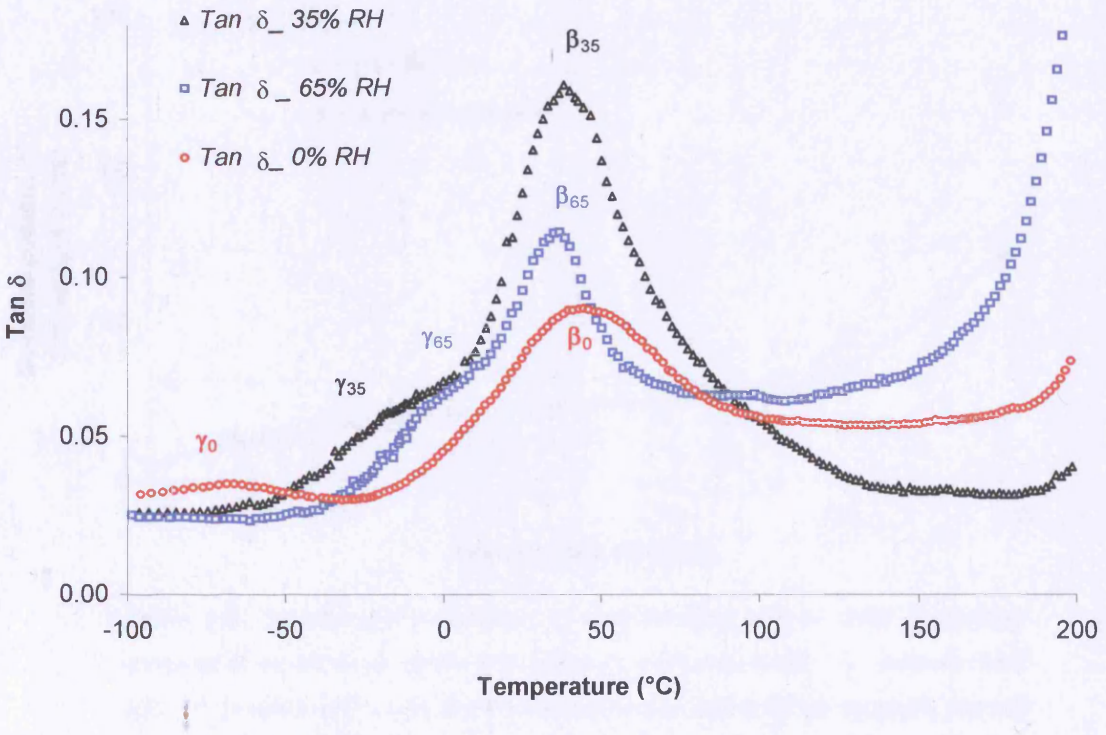

Figure 2.5: Loss tangent, tan δ, as a function of temperature for air-dried skin samples pre-conditioned in a given relative humidity environment (0, 35, 65% RH).

The moisture absorption isotherms for air-dried skin and acetone-dried skin are given in Figure 2.6. They indicate that, if the samples were conditioned below 65% RH, then the amount of absorbed water is less than 0.25 g/g on dry weight basis. Bienkiewicz stated that, in the range 0.07 to 0.25 g/g, of water absorbed onto the collagen forms two hydrogen bonds[63]. Thus all the water which is present in the samples conditioned below 65% RH is linked to collagen with two hydrogen bonds. Moreover, as illustrated in Figure 2.7, when such water molecules bind to hydrophilic side chains, the free rotation of the side chains is inhibited by the formation of hydrogen bonds with the water. If this assumption holds, then any absorbed structural water molecules will increase the temperature at which the side chain transition takes place.

The β transition appears not to be as sensitive as the γ transition to frequency (Figure 2.4) or moisture content (Figure 2.5). During this transition, the storage modulus decreases towards a minimum point, at 40°C (for samples preconditioned at 0% RH), where the maximum tan δ value

is observed. This is the classical type of behaviour associated with main T_g of polymers. Therefore, the β transition is assigned to a transition of the collagen backbone.

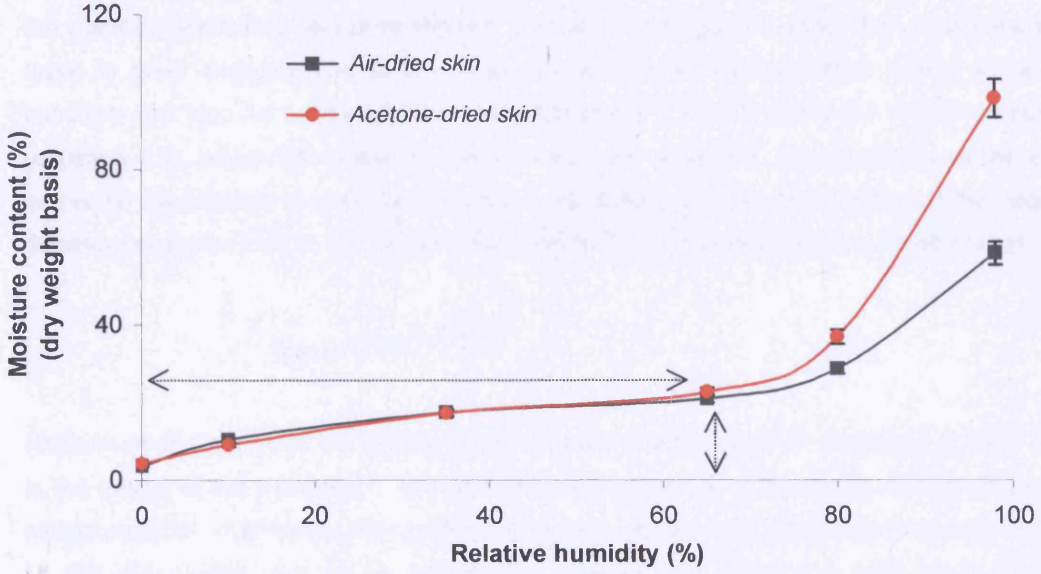

Figure 2.6: The absorption isotherms of acetone-dried and air dried skin (water contents of samples conditioned at different relative humidity), — acetone-dried skin, + air-dried dried skin. Double headed arrow indicates the moisture content of the samples that were conditioned at 65% RH.

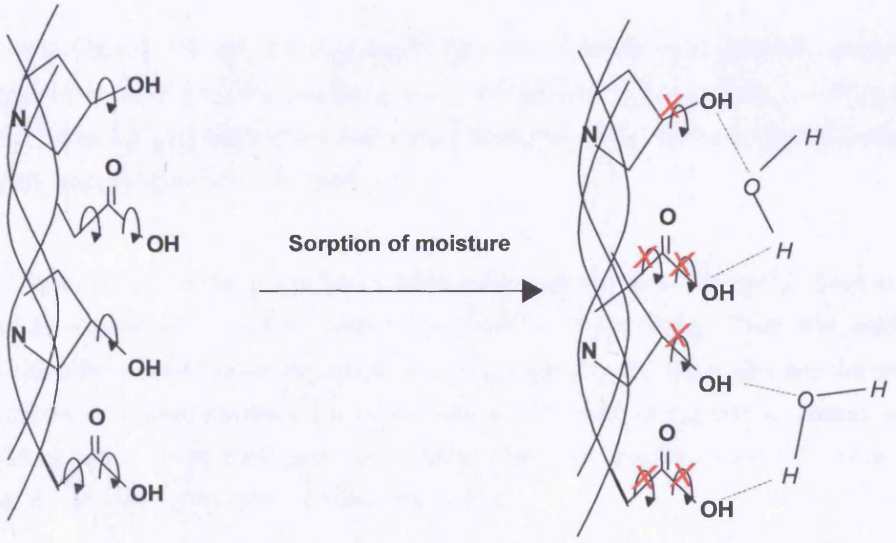

Figure 2.7: Schematic illustration of how the free rotation of hydrophilic side chain amino acids could be prevented when moisture is absorbed into the inter-fibril region.

A frequency scan during DMTA is often performed on polymeric materials for several reasons. Usually, the frequency at which the temperature scan is run will affect the temperature of a transition. The general trend is that higher order transitions like T_g move to lower temperatures as the frequency decreases. Figure 2.4 shows a temperature scan at different frequencies across the γ and β transition temperature regions. It is clear from Figure 2.4 that the γ and β transitions move to lower temperatures as the frequency decreases. The activation energy for a given transition can also be estimated from these frequency scans by using the Arrhenius equation (equation 2.1), where ΔE is the activation energy for relaxation, corresponding to the energy barrier for the polymer to undergo a transition. By plotting the natural logarithm of the frequency dependence against 1/T in °K, the activation energy for a given transition can be estimated.

$$\nu_{peak} = A\, e^{(-\Delta E/RT)} \qquad (2.1)$$

McCrum *et al.* stated that the degree of dependency of a transition on frequency is often related to the nature of the transition[13]. The activation energy for the β transition of air-dried skin was estimated to be ~139 kJ/mol. For synthetic polymers, Menard has stated that activation energies of 300-400 kJ/mol and 20-30 kJ/mol are expected for glass and side chain transitions respectively[12]. Clearly, the activation energy estimated for the β transition of air-dried skin falls neither within the range of activation energies for a glass transition nor within the side chain transition energy range reported by Menard. It is therefore not possible to identify the nature of the β transition from the activation energy data alone.

It is clear from Figures 2.5 and 2.8 that the β transition is sensitive to moisture content. The results suggest that the β transition moves to lower temperature with increasing moisture content (also refer to Table 2.2), although this is not always absolutely clear, because peak broadening is observed with increasing moisture content.

Breaking of secondary bonding in a polymer (electrostatic/van der waals forces) by heat or by the introduction of a plasticiser enables large-scale motions of the chain. Thus, the addition of moisture to air-dried skin reduces the cohesive energy between the molecules and hence the β transition moves to a lower temperature. As the moisture content of the skin increases above a critical moisture value, water molecules will be free to form ice crystals below 0°C. Thus for the wet sample, an ice melting transition is observed at 0°C.

As indicated by Figure 2.8, when the moisture content exceeds a limiting value, another distinct peak, β^*, appears at around 45°C. The β^* transition may be related either to a pre-shrinkage phenomenon, such as a helix-coil transition or to the partitioning of the β transition (this may be

due to the preferential hydration of the hydrophilic amino acid residues). Figure 2.9 shows that the β* transition progressively moves to a lower temperature as the moisture content increases and indicates that this transition must be closely associated with shrinking. However, the measured shrinkage temperature of hydrated collagen (59 ± 2°C), is higher than that of the β* transition. Since, DMTA measures the molecular mobility of materials, the β* transition may be viewed as a softening of the collagen. These results clearly demonstrate that, even before actual shrinking, the molecules are becoming flexible.

Leather also undergoes a shrinking transition in the presence of water. It is well known that the shrinkage transition of leather progressively moves to lower temperatures, until a limiting value, as the moisture content of the sample increases. The β* transition is therefore attributed to a shrinking related transition of the hydrated collagen, as it follows the expected trend. The phase transition of ice and the shrinking related transition, β*, contribute to the masking and broadening of the β transition peak.

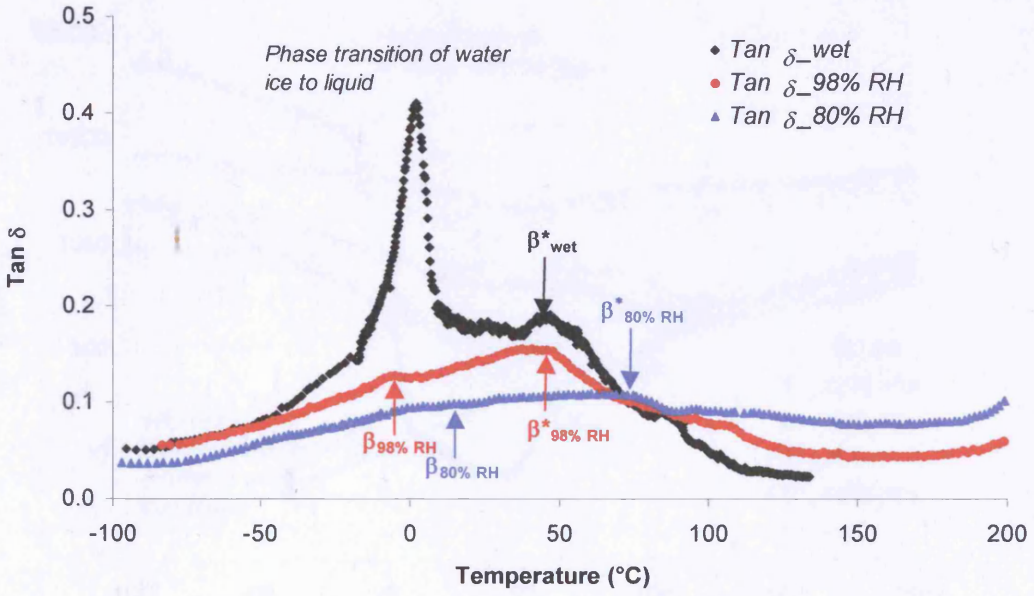

Figure 2.8: Loss tangent, tan δ, as a function of temperature for air dried skin samples preconditioned at 80% and 98% RH and for hydrated skin containing 160% moisture on a dry weight basis.

Figure 2.9 presents the storage modulus data, as a function of temperature, for samples initially conditioned to specific moisture contents. At higher moisture contents, the storage modulus curve shows two distinct inflection points, indicative of two different softening transitions. The inflection points, labelled as 1 and 2 in Figure 2.9, indicate the β transition and β* transition respectively.

Relative humidity (%)	β transition temperature (°C)	β* transition temperature (°C)
0	42 ± 2	
35	38 ± 3	
65	37 ± 2	
80	0.6 ± 1	77 ± 2
98	-5 ± 1	48 ± 5
wet	obscured by the phase transition of water	46 ± 2

Table 2.2: β and β transition temperatures obtained from DMTA scans of air-dried skin samples preconditioned to a given humidity.*

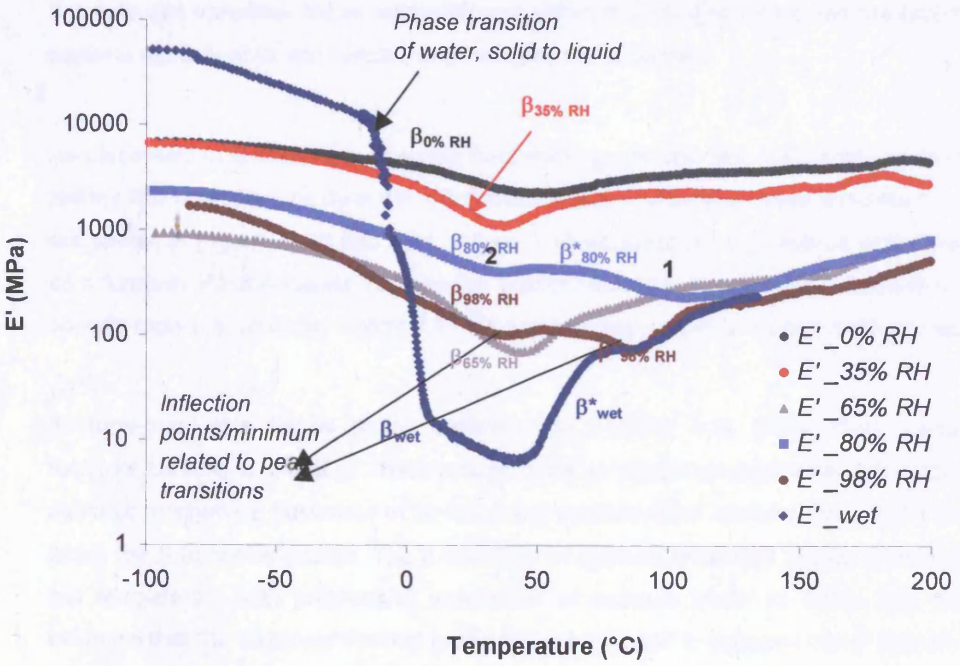

Figure 2.9: Storage modulus, E', as a function of temperature for air-dried skin samples preconditioned to a given humidity.

It is clear that DMTA detects the molecular motions associated with the shrinking event before actual shrinking occurs. Several researchers have reported that the helix-coil transition of collagen in solution to be 10 to 15°C below the shrinkage temperature[86,78-79]. However, the

collagen fibres do not normally exhibit a helix-coil transition. In dilute solution, during the helix-coil transition, the collagen molecules must undergo some type of relaxation or molecular motion. Since it is a transition associated with collagen molecules, a similar type of transition is expected in the solid state. However, so far there is no published evidence suggesting the presence of a helix-coil transition in fibres.

The helix to random coil transition can occur in single, double or triple stranded protein and the transition is reported to go from diffuse, to second order, to first order with the increase of strands from 1 to 3[39]. Hence, for triple stranded collagen, this transition is expected to be first order in solution. When molecules undergo a helix-coil transition, the energy released or absorbed by the system is the difference in the potential energy of the two states. The helical portions have a high conformational enthalpy, stabilising the helical structure(s), while the random portions have configurational entropy stabilising the random coil. When collagen molecules are arranged as fibres, total collapse from helix-coil to random coil will be restricted by the external crosslinks. Therefore, a first order helix-coil transition for a collagen fibre is not normally observed, whereas molecular relaxation is observed in the DMTA trace. Therefore, the β^* transition may be related to this helix-coil transition. When internal forces within the collagen molecules are broken, molecules become more flexible and hence the β^* transition is observed.

As discussed in Section 2.1, to avoid fibre sticking, pickled skin was acetone-dried to obtain a leather-like character. Its dynamic mechanical thermal properties were examined and the results are shown in Figures 2.10 and 2.11. Figure 2.10 presents tan δ (obtained at the frequency 1Hz) as a function of temperature, for samples initially conditioned at various relative humidities to give specific moisture contents. Figure 2.11 shows the corresponding storage modulus data.

Acetone-dried skin shows similar behaviour to air-dried skin, giving three transitions at low moisture content (α, β and γ). There is apparently no significant qualitative difference between the dynamic mechanical behaviour of air-dried and acetone-dried samples, except the temperature at which the β transition occurs. The β transition of acetone-dried skin shows a pronounced shift to low temperature with progressive absorption of moisture (refer to Table 2.3). This is further evidence that the observed thermal properties are inherent to collagen rather than an artefact due to fibre rubbing. Storage modulus data (Figure 2.11) also indicates that more than one softening transition occurs at high moisture contents.

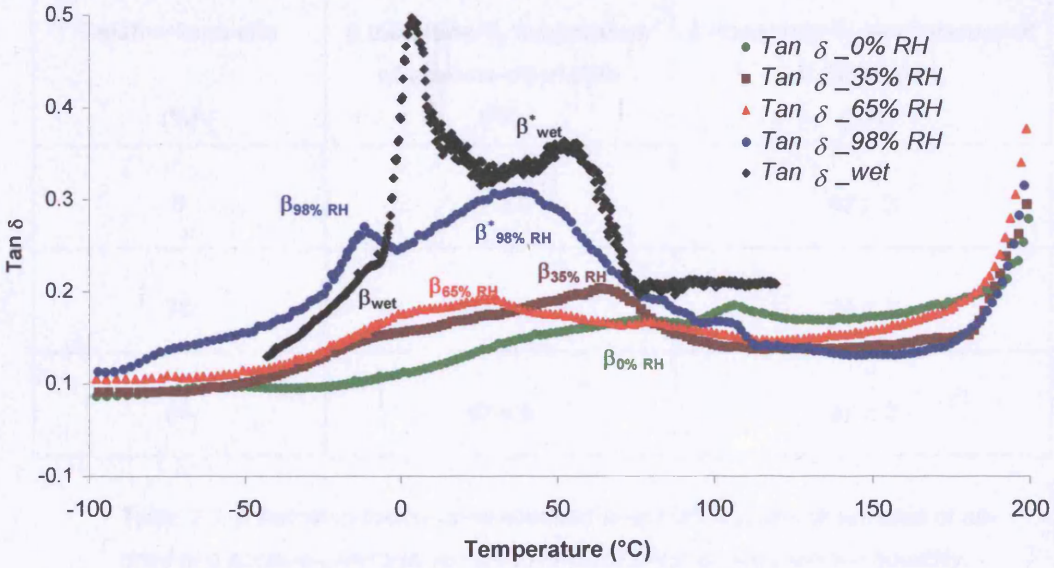

Figure 2.10: Tan δ as a function of temperature for acetone-dried skin samples preconditioned at given relative humidity.

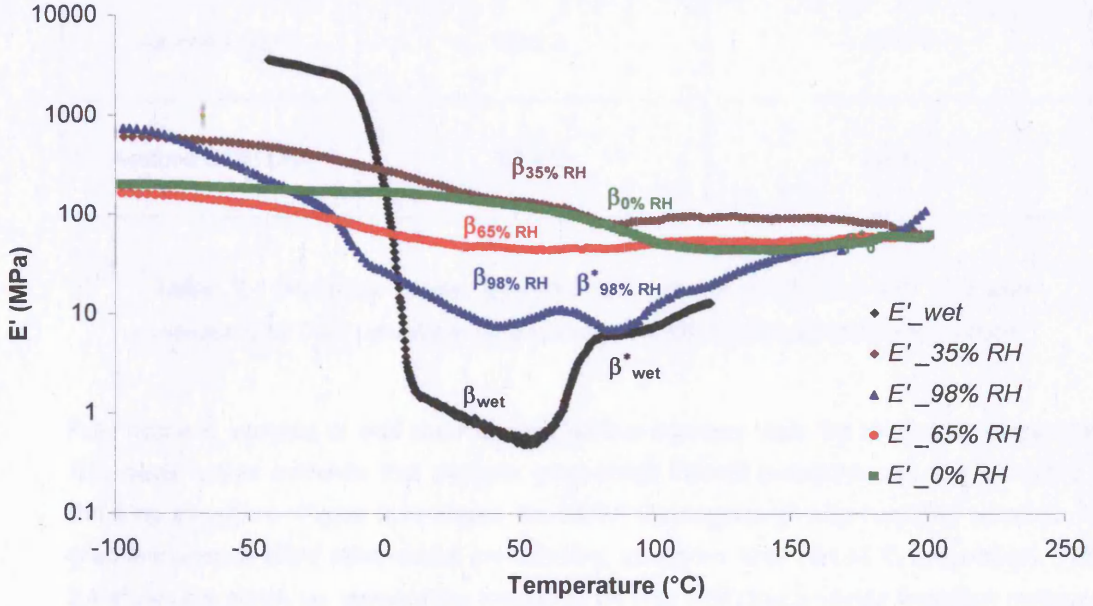

Figure 2.11: Storage modulus, E' as a function of temperature for acetone-dried skin samples preconditioned at given relative humidity.

Relative humidity (%)	β transition/T_g temperature of acetone-dried skin (°C)	β transition/ T_g temperature of air-dried skin (°C)
0	77 ± 2	42 ± 2
35	64 ± 4	38 ± 3
65	57 ± 3	37 ± 2

Table 2.3: β transition temperature obtained from DMTA scans of samples of air-dried and acetone-dried skin samples preconditioned at given relative humidity.

Sample	Shrinkage temperature (onset, DSC) (°C)	Pre- shrinkage transition (loss tangent peak, DMTA) (°C)
Air-dried skin	59 ± 2	47 ± 1
Acetone-dried skin	67 ± 2	54 ± 4

Table: 2.4 Shrinkage related transition temperature of air-dried skin and skin measured by DSC (shrinkage temperature) and DMTA (pre-shrinkage transition).

Fully hydrated samples of skin show another distinct transition near the shrinkage temperature. This gives further evidence that dynamic mechanical thermal properties are also sensitive to shrinking transitions. Figure 2.12 shows the DMTA thermogram of fully hydrated samples. Air-dried and acetone-dried skins exhibit pre-shrinking transitions at 47 and 52°C respectively. Table 2.4 shows the shrinkage temperature measured by DSC and pre-shrinkage transition measured by DMTA. Shrinkage temperature measured by DSC is 10 to 15°C higher than the pre-shrinking transition.

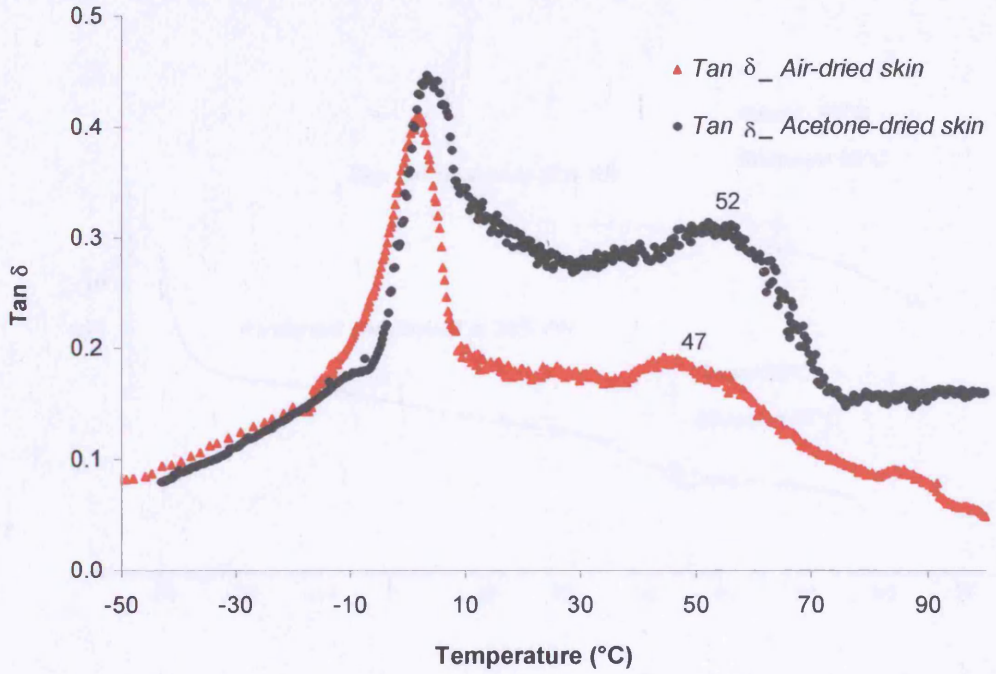

Figure 2.12: DMTA traces of fully hydrated air-dried and acetone-dried skin samples, showing pre-shrinking β transitions at 47°C and 52°C respectively.*

The DMTA in bending mode is sensitive to detecting molecular motion and in this case it appears to be detecting a pre-shrinking transition (possibly a helix-coil transition) of collagen. The detection of a shrinkage temperature in collagen and leather by DMTA used in a tensile mode has been reported[93,96]. If the sample is in the tensile mode, gross macroscopic shrinkage can also be detected, whereas in the bending mode it was not possible to detect tension related changes. Thus, the shrinkage temperature of the sample was not detected.

In order to clarify the origin of the β transition, DSC experiments were performed at a heating rate of 20°C/min. This relatively high heating rate was used because, when heated at a slower rate, the second order transition tends to be broader and undetectable. Figure 2.13 shows typical DSC traces for skin. It is clear that a thermal event associated with a change in heat capacity is detectable at the temperature where a β transition was observed by DMTA. This supports the DMTA evidence that the β transition is in fact a second order transition of collagen.

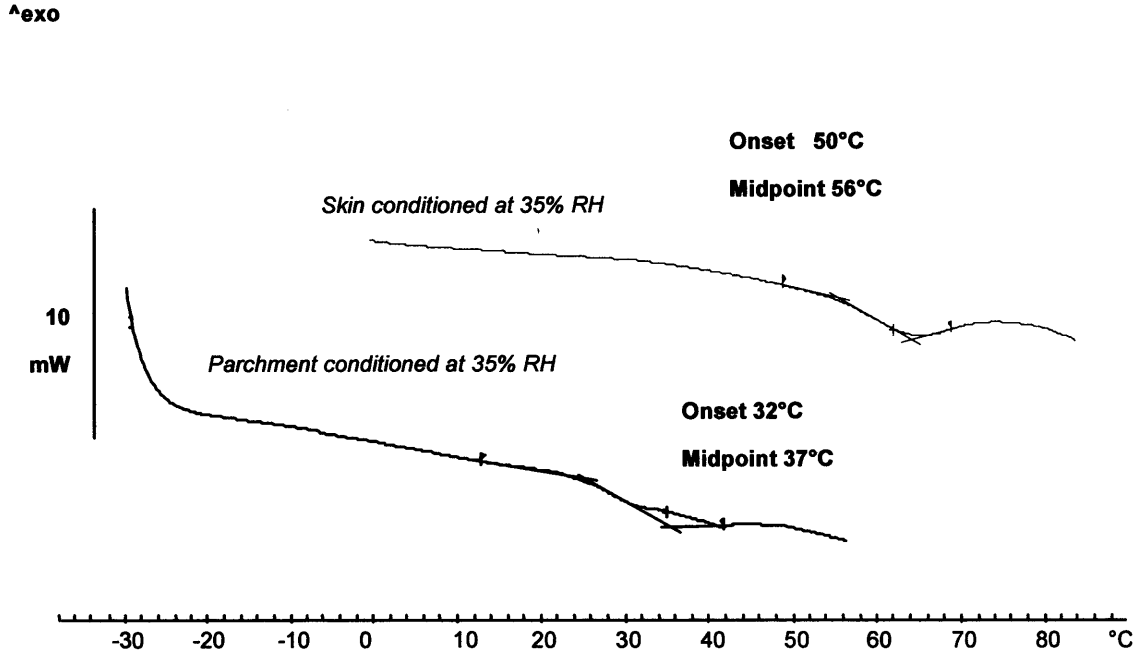

Figure 2.13: DSC thermograms of air-dried and acetone-dried skins conditioned at 35% RH heated at 20°C/min, showing the glass transition temperature.

Figures 2.14 and 2.15 show the relationship between the β transition temperature/T_g and moisture content. It is clear that the T_g decreases with increasing moisture content. This is due to the plasticising effect of water on the hydrophilic substrate (collagen). It appears that no further plasticisation occurs after a limiting moisture level (~ 30%) has been reached.

The plasticing effect may also be related to the swelling of fibres, i.e., the amount of water within the intra-fibril spaces. Several researchers have pointed out that the equatorial spacing on the X-ray diffraction pattern increases with the absorption of moisture until a characteristic limiting value is reached[68-70]. They also stated that this value depends on the origin of the collagen. It is therefore reasonable to assume that the collagen molecules are forced apart laterally with the accretion of water. When the water content exceeds a limit, there is no further expansion. This indicates that further addition of water no longer affects the molecular motion of collagen and hence the β/glass transition maintains a constant value (Figures 2.14 and 2.15).

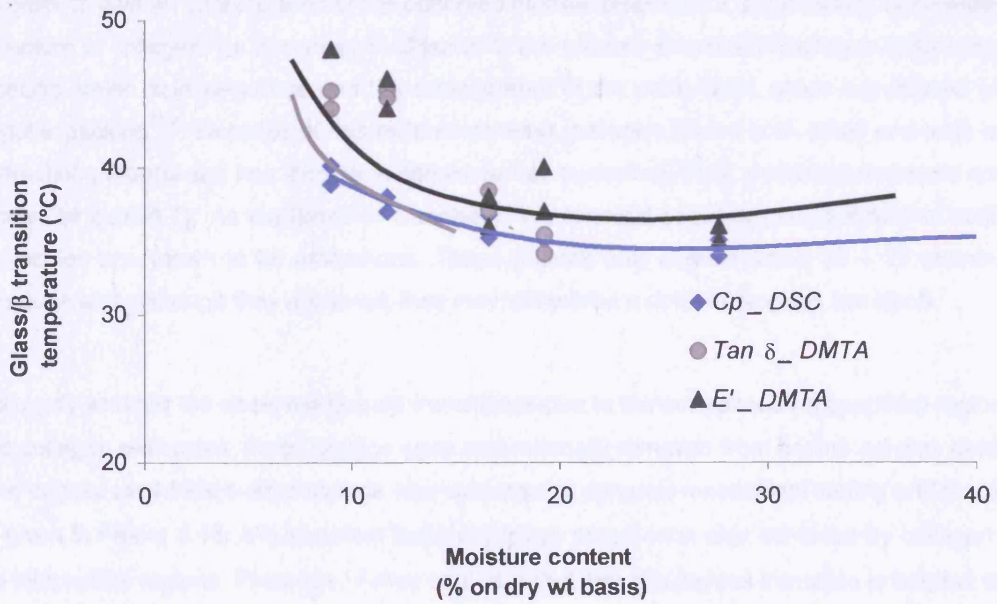

Figure 2.14: The glass/β transition temperatures of air-dried skin detected by various methods, (υ) mid-point of C_p changes by DSC, (▲) maximum loss tangent by DMTA, (●) minimum point of bend modulus.

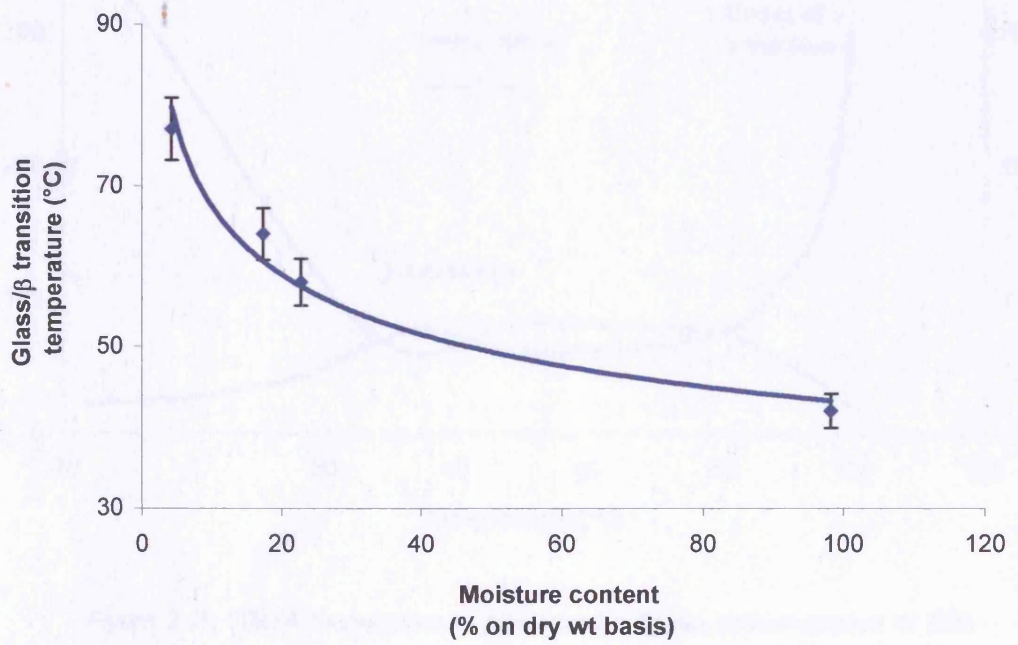

Figure 2.15: The β/glass transition temperatures of acetone-dried skin detected by DMTA.

In order to give an interpretation of the observed thermal properties it is necessary to consider the structure of collagen. As described in Chapter 1, the ordered structure of collagen arises from its specific amino acid sequence and the arrangement of the proto-fibrils which are aligned with a regular packing[5,69]. Because of this ordered packing, collagen shows both small and wide-angle diffraction patterns and has long been considered as crystalline. Fully crystalline materials are not known to exhibit T_g. As explained in Chapter 1, the terminal sections (telopeptides) of collagen molecules are known to be amorphous. These regions only contain about 10 – 20 amino acid residues and, although they are small, they may still exhibit a detectable glass transition.

To clarify whether the observed glass/β transition is due to the amorphous (telopeptide) regions of the collagen molecules, those regions were enzymatically removed from bovine achilles tendons. The compressed freeze-dried sample was subjected to dynamic mechanical testing and the result is given in Figure 2.16. It is apparent that the β/glass transition is also exhibited by collagen with no telopeptide regions. Therefore, it may be concluded that this β/glass transition is not due to the telopeptide regions, but rather to the behaviour of the structured regions of the collagen molecules.

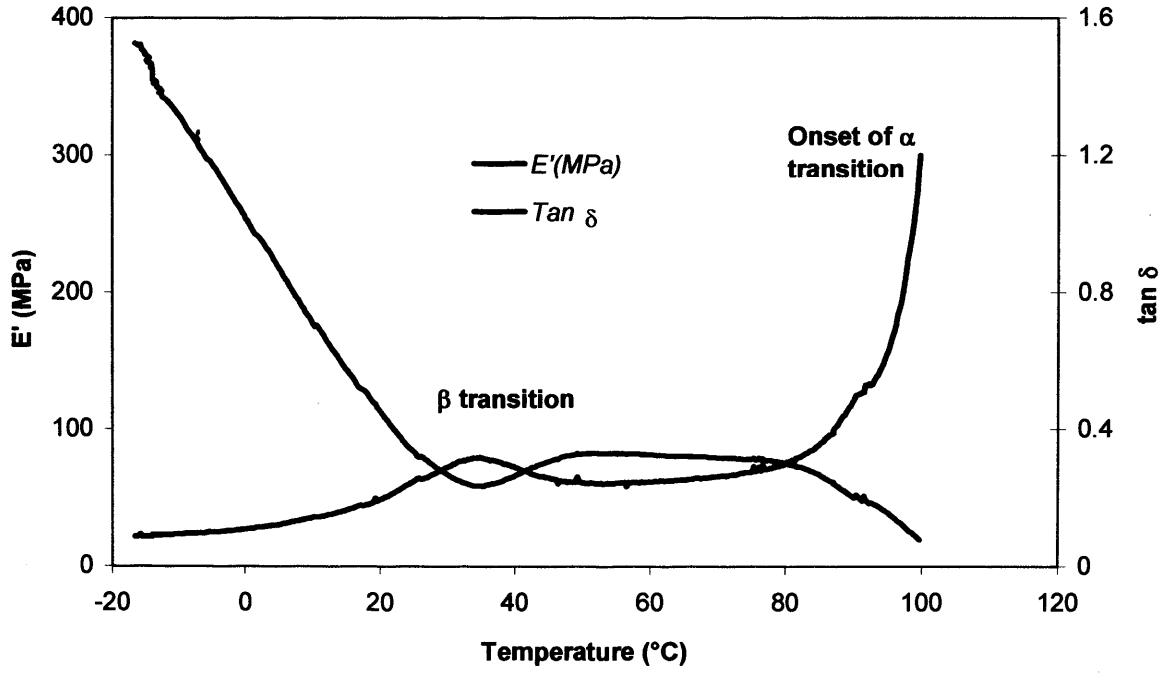

Figure 2.16: DMTA thermogram of pepsinised collagen, preconditioned at 65% RH, showing β transition and onset of α transition.

Pepsinised collagen is known to be mechanically weaker than native collagen because of the absence of telopeptide regions[98]. During the biosynthesis of collagen, after the fibrillogenesis step, the enzyme lysyl oxidase facilitates covalent crosslinking between the collagen molecules at the telopeptide ends. Without these crosslinks, the mechanical strength of fibres is lower. The onset of the α transition for pepsinised collagen is approximately 80°C. This is lower than the value obtained for air-dried skin or acetone-dried skin (approximately 145 and 150°C respectively for samples conditioned at 65% RH). Therefore, it is clear that the thermal stability of collagen is also decreased by the removal of the telopeptide regions.

It is accepted that the primary structure of collagen is that of a block copolymer, composed of sequences of so called "soft blocks" and "hard blocks" (refer to Section 1.2.4). If two pyrrolidine rings are in sequence, this determines the position of nine bonds of the backbone, which comprise one complete turn of the polyproline helix. These imino acids together constitute almost one-fourth of the residues. This implies that rotation around the collagen backbone would be restricted in some parts of the molecules. If two α-amino acids are present in sequence, then this section of the molecule is flexible. Above a characteristic temperature, because of an increase in free volume, a partial relaxation of the backbone can take place. The observed T_g in collagen is attributed to this relaxation. When imino groups begin to rotate freely due to applied thermal energy, the total collapse of the structure is expected and hence the α-transition is attributed to a relaxation in the rigid block of the collagen molecules. Further evidence for the heterogeneity of the collagen molecule comes from the thermal behaviour of gelatin, the amorphous state of collagen, which exhibits two glass transitions[58].

The suggestion of the presence of a glass transition in collagen is problematic, if collagen is considered to be a highly ordered crystalline material. The X-ray diffraction patterns observed for collagen are due to the molecular packing of the proto-fibrils, whereas the subtle molecular changes detected by DMTA are within the individual molecules, where the presence of less structured regions is possible. A recent publication on the molecular packing of collagen fibrils by Wess and co-workers indicates that collagen proto-fibrils contain regions of three-dimensional order (crystallinity), as well as regions of disorder[6]. This is further evidence that there are less ordered regions present in collagen proto-fibrils, which can take part in relaxation processes and it is not unreasonable to call this relaxation process a glass transition.

2.4 Summary

It has been shown that DMTA is sensitive in detecting the thermal transitions of collagenous material. There is compelling evidence that collagenous materials show viscoelastic transitions below their shrinkage temperature. It was also established that these are higher order transitions, as they have dependency on the frequency of the applied stress. These thermal transitions are also sensitive to moisture content.

It is useful to consider the collagen molecule as a semi-crystalline biopolymer with ordered regions (crystalline) as well as less ordered (amorphous) regions, thus it exhibits characteristic thermal transitions associated with crystalline polymers and amorphous polymers. The β transition is assigned to the glass transition of the "amorphous/less ordered" portion of the collagen molecular structure. DMTA is also sensitive in detecting the pre-shrinkage transition and β^* is assigned to the pre-shrinkage transition, which might be associated with the helix-coil transition temperature.

Chapter 3

EFFECT OF TANNINS ON THE VISCOELASTIC TRANSITIONS OF COLLAGEN

3.1 Introduction

Collagen is one of the most resilient natural polymers known to man. It is converted into leather through the tanning process in order to increase its resistance to microbial attack. As a result of its biocompatibility, collagen is also used extensively in medical applications. When collagen is turned into leather or biomaterials, its physical, chemical and thermal properties are modified considerably. Conventionally, hydrothermal stability or T_s measurement is used as an indicator to monitor the effectiveness of the process. While hydrothermal stability gives information regarding the stability of the collagen based material to wet heat, it does not reveal any useful information regarding other aspects of the material's performance. For example, the T_s of leather gives no indication of its combustion temperature[99] or its rheological properties. On the other hand, the viscoelastic transition temperatures, in particularly the T_g, can predict a material's performance at a given temperature[2].

In Chapter 2, a detailed account of the viscoelastic transitions of fibrous collagen is given. This Chapter is therefore a continuation of that account, in which the effects of some commonly used tannages on the β/glass transition are examined. A discussion of the relationship between T_s and both α and β transition temperatures will also be presented.

3.1.1 Tanning process

The processing of animal skins into fur or leather is one of the oldest technologies known to humankind. In the first known records on the subject of tanning, the Babylonians recommended the use of flour, wine and beer as well as nut-gall, alum and bull fat, then to aromatise with plant extracts[100]. Until the start of the twentieth century, tanning was a craft-based industry with guarded secrets passed down from generation to generation. The senses, smell, feel, colour, taste, touch, and experience controlled the various processes used in tanning. The process times

were long, taking months to complete the operations. In a tannery today, all the benefits of modern science are used to complete the tanning within hours/days.

The manufacturing process for leather is a combination of many mechanical and chemical operations that can be divided into three broad areas, namely, pre-tanning, tanning and post-tanning operations. Salt cured animal skins are often the starting materials for the modern leather industry. During the initial beamhouse processing, the epidermis, subcutaneous fat, hair, globular proteins, cementing materials (dermatan sulphate, and hyaluronic acid) are removed chemically, leaving the network structures of fibrous collagen and elastin intact. The liming process, which ensures the "opening up" of fibres (i.e separating fibres and fibrils), is considered to be one of the most important processes. The opening up of the structures is important for the penetration of chemicals in the later stages of leather processing. The hydrolysis of asparagine and glutamine into aspartic and glutamic acid is also known to occur in the liming process[101].

In the tanning process, collagen is treated with so called "tanning agents" in order to confer the ability to resist biochemical attack. The most common tanning agents are chromium(III) salts and plant polyphenols. However other tanning agents such as aluminium(III), syntans, aldehyde, zirconium(IV) and titanium(III/IV) are also used. Table 1.3 gives a summary of the common types of tanning agents and the shrinkage temperatures of the leather such tanning agents produce.

Tanning agents	Plant polyphenols	Chrome(III)	Zirconium(IV) Titanium(III/IV)	Aluminium(III)	Aldehyde	Syntan
T_s (°C)	75-85	>100	85	80	85-90	80

Table 3.1: Tanning materials and the thermal properties of leather produced[102-109].

(a) Mineral tannages

Mineral tannage can be achieved with salts of Al(III), Ti(III/IV), Cr(III), Fe(III) and Zr(IV). It is arguable whether other metal compounds used in histological staining, such as osmium, tungsten and molybdenum, show any tanning ability. However, uranyl salt shows some tanning action[105]. Chromium(III) and aluminium(III) salts are the most commonly used mineral tanning agents.

Chromium(III) tanning

90% of all leathers produced today contain chromium(III)[106]. The chrome tanning reaction has always been thought of as unique, because of its ability to produce a leather with high hydrothermal stability. Unfortunately, the effects of Cr(III) on the environment are widely misunderstood and the future of chrome tanning in some countries is under threat. In fact, Cr(III) has very low toxicity, unless it is oxidised to Cr(VI)[117].

Aluminium(III) tanning

Sulfate of aluminium or alum is always used for leather making (or tawing) in conjunction with common salt[105]. Although, it may be viewed that aluminium(III) forms complexes with carboxyl compounds, their formation is based in ion pair interaction[110]. It is a poor tanning agent because of its easily hydrolysable carboxyl-aluminium bond[105]. Fixation of aluminium to collagen is pH dependent and maximum shrinkage temperature of 80-85°C can be achieved with aluminium salts as a sole tanning agent[111]. Introduction of carboxyl groups into collagen is reported to facilitate aluminium uptake[112].

(b) Vegetable Tannins

Natural polyphenols that have the ability to turn hides and skins into leathers are termed vegetable tannins. These are widely distributed in plants as protective substances against harmful external influences and hence are generally referred to as secondary metabolites[113]. These complex polyphenolics are extracted from ground-up plant materials by steeping in hot water. Until the beginning of this century, there was a wide range of vegetable tannins used by tanners throughout the world. Nowadays only a few vegetable tannins are in regular use. Examples are; mimosa, myrabolans, valonia, sumac, quebracho, oak, tara and chestnut. Plant polyphenols are broadly divisible into two major groups; they are:

1. Proanthocyanidins, so called catechol or condensed tannins.
2. Polyesters based on gallic / hexahydroxydiphenic acids, so called pyrogallol or hydrolysable tannins.

Condensed tannins (proanthocyanidins)

Plant proanthocyanidins are based on a polyflavan-3-ol structure[113-116] (Figure 3.1). The proanthocyanidins are reported[113] to be formed as byproducts of the processes by which the parent flavan-3-ols are biosynthesised in the plant tissue.

Procyanidins are the most abundant group of proanthocyanidins in plants[113]. Fruit bearing plants have proven to be particularly rich sources of oligomeric procyanidins They occur free, unglycosylated and almost invariably with one or both of the flaven-3-ols, (+) - catechin (Figure

3.2 (b)) or (-) - epicatechin (Figure 3.2 (a)). Condensed tannins do not generally undergo hydrolysis but they are liable to oxidation and polymerisation to form insoluble products[113]. Gambier, mimosa and quebracho are well known condensed tannins widely in use today.

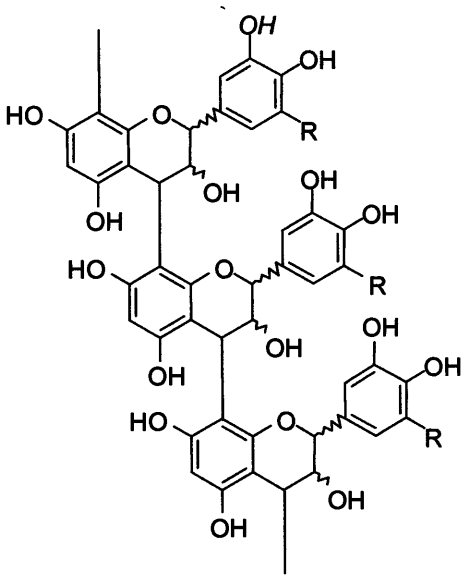

Figure 3.1: Molecular structures of condensed tannins[113] (R=H procyanidins; R=OH prodelphinidins).

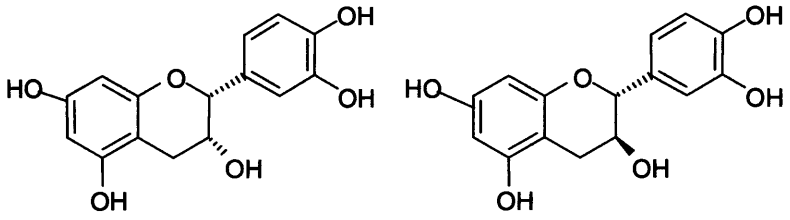

Figure 3.2: Monomers of condensed polyphenols[113].
(a): (-) - epicatechin,(b): (+) - catechin.

Hydrolysable tannins

Hydrolysable tannins are esters of hydroxybenzoic acids. Depending on the nature of the phenolic carboxylic acid, the hydrolysable tannins are usually subdivided into gallotannins and ellagitannins This group of tannins undergoes rapid hydrolysis at raised temperature above 60°C[113-115]. Hydrolysis of gallotannins yields gallic acid while that of ellagitannins yields hexahydroxydiphenic acid, which is isolated normally as ellagic acid. Gallotannins used for

tanning are oak galls, sumac, tara and chinese gallotanninn. Ellagitannins are widespread in nature, e.g chestnut, valonia, oak, myrabolam and divi divi. An example of the structure of hydrolysable tannins is given in Figure 3.3.

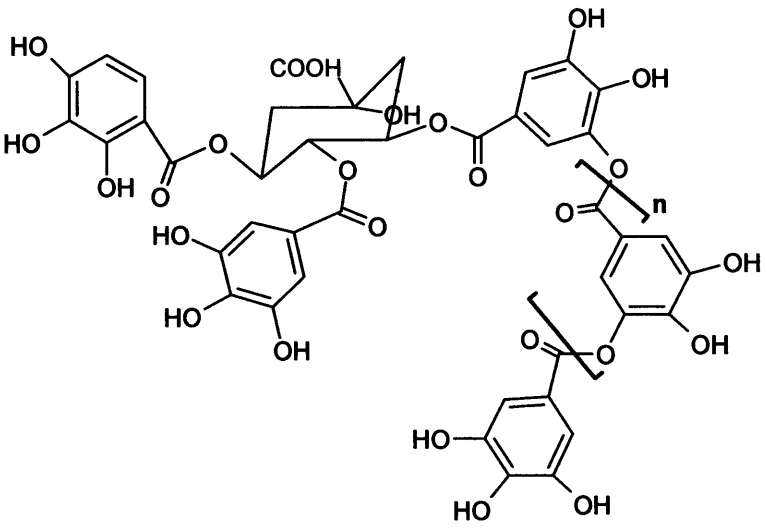

Figure 3.3: Galloylated quinic acid structure of Caesalpinia spinosa (tara; an extract from fruit pods)[116].

(c) Semi-metal tannages

The combination of metals and vegetable tannins is well established[34]. Iron, titanium, aluminium, zirconium and chromium have been used in semi-metal leather production[103]. Semi-metal leathers tanned with transition metals give intense coloration, due to the formation of charge transfer complexes. Although similar types of complexes are formed with Al(III), these are colourless. This is due the unavailability of the d-orbital to form charge transfer complexes.

3.1.2 Tanning mechanisms

The early work by the Bear suggested that collagen molecules can be viewed as having the "band" and "interband" structure given in Figure 3.4[4]. He suggested that the presence of the sterically bulky acidic and basic amino acid residues in the "band" region make it open and vulnerable to bacterial invasion. However, the "interband" region is compact and orderly, hence less susceptible to bacterial attack. Therefore, interband regions do not require stabilisation but band regions do. During the tanning processes, the accessibility of the band region would be increased by osmotic swelling in the acidic environment. Once tanning agents penetrate into this region, acidic and basic amino acid residues provide reactive sites for binding.

To what extent the tanning molecule actually crosslinks the collagen is still an open question. However, there is a general agreement amongst many leather chemists that chrome tanning occurs by inter-fibrillar crosslinking of carboxyl groups, which occurs along the surface of tropocollagen molecules. Conventionally, it was believed that chromium forms covalent crosslinks involving carboxyl groups of aspartic and glutamic acid residues[118-119]. The dichromium complexes, as indicated by Figure 3.5(a), were believed to bind via multi point crosslinking. Following the study of chrome tanned leather by Extended X-ray Absorption Fine Structure (EXAFS), it is now believed that the chromium species involved in tanning reactions are linear chains of four chromium ions, linked by oxy-bridges (Figure 3.5(b)) and may bind with collagen by single point binding. Following all the recent experimental development, Covington has proposed a new tanning theory: chromium sulphate not only forms covalent binding with collagen but also polymerises itself to form a rigid matrix around the collagen, preferably by displacing the supramolecular water or even incorporating some of this water as part of the matrix structure[107].

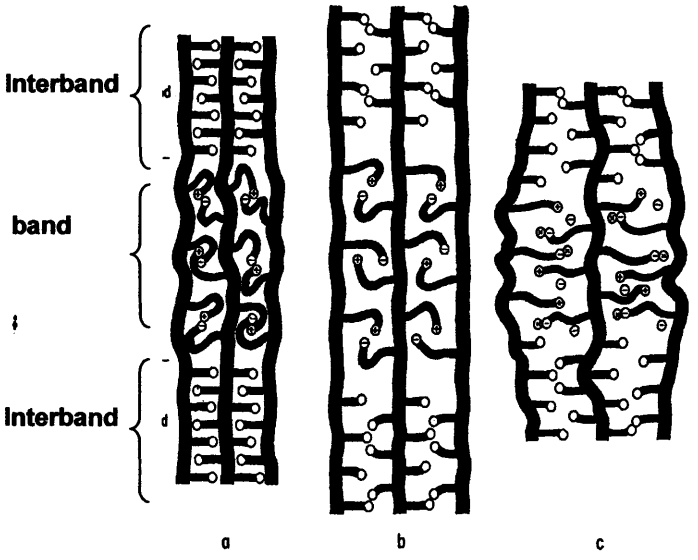

Figure 3.4: Diagrammatic representations of the "band-interband" structure of collagen showing (a) a dry fibril, (b) a fibril in water, naturally swelling and (c) an acid swollen fibril. Originally printed by Bear[4].

Based on the results of isometric tension produced during shrinking transition of leathers, Covington and Song proposed that chromium complexes *do not* crosslink the collagen molecules[121]. Although the authors rightly pointed out that there are differences in the tension produced during the shrinking transition, they failed to account for the effect of temperature upon the subsequent stress relaxation process. As the leathers shrink at different temperatures, they will also undergo simultaneous temperature dependent stress relaxation. Such relaxation is greater at high temperature and hence leathers tanned with different tanning agents will show different tension-time profiles at the shrinkage temperature. This relaxation effect will contribute to

the value of the tension produced during the shrinking transition and this might be an alternative explanation for their observed result. The authors proposed that the tanning mechanism of chromium salts is due to a matrix formation with collagen and water rather than crosslinking of two collagen molecules. However, their theory does not rule out multi point crosslinking.

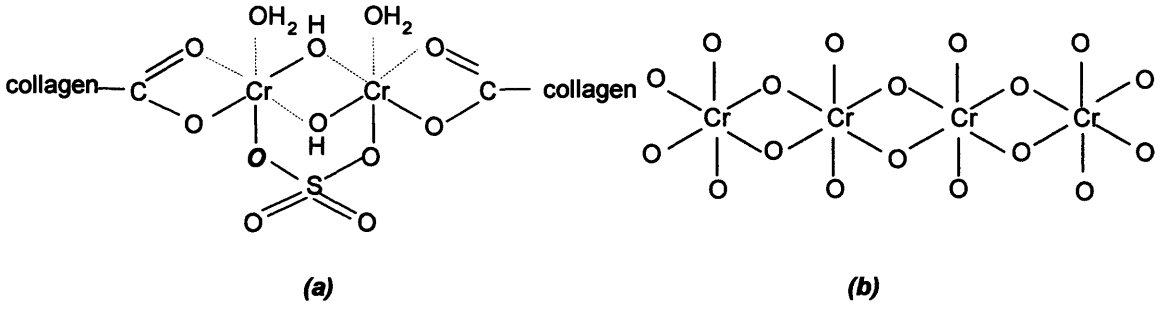

Figure 35: Possible mechanisms of covalent crosslinking of collagen with chromium salt with collagen, (a) The conventional concept and (b) the new concept of chrome tanning.

Interaction between polyphenols and protein may be either reversible or irreversible. Many workers believe that the deposition of the vegetable tannin takes place within the charged fibers along the collagen molecules. Gustavson[118-119] and Bear[4] suggested that vegetable tannins give hydrothermal stability to collagen fibrils predominantly by interaction with basic groups, e.g. lysine and arginine. Later, Haslam provided further evidence for this theory and favoured the view that, once the vegetable tannins had successfully penetrated into the inter-fibrillar regions, peptide groups would provide additional reactive sites for hydrogen bonding[113]. He further suggested that the gap ozone is most probable site for vegetable tannin fixation[112]. However, it is generally believed that vegetable tannins are fixed in leather by hydrophobic bonding and hydrogen bonding.

The reaction mechanism of semi-metal tanning has been explained in terms of the metal species crosslinking polyphenol moieties to create a matrix that interacts with collagen[107]. It has been demonstrated that for optimum stabilisation, 3,4,5- trihydroxy phenol moieties (pyrogallol) are needed for the formation of charge transfer compounds[110-111]. Therefore, hydrolysable tannins are better candidates for effective crosslinking with metal salts than condensed tannins. However, mimosa, which is a condensed tannin, has a major component that has trihydroxyl group in the B ring (refer to Figure 3.2), so it shows high affinity for aluminium (III)[122]. Titanium has shown strong affinity to hydroxyl groups and therefore is very effective in crosslinking the hydrolysable tannins

as well as the condensed tannins. It was reported that titanium produces high hydrothermally stable leather with tara[123].

Chromium (III) has less affinity to the hydroxyl groups of polyphenols and hence a semi-chrome tanning reaction is less easily accomplished than the corresponding tannages of semi-alum and semi-titan[107]. This is related to its relative reactivity towards carboxyl groups of collagen: instead of crosslinking the polyphenolic species, it forms covalent bonds with the protein. Therefore, semi-chrome is a combination of the two separate reactions, because it is actually a mixed vegetable and metal tannage.

3.1.3 Literature review

Although the thermal stability of wet leather remains a topic of interest to the leather industry, it can only give information regarding the maximum temperature and humidity conditions for the safe use of a leather without degrading it. Whereas the viscoelastic transition temperatures of leather, which may give practical information regarding physical performance, have typically not been measured and characterised.

Recently, Cot *et al.* published two research papers indicating the presence of a glass transition in chrome tanned leather, and reporting it to be approximately 45°C for leather conditioned at room temperature[10,11]. Odlyha *et al.* have reported two transitional events below the shrinkage temperature and they associated these transitions with relaxation of the polypeptide chains of collagen[93].

3.2 Experimental procedure

3.2.1 Materials

A calfskin was taken to the pickled condition by a conventional process, after which six rectangular pieces were cut from the leather as indicated in Figure 3.6. Each piece of skin was treated with a different tanning agent and processed into leather. Sample 3 was treated with an acetate buffer of pH 4.5 for 3 hours until equilibrium was reached, after which the sample was acetone dried. Sample 4 was processed into leather by a typical chrome tanning process with an 8% offer of 33% basic chromium (III) sulfate (25% Cr_2O_3). Samples 5 to 8 were processed into leather by 20% offer of tara (hydrolysable tanning agent). Three pieces of vegetable tanned leather were retanned with 2% oxide offers of metal salts (Ti(III), Al (III) and Cr(III)). The final pH during processing was maintained between 4.3 to 4.5 for all leathers. All the samples were air dried without stretching. Detailed accounts of the tanning processes are given in Appendix 5.

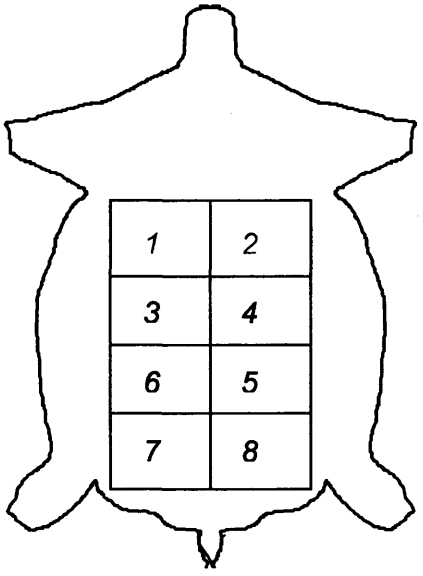

Figure 3.6: Shows the position where samples were taken to make different types of leathers; (3) untanned skin, (4) chrome, (5) vegetable, (6) semi-chrome, (7) semi-alum and (8) semi-titan, (1 and 2 were used in obtaining results described in Chapter 2).

(a) Preparation of titanium (III) as a retanning agent

Meta-stable titanium(III) ions are easily oxidised to titanium(IV) but show better tanning ability. Titanium(III) ions for combination tanning were prepared as follows; 50 g of metallic titanium was

added to 400 ml of 3M sulfuric acid in a dark flask. This mixture was then heated to 60°C with vigorous stirring under nitrogen until all the metals were dissolved. The mixture was then cooled and stored under nitrogen.

(b) Preparation of aluminium (III) as a retanning agent

One mole of aluminium sulphate and 0.5 mole of sodium acetate were dissolved in 300 ml of water and heated to 55°C. One mole of sodium carbonate was made into a 20% solution and was added drop-wise to the stirred mixture of aluminium sulphate. The mixture was left to cool overnight and the pH was recorded.

(c) Sample preparation for DMTA studies

Prior to dynamic mechanical testing, samples were conditioned in controlled relative humidities of 0, 35, 65, and 98% for 48 hours over a saturated salt solution (refer to Appendix 4) at 20°C. Rectangular (30X10 mm) samples were cut parallel to the backbone for the DMTA experiments. The moisture content of the samples was calculated by following the official Method IUC 5^{95}.

3.2.2 Dynamic Mechanical Thermal Analysis

Thermal transitions of the pre-conditioned samples were monitored by observing changes of storage modulus (E′) and loss tangent (tan δ) with temperature. A Polymer Laboratories Mark II, DMTA was used in the dual-cantilever-bending mode at a frequency of 1Hz and an amplitude of 64 μm. The sample was heated at a rate of 2°C/min from -100°C to +200°C. The transition temperature values reported are the average from three scans.

3.2.3 Differential Scanning Calorimetry (DSC)

Calorimetry measurements were carried-out in a dry nitrogen atmosphere using a heat flux Mettler Toledo DSC 822^e differential scanning calorimeter. Fully hydrated samples, 20 to 60 mg, were weighed and placed in medium pressure stainless steel pans, which were heated at a rate of 2°C/min, with an empty pan as reference. The onset of the endothermic transition was taken to be the shrinkage temperature of the samples.

3.2.4 Determination of the collagen content of leather

(a) *Digestion of hide for hydroxyproline determination*

0.200-0.400 g of dry leather was placed in a digestion tube. 10 cm^3 of 50% hydrochloric acid was added to the tube which was closed immediately with a lid containing a PTFE insert. Tubes were incubated at 100°C for 16 hours, the mixture was then cooled and diluted to 100 cm^3.

(b) Calibration curve with hydroxyproline

A stock solution of 100 mg/dm^3 of hydroxyproline was diluted with an appropriate amount of water to concentrations of 2.5, 5,10, 15 and 20 mg/dm^3.

(c) *Assay for the measurements of hydroxyproline*

Reagents

Buffer: 34.38 g of anhydrous sodium acetate, 37.50 g of sodium acetate and 5.50 g of citric acid were dissolved in 300-400 ml of distilled water and 400 ml of propan-2-ol then added. The mixture was then made up to a litre with distilled water.

Chloramine-T: 0.01 g/cm^3 of chloramine-T was made with 1:5 ratio of distilled water and buffer.

Ehrlichs reagent: 24 g of dimethylaminobenzaldehyde was dissolved in 36 ml of perchloric acid (60%) and diluted with 200 ml of propan-2-ol immediately prior to use.

Procedure

0.55 ml of samples, blank (water) and standard hydroxyproline solutions were measured out accurately with a calibrated pipette and placed in test tubes. 1.57 ml of 2:1 propanol, water mixture and then 0.88 ml of chloramine-T were added to the test tube. These mixtures were shaken gently and left at room temperature for 5 minutes. The mixtures were incubated at 70°C followed by the addition of 2.3 ml of Ehrlichs reagent. Finally the absorbance of rapidly cooled mixture was measured at the wavelength of 555 nm. The concentration of hydroxyproline and hence the amount collagen content (12% of amino acids residues of collagen type I is hydroxyproline) by weight were calculated from the calibration curve.

3.3 Results and discussion

Figure 3.7 displays a typical DMTA response of a leather conditioned at 0% RH and shows three tan δ peaks of interest, labelled α, β and γ. As discussed in Chapter 2, the β peak is assigned to the glass transition and the α peak is assigned to the shrinking related transition. When α and β peak temperatures were plotted against wet shrinkage temperature obtained by DSC, it was found that only the α peak temperatures show a correlation with shrinking transition, as indicated in Figure 3.8. This strongly suggests that they are associated with the same transition. The relatively low correlation coefficient value (R=0.85) can be explained in terms of firstly, an overlapping of thermal degradation (carbonisation) and the α transition and secondly, the broadness of the α peak. These will hinder accurate determination of the transition temperatures.

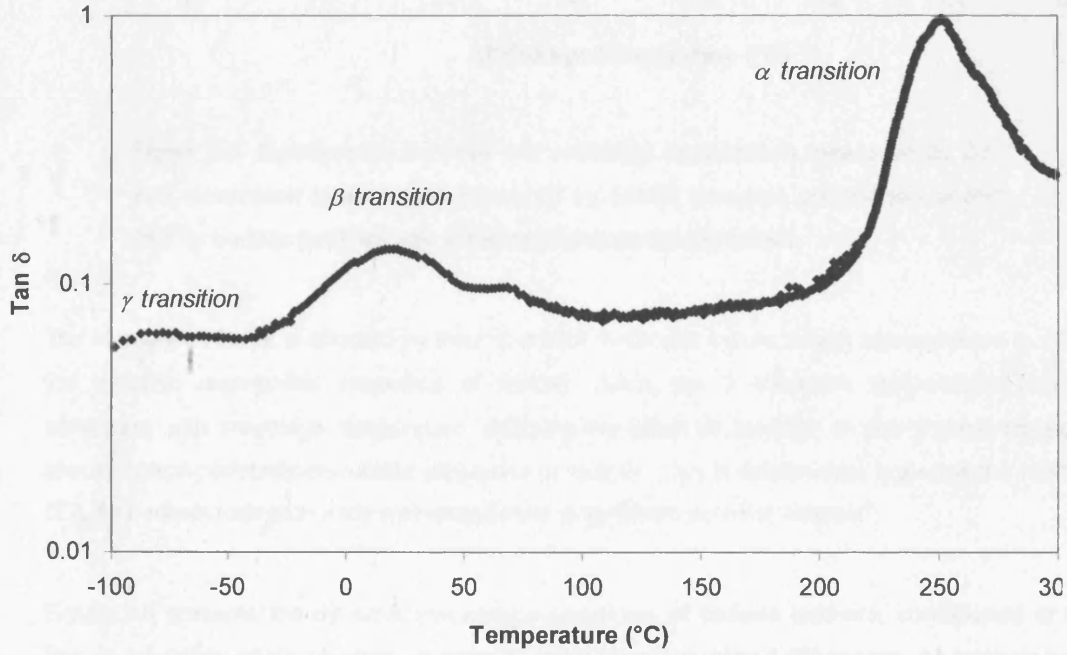

Figure 3.7: A typical DMTA thermogram of a leather tanned with vegetable conditioned at 0% RH.

Generally tanning is perceived as a process of increasing the stability of the collagen matrix. According to some literature, tanning is meant to increase the fibre strength but investigation of the tensile strength of single fibres shows that tanning actually weakens the fibres[124]. Some researchers explain such an observation in terms of the relative amount of collagen within the sample. Addition of tanning agents to collagen "dilutes" the number of collagen molecules in a unit volume and consequently material strength might be reduced[125].

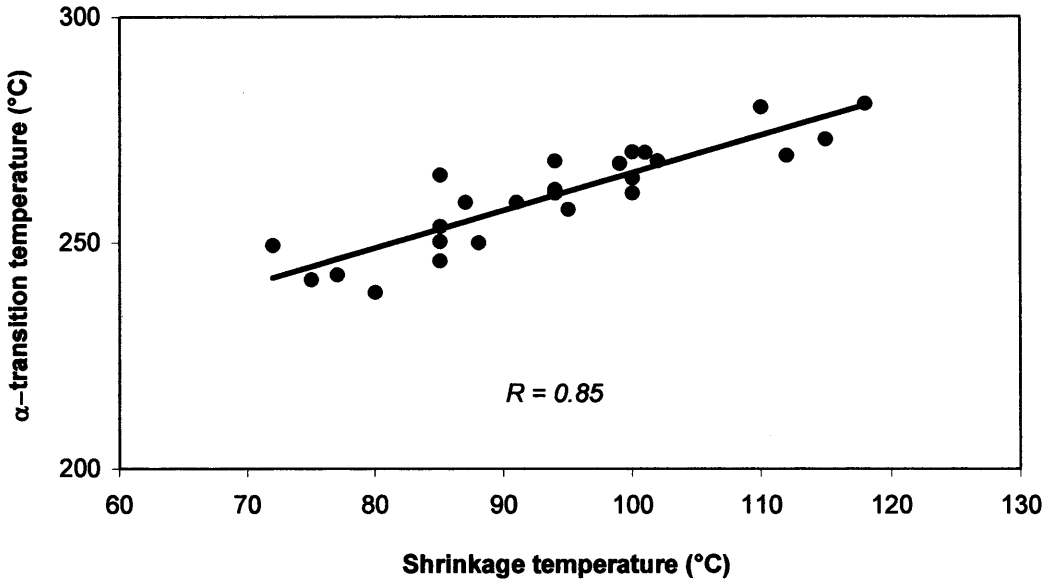

Figure 3.8: Relationship between wet shrinkage temperature measured by DSC and α-transition temperature measured by DMTA (samples conditioned at 65% RH) for various leathers with different shrinkage temperatures.

The strength of fibres is affected by inter and intra molecular bonds, which are expected to affect the dynamic mechanical properties of leather. Since the β transition temperature has no correlation with shrinkage temperature, studying the effect of tannage on the β/glass transition should reveal performance-related properties of leather. This is reasonable, because the relation of T_g to performance is already well established in synthetic polymer science[2].

Figure 3.9 presents the dynamic mechanical properties of calfskin leathers, conditioned at 0% RH, as a function of temperature. In order to avoid structure related differences, all leathers were made from the same skin (with a 2% oxide offer of basic chromium salt and a 20% offer of hydrolysable vegetable tannin (tara)). Results are compared with that of acetone-dried untanned calfskin. From Figure 3.9 a number of important observations can be made. Firstly, the progressive decrease of storage modulus from -100 to +100°C indicates a broad viscoelastic transitional region for all samples. However, the magnitude of the decrease in modulus is dependent on the tannage and corresponds to the regions where the β transition is observed. Secondly, the tanned leathers show the β/glass transitions at a lower temperature than that of untanned skin. This demonstrates that tanning molecules are acting as a plasticiser.

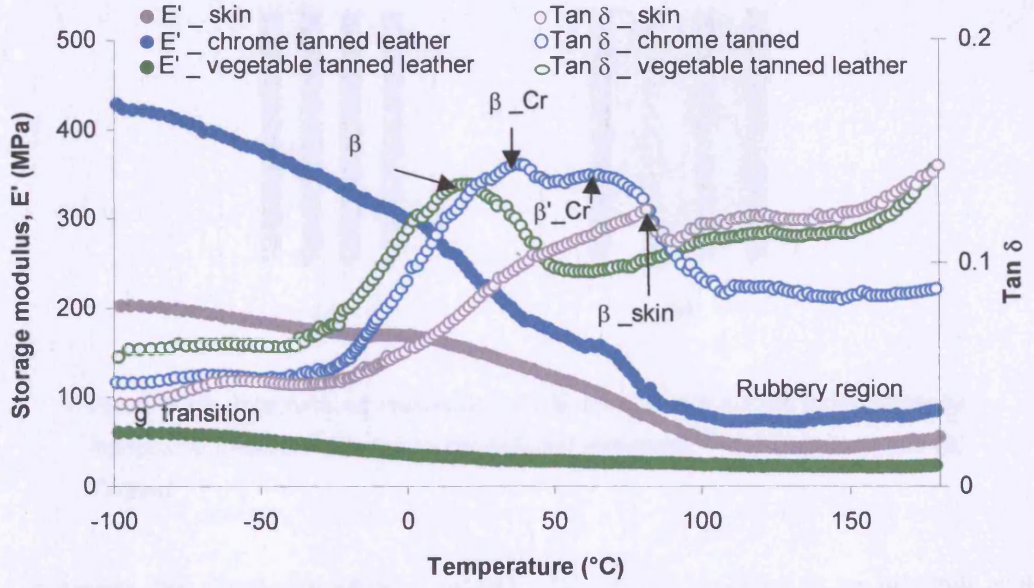

Figure 3.9: DMTA thermograms of chrome tanned skin, vegetable tanned skin and untanned skin, all preconditioned at 0% RH.

Some believe that vegetable tannins are deposited between the fibres, but that chromium penetrates deeper into the fibril structure and thus gives higher hydrothermal stability[113]. However, X-ray studies of tanned collagen carried out by Heidemann and Keller have revealed that vegetable and chrome tanning agents reduce the X-ray intensity of side-chain reflections, indicating deposition of both types of tanning materials inside the fibrils[70]. If this result holds, then DMTA is sensitive in detecting viscoelastic changes in the tropocollagen molecules. Finally, it is clear that the dynamic mechanical properties exhibited by vegetable tanned leather are quite different from the leather tanned with chrome. Leather tanned with vegetable tannin shows two distinct tan δ peaks, corresponding to the γ and β transition, as is exhibited by untanned skin, whereas chrome tanned leather shows three peaks, γ, β and β'.

The action of a tanning agent may be to interpose itself between the polymer chains and alter the forces holding the chains together. Due to this plasticisation, viscoelastic transitions, including T_g, are depressed. The plasticising effect of tanning molecules on collagen is schematically represented in Figure 3.10.

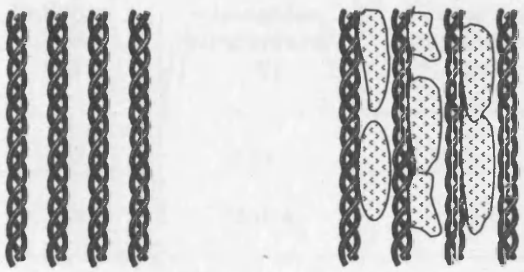

(a) *(b)*

Figure 3.10: Schematic representation of how tannins may act like a plasticiser by interposing themselves between the collagen molecules[125]. (a) Untanned and (b) Tanned.

Furthermore, the plasticising effect of tannins may also be expected to be reflected in the modulus values. This is because the plasticisation will impose greater molecular flexibility by reducing cohesive forces between the molecules and thus lowering storage modulus in the rubbery region (refer to Figure 3.9). The temperature range or magnitude of this region is dependent on the molecular weight between entanglements or crosslinks[12]. The modulus value of the rubbery plateau region of amorphous synthetic polymer is related to the molecular weight by the expression given in Equation 3.1[12].

$$G' \cong (\rho RT)/M_e \qquad (3.1)$$

Where G' is the modulus of the plateau region at a specific temperature, ρ is the polymer density and M_e is the molecular weight between entanglements. This equation is mainly applicable to rubber like polymers. However, in practice the relative modulus of the plateau region of semi-crystalline material would also indicate the relative changes in M_e or the number of crosslinks compared to a standard[12].

When the rubbery plateau regions in Figure 3.9 were analysed, the values of 140, 150 and 130 MPa were obtained for untanned skin, chromium and vegetable tanned leathers respectively. These values indicate that no significant crosslinking may exist between fibrils when skin is tanned with vegetable tannins. The high value obtained for skin in the absence of water, suggests possible fibre sticking. Moreover, in the case of chrome tanned leather, a slight increase of modulus signifies some crosslinking.

Tannage	Collagen content (%)	γ transition temperature (°C)	β transition temperature (°C)	β′ transition temperature (°C)
None (skin)	~ 93	-53 ± 7	81 ± 5	-
Chrome	~ 89	-66± 4	38 ± 8	65 ± 3
Vegetable	~ 67	-78 ± 5	20 ± 3	-

Table 3.2: Transition temperatures of tanned and untanned skin conditioned at 0% RH.

Figure 3.9 also suggests that the vegetable tannin gives greater plasticisation than the chromium salt, since it has depressed the β/glass transition to a lower temperature (see Table 3.2). Three possible explanations can be given for this observation. They are;

1. Relative amounts of tannin: Hydroxyproline determination of leathers conditioned at 0% RH shows that chrome tanned leather has ~89% collagen content, whereas vegetable tanned leather only contains ~67% collagen. A greater presence of vegetable tannins inside the fibril structure leads to greater depression of T_g.
2. Relative size of the tanning molecules: Vegetable tannins are high molecular weight polyphenols and will give multipoint reactive sites for hydrogen bonding and hydrophobic interaction with the fibre[113]. Thus, they are effective in reducing the chain rigidity of collagen by intermolecular hydrogen bonds.
3. Chromium salt binds to carboxyl groups, which occur along the surface of tropocollagen molecules. As a result of this, the temperature at which segment motion of collagen molecules becomes thermally activated is increased. However, chromium complexes that form an interpenetrating network between the collagen molecules are acting as the distance holders and thus T_g is depressed to lower temperature.

Tanning agents are considered to preserve collagen by introducing crosslinking between collagen molecules[126]. Viscoelastic transitions would then be expected to move to higher temperatures. Because this was not observed for any of the leathers examined, it suggests that the mechanism of tanning is matrix formation around the collagen molecules. This is in line with the latest thinking of the tanning mechanism[121]. In the case of vegetable tannage, polyols are well known plasticising agents for protein[85]. Vegetable tannins can be viewed as a polyols. Hydroxyls groups of polyphenols form hydrogen bonds with collagen and hence reduce the cohesive forces between adjacent tropocollagen molecules.

Table 3.2 shows that all the viscoelastic transitions are plasticised by the presence of tanning agents. However, in the case of chromium tanned leather, an unusual second transition, labelled β', is observed (refer to Figure 3.8). This may be due to separation of clusters of amino acids that are modified by chromium.

It has been widely accepted that chromium species react and form covalent bonds with the carboxyl groups of aspartic acid and glutamic acid residues. Therefore, this splitting could be due to increased rigidity imparted to the sequences of amino acids containing carboxyl groups where chromium salt binds. Thus the T_g of this region of tropocollagen will be separated from the rest of the molecule. A "cluster like" appearance of chrome tanned leather under SEM may be reflective of this "phase separation" type of behaviour[128]. Similar behaviour of the binary mixtures of polymers and biopolymers has been reported[129-131]. In these cases, due to different water activity of the individual polymers in the mixture, above a critical moisture content the polymer exhibits splitting of the glass transition temperatures. In the case of binary mixtures at low moisture contents, the mixture shows just one T_g. However, if the individual components of binary mixtures have different miscibilities with water, then at a high moisture content the mixture shows two or more distinct glass transition temperatures. The experimental evidence reported by Kalichevsky and Blanshard shows clearly that amylopectin/gluten mixtures exhibit two values of T_g at intermediate degrees of hydration, 5 - 85% RH, but only a single transition at low and high water contents[131]. The authors suggested that phase separation due to the relative miscibility of individual components with water as the probable explanation for such observation. In the case of immiscible copolymers, due to the inability of the components to mix, the polymer shows the individual T_g of each of the individual components[132].

Even though collagen shows heterogeneity (Chapter 1, Section 1.2.4), the question that needs to be answered is, does the proposed model of "hard block, soft block" give a true representation of the amino acid sequences in the collagen molecule? It is clear from the amino acid sequences (Table 3.3), that the imino acid containing tripeptides, $(Gly\text{-}Pro\text{-}Hyp)_m$, are not sufficiently clustered for collagen to be classified as a true block copolymer. In order to understand the true structural heterogeneity of collagen, it is necessary to examine the sequences of amino acids residues in collagen molecules. Table 3.3 shows the amino acid sequences of the α-chain of collagen type I[34]. This clearly indicates that the "band" and "interband" model (refer to Section 3.1.2) suggested by Bear[4], will represent the collagen structural heterogeneity better than any other proposed models. Here, the presence of sterically bulky acidic and basic amino acid residues gives less order to the molecules in the band region. Therefore, the β transition may be attributed to the band regions of collagen molecule.

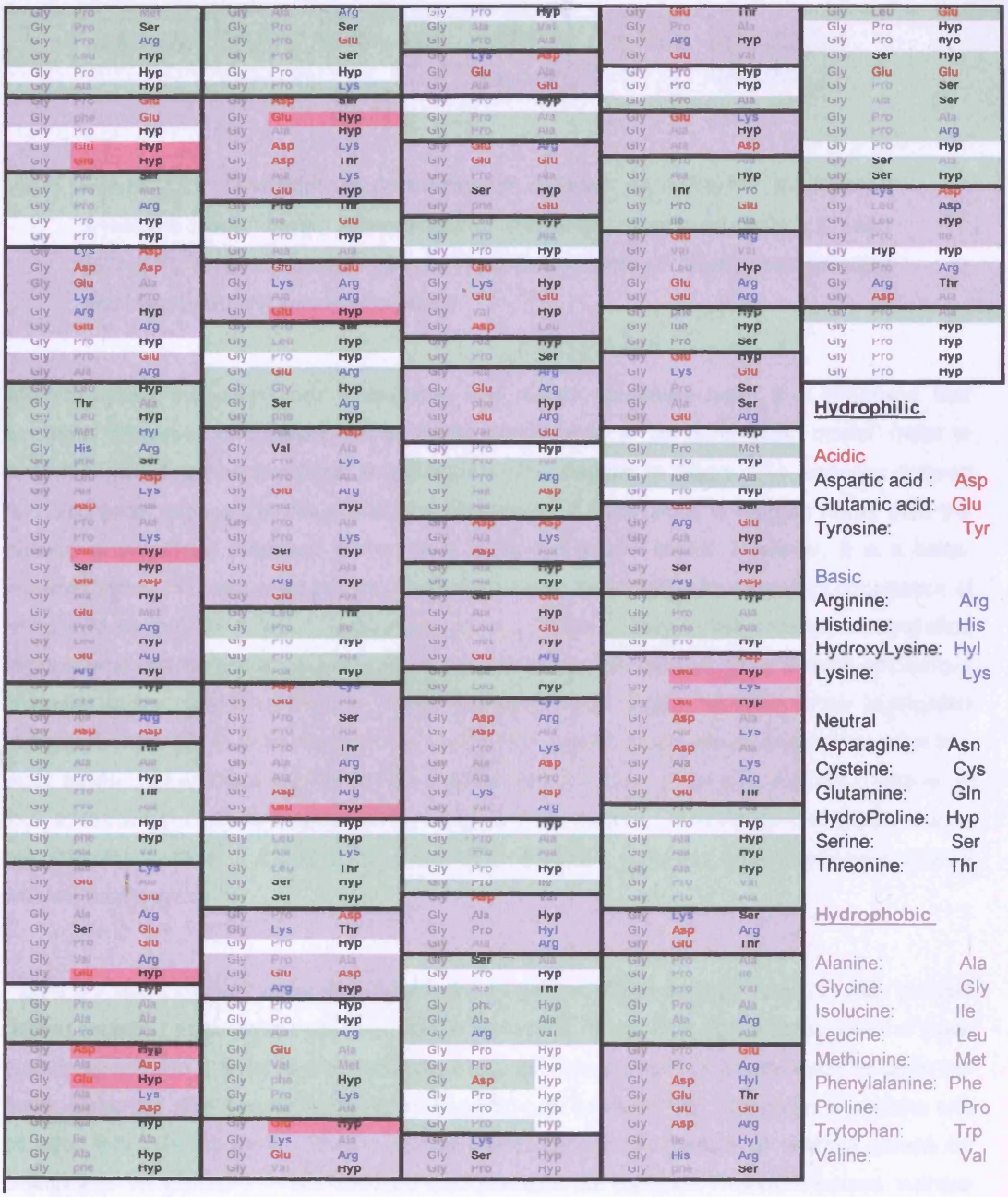

Hydrophilic

Acidic
- Aspartic acid : Asp
- Glutamic acid: Glu
- Tyrosine: Tyr

Basic
- Arginine: Arg
- Histidine: His
- HydroxyLysine: Hyl
- Lysine: Lys

Neutral
- Asparagine: Asn
- Cysteine: Cys
- Glutamine: Gln
- HydroProline: Hyp
- Serine: Ser
- Threonine: Thr

Hydrophobic
- Alanine: Ala
- Glycine: Gly
- Isolucine: Ile
- Leucine: Leu
- Methionine: Met
- Phenylalanine: Phe
- Proline: Pro
- Trytophan: Trp
- Valine: Val

Table 3.3: Amino acid sequence of type I collagen34. The liming process is known to hydrolyse (typically about half) asparagine and glutamine into aspartic acid and glutamic acid respectively, therefore "asn" and "gln" from the original sequences are changed to acidic "glu" and "asp" residues respectively. Green highlighted areas represent regions deficient in acidic and basic amino acid residues, grey highlighted areas represent regions of rich in acidic and basic amino acid residues, white highlighted areas represent regions with an occurrence of two pyrrolidine rings in sequence and pink highlighted areas represent regions with sequences of acidic amino acids with hydroxyproline.

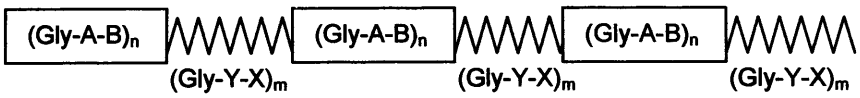

Figure 3.11: Schematic representation of collagen as a "cluster model/semi crystalline model" having a sequences of $(Gly\text{-}A\text{-}B)_m$ as ordered regions (□) and $(Gly\text{-}X\text{-}Y)_n$ as a disordered regions (/\/\/\). Where ordered blocks are crystalline and disordered blocks are amorphous.

After analysing the amino acid sequences and results presented here, it is proposed that functional properties of collagen can be better explained by a "band-interband model" (refer to 3.4). This model can be simplified as indicated by the diagram in Figure 3.11, showing ordered and disordered regions[4]. In this model, the distribution of imino acids is random rather than the ordered arrangement proposed in the "hard block soft block" model. However, it is a better representation of the actual amino acid sequences (refer Table 3.3). The persistent occurrence of imino acid clusters in A and B sequences gives a higher rigidity to the ordered or crystalline regions, whereas the occurrence of acidic and basic amino acid clusters gives a more amorphous character to the disordered regions. These differences can readily be seen in the highlighted regions of Table 3.3. In this interpretation, the ordered regions frequently do contain nonpolar and polar amino acid residues but the flexible regions mainly contain polar amino acids. There is, in fact, a less sharp distinction between polar and nonpolar regions. This model can explain the X-ray diffraction pattern[5-6]. It also explains the banding pattern observed when collagen is stained with the uranyl cation[45].

Figure 3.7 and Table 3.2 show that untanned skin gives a higher β/glass transition than chrome tanned leather. This unusual behaviour can be explained. Firstly, from the structural point of view, tanning agents not only act as crosslinkers but also as distance-holders (plasticisers) between the fibrils. Secondly, there is no evidence in the literature showing that chromium crosslinks two collagen molecules together. Finally, tanning agents reduce the number of reactive groups on collagen so the attractive forces between the molecules are reduced. Therefore tanned leathers undergo transition at a lower temperature than that of untanned skin.

Figures 3.12 and 3.13 show the DMTA thermograms obtained for tanned leather samples conditioned to different moisture contents. The viscoelastic transition temperatures are also tabulated in Tables 3.4 and 3.5. The results indicate that the glass/β transition is well defined for vegetable tanned leather at lower moisture content. As might be expected, due to the plasticising effect of water on collagen, the T_g as indicated by the β peak, shifts to lower temperatures as the moisture content increases.

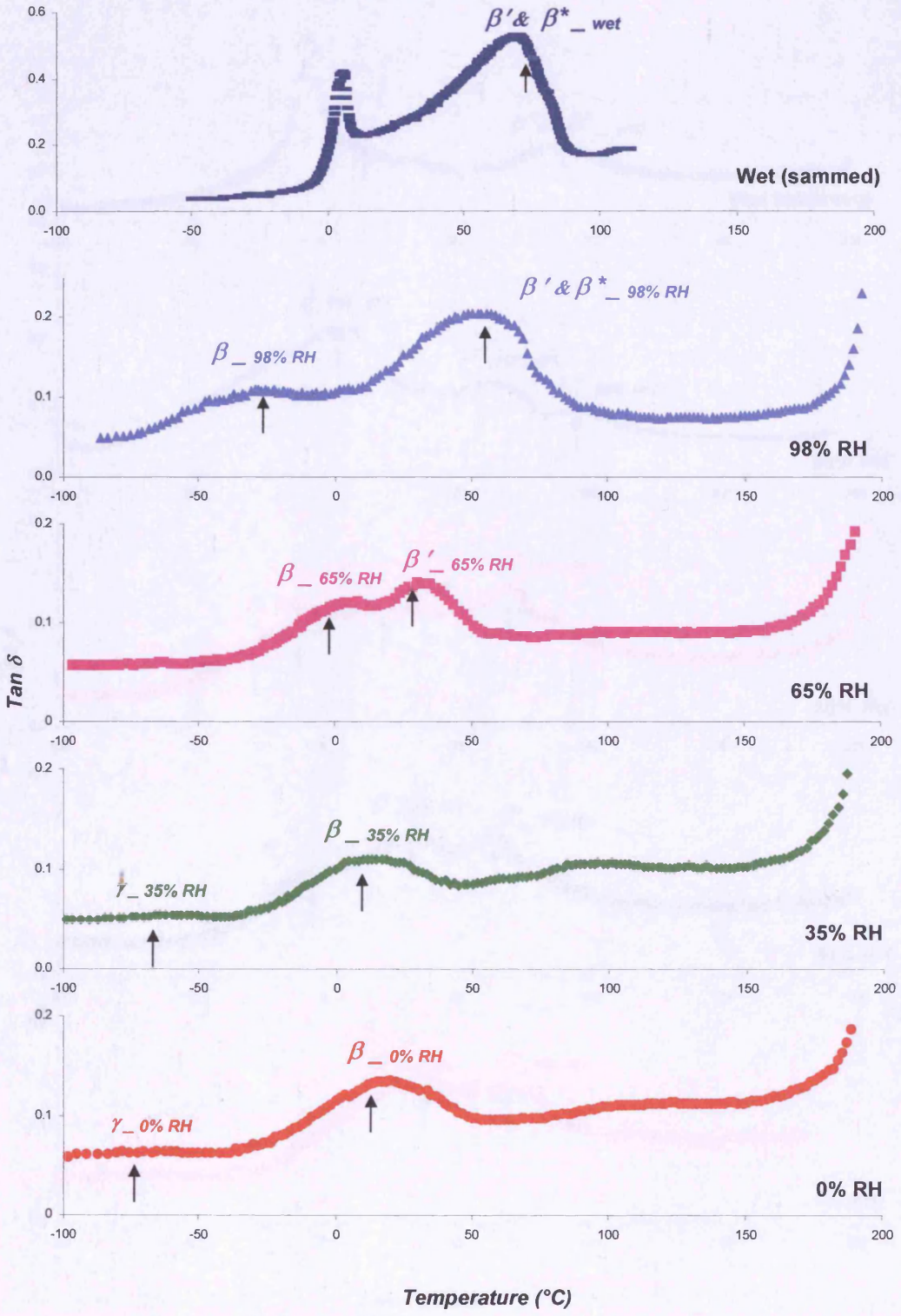

Figure 3.12: DMTA thermograms of vegetable tanned leather. Different leather samples were initially conditioned at 0, 35, 65, 98% RH for 48 hours and the wet sample was soaked in distilled water for 12 hours.

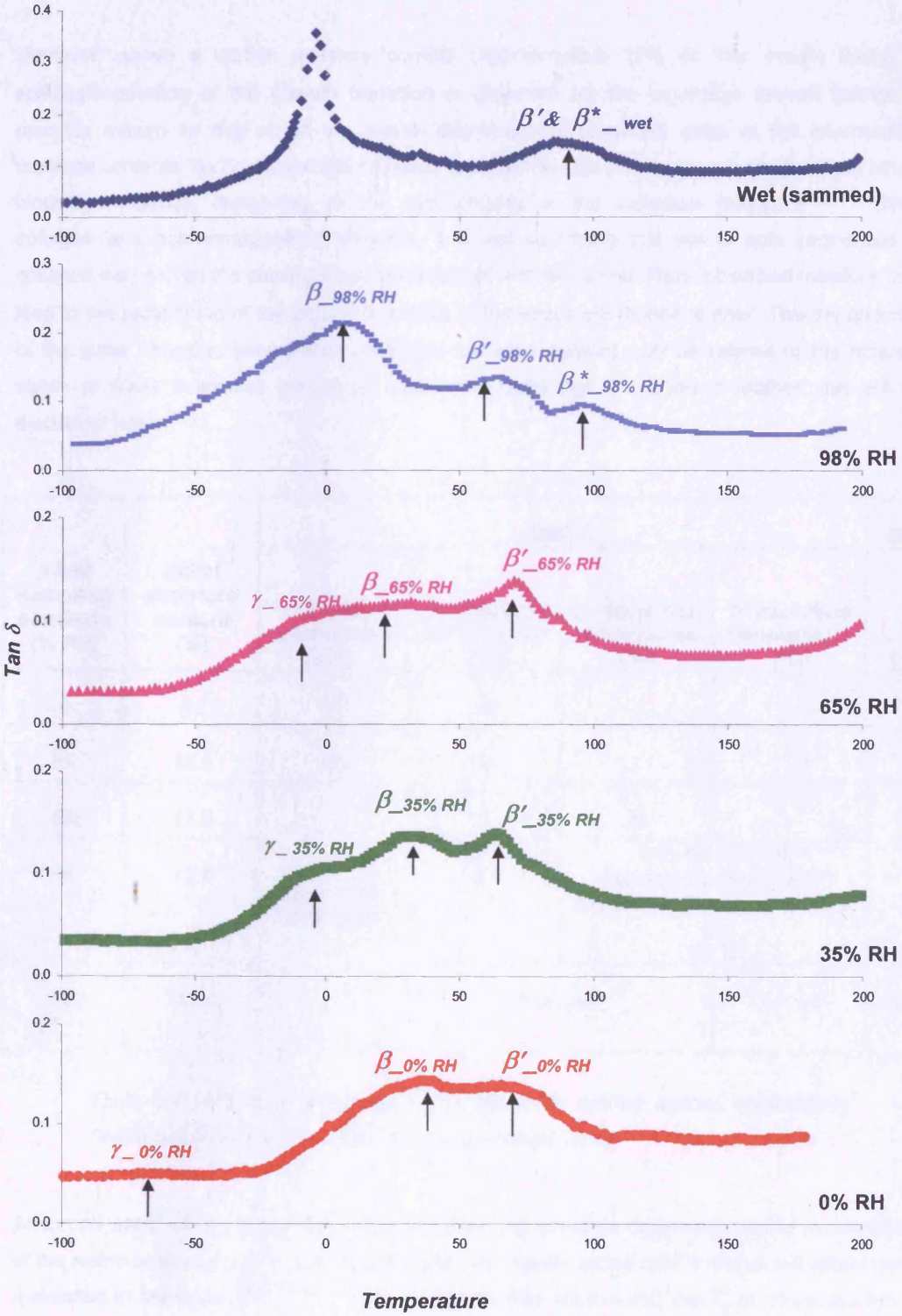

Figure 3.13: DMTA thermograms of chrome tanned leather. Different leather samples were conditioned at 0, 35, 65, 98% RH for 48 hours and a wet sample was soaked in distilled water for 12 hours.

However, above a certain moisture content (approximately 17% on dry weight basis), a splitting/separation of the glass/β transition is observed for the vegetable tanned leather. A possible reason for this would be uneven distribution of absorbed water at the intermediate moisture contents. As discussed before, water is known to split or phase separate the T_g of binary biopolymer blends, depending on the hydrophilicity of the individual polymers[129-131]. Since collagen is a non-homogeneous polymer, it is not surprising that amino acid sequences in collagen may exhibit the characteristic behaviour of a binary blend. Thus, absorbed moisture may lead to the partitioning of the β/glass transition of the vegetable tanned leather. The dependency of the glass transition temperature of leather on water content may be related to the different states of water molecules (structural, bound and bulk) that are found in leather, this will be discussed later.

<table>
<tr><th rowspan="2">Initial sampling condition (% RH)</th><th rowspan="2">Initial moisture content (%)</th><th colspan="4">DMTA</th><th>DSC</th></tr>
<tr><th>γ transition temperature (°C)</th><th>β transition temperature (°C)</th><th>β' transition temperature (°C)</th><th>β* transition temperature (°C)</th><th>T_s (°C)</th></tr>
<tr><td>0</td><td>4.2</td><td>-67</td><td>18</td><td></td><td></td><td></td></tr>
<tr><td>35</td><td>12.6</td><td>-50</td><td>13</td><td></td><td></td><td></td></tr>
<tr><td>65</td><td>17.9</td><td rowspan="3">Not very clear peak</td><td>7</td><td>33</td><td></td><td></td></tr>
<tr><td>98</td><td>72.8</td><td>-21</td><td colspan="2">Very broad peak
Possibly merged β' & β* transitions showing maximum at
62°C</td><td></td></tr>
<tr><td>Wet</td><td>162.0</td><td colspan="2">Not clear</td><td>67 ± 4</td><td>66 ± 2</td></tr>
</table>

Table 3.4: Transition temperatures of vegetable tanned leather obtained by DMTA and DSC; moisture content is on dry weight basis.

Absorbed water will distribute unevenly throughout the structure depending on the hydrophilicity of the amino acid residues. In a particular region, hydrophilic amino acid residues will attract water molecules to themselves[60-63,133-135]. This will restrict free volume and the T_g of these clusters of amino acids will occur at the elevated temperature. Thus, the splitting of the β-transition is observed. The relative amplitude of the β' peak (refer to Figure 3.12) after splitting is dependent on the moisture content. This implies that the origin of this peak is associated with water molecules.

Initial sampling condition (% RH)	Initial moisture content (%)	DMTA				DSC
		γ transition temperature (°C)	β transition temperature (°C)	β′ transition temperature (°C)	β* transition temperature (°C)	Ts (°C)
0	2.9	-66	38	65		
35	10.7	-1	31	63		
65	14.7	Mereged with β transition and hence no separate peak was observed	25	67		
98	65.0		6	62	94 ± 3	
Wet	160.3		Not clear		91 ± 4	98 ± 4

Table 3.5: Transition temperatures of chrome tanned leather obtained by DMTA and DSC; moisture content is on dry weight basis.

The β transition shows a decay relationship with absorbed water (Figure 3.14); this relationship is also reported in the literature[89]. The β* transition represents the shrinking related transition of hydrated leather. The relationship between β* and moisture content cannot be easily studied by DMTA, due to the free evaporation of moisture during the experiment. Figure 3.14 also displays tan δ as a function of temperature at different moisture contents for leathers tanned with chromium. Despite the broadness of the β transition, it shows the expected decay relationship with water content, whereas the β′ transition temperature remains unaffected by the moisture content. Additionally, unlike vegetable tanned leather, no further splitting of the β transition was observed at high moisture content. This indicates that the β′ peak, observed for both leathers, is possibly due to the same cluster of amino acid residues. If that supposition is true, then it would explain the hydrophobic nature of dried chrome tanned leather, which exhibits high resistance to rehydration. This could be due either to the hydrophobic nature of the chromium complexes formed or to the chromium complexes blocking the nucleation sites for growth of the hydration shell. Many researchers believe that hydroxyproline is the nucleation side for a hydration shell around the collagen molecule[60-64,134-135]. The amino acid sequences, given in Table 3.3, show that those hydroxyproline groups are often surrounded by acidic amino acid residues. Thus, chromium complexes could block this nucleation site for hydration.

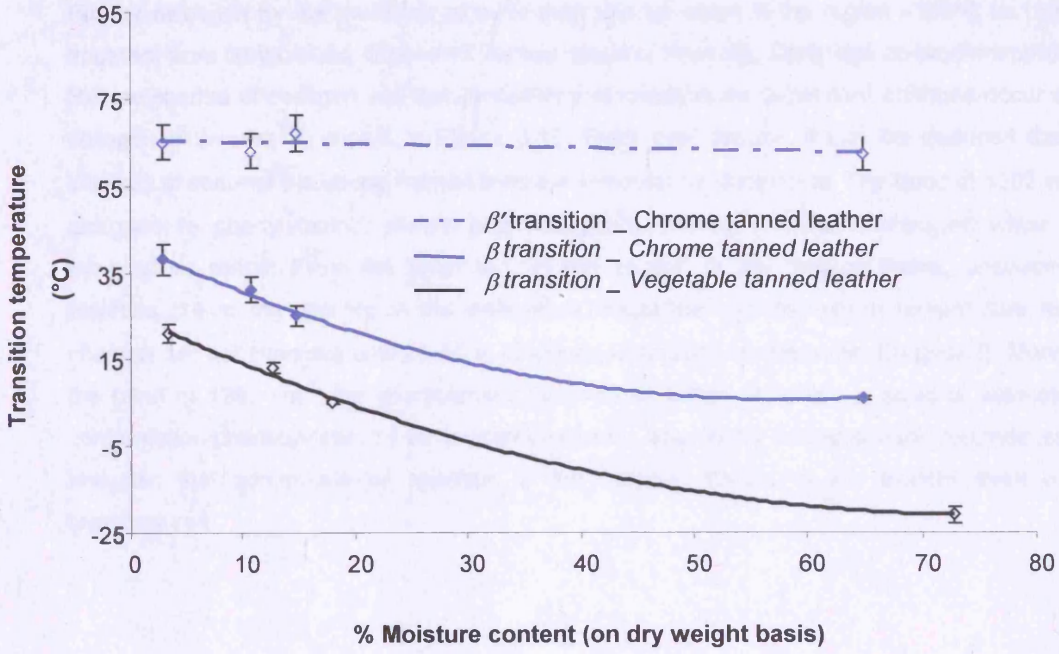

Figure 3.14: The glass transition temperatures of pre-conditioned vegetable tanned leather samples obtained from the DMTA tan δ peak (β and β' transitions of Figure 3.9).

The γ transition, as shown in Figures 3.12 and 3.13, which is attributed to side chain vibration, is unaffected by tanning. Such side chains clearly remain free (without crosslinking) to undergo a transition at low temperature in the absence of water. However, the position and the height of the γ relaxation is altered by absorption of water and above a certain value of absorbed water content, it remains unaltered at around -10°C. For samples that have been conditioned at or above 35% RH, the γ transition is seen as a shoulder on the β transition peak. These observations suggest that the side chains responsible for the γ transition do not get involved in the crosslinking reaction with tanning agents, but rather are fixed by the presence of structural water. The most probable group is therefore hydroxyproline.

When studying the water-collagen interaction, Pineri and his co-workers[66] found similar behaviour for a transition that occurred at –15°C: their β transition remained unaltered above the moisture content of 0.08 g water/g of collagen. Stefonou *et al.*[136] interpreted this peak as corresponding to the oscillation of the proline group, based on the known relaxation processes shown by the synthetic poly(L-proline) polymer. It is therefore reasonable to attribute the γ transition to the secondary vibration of hydroxyproline.

Further evidence for the presence of more than one transition in the region –100°C to 100°C is apparent from temperature dependent Raman spectra. Recently, Dong and co-workers published Raman spectra of collagen and demonstrated that temperature dependent changes occur within collagen molecules[137], shown in Figure 3.15. From their results, it can be deduced that the intensity of some of the strong Raman lines are temperature dependent. The band at 1002 cm^{-1} is assigned to phenylalanine, whose characteristic frequency remains unchanged within their temperature range. From the proposed "cluster model" in the present thesis, phenylalanine residues are mainly located in the ordered or crystalline regions, where temperature related changes are not expected until 210°C is reached (α transition temperature, Chapter 2). Moreover, the band at 1263 cm^{-1}, the characteristic vibration of Amide III, which is used to estimate the conformation characteristics of the protein backbone, does show a temperature dependency and indicates that conformational changes to the collagen backbone are evident even at low temperatures.

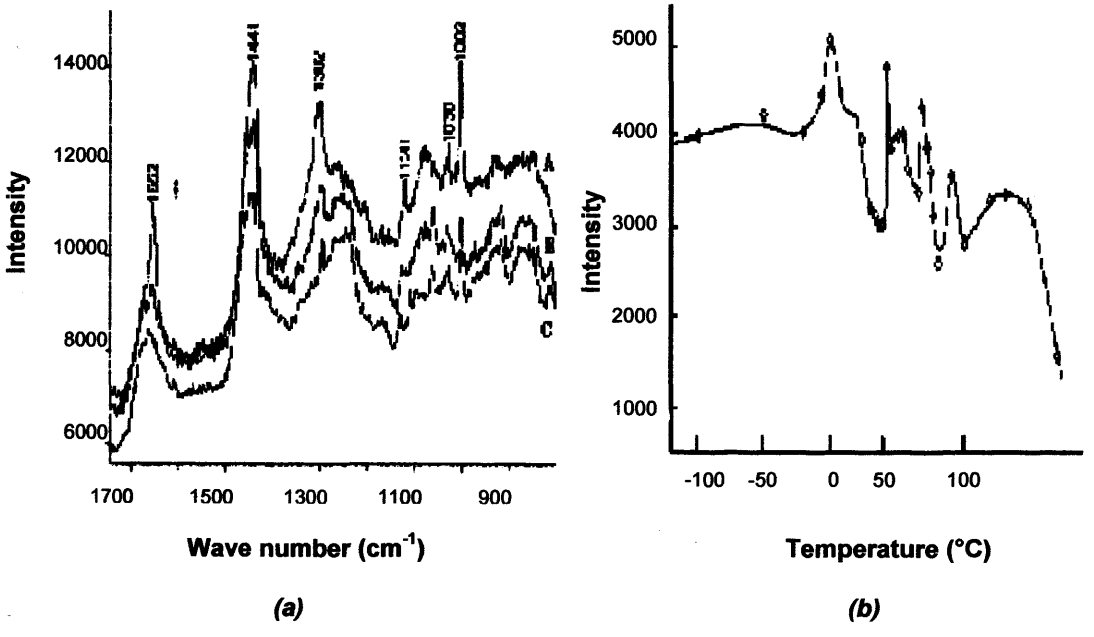

Figure 3.15: (a) Raman spectra of collagen I fibre from 750 to 1750 cm^{-1} (A) at 80°C; (B) at 20°C and (C) at –100°C. (b). Temperature-dependence of Raman intensity of collagen I by characteristic vibration band at 1443 cm^{-1} assigned to methyl and methylene groups, from Ref[137].

The temperature dependence of the characteristic band at 1443 cm^{-1}, assigned to methyl and methylene, is shown in Figure 3.15(b) and it is clear that four discrete transitions occur within the studied temperature range. There are no changes to the Raman intensity below 0°C, suggesting

that no structural changes take place. It is clear from Figure 3.15(b) that at least two major changes to molecular conformations take place between 0 to 50°C (assuming the sample is conditioned at 65% RH and 20°C, however the authors failed to mention the moisture content of the sample). These results provide further proof that the β transition is associated with molecular motions of the collagen backbone rather than the changes to the side chains. The Raman spectra also indicate that there is more than one transition taking place within the region where the β transition is observed, thus providing an explanation of the broadness and splitting of the β transition.

Figure 3.16 shows DMTA thermograms of semi-metal leathers preconditioned in different humidities. It is quite clear that semi-chrome leather shows different viscoelastic thermal behaviour to other semi-metal leathers. At 0% RH, all leathers show a single tan δ peak indicating the β/glass transition. However, with increasing moisture content, the β/glass transitions of semi-titan and semi-alum tanned leather split into two separate transitions, while the β/glass transition in semi-chrome leather remains as a single peak.

The position of the β transition of semi-titan leather is moisture dependent, but the β' transition is independent of moisture content and remains at 30°C for samples conditioned at 35 and 65% RH. This suggests that, even at 0% RH, this transition is present but is masked by the moisture dependent β transition. Therefore it is reasonable to assume that the β' peak is due to the covalent crosslinking of polyphenol modified collagen by titanium and thus the amino acid sequences where titanium crosslinks are not affected by moisture.

The viscoelastic properties of semi-alum leather are also similar to those of semi-titan leather but the β' transition shows a moisture dependent behaviour. This may be due to the hydrolysable aluminium-collagen (carboxyl-Al(III)) bond. The viscoelastic behaviour of semi-chrome leather is somewhat similar to the vegetable tanned leather (refer to Figure 3.11), showing a β peak splitting at high moisture content.

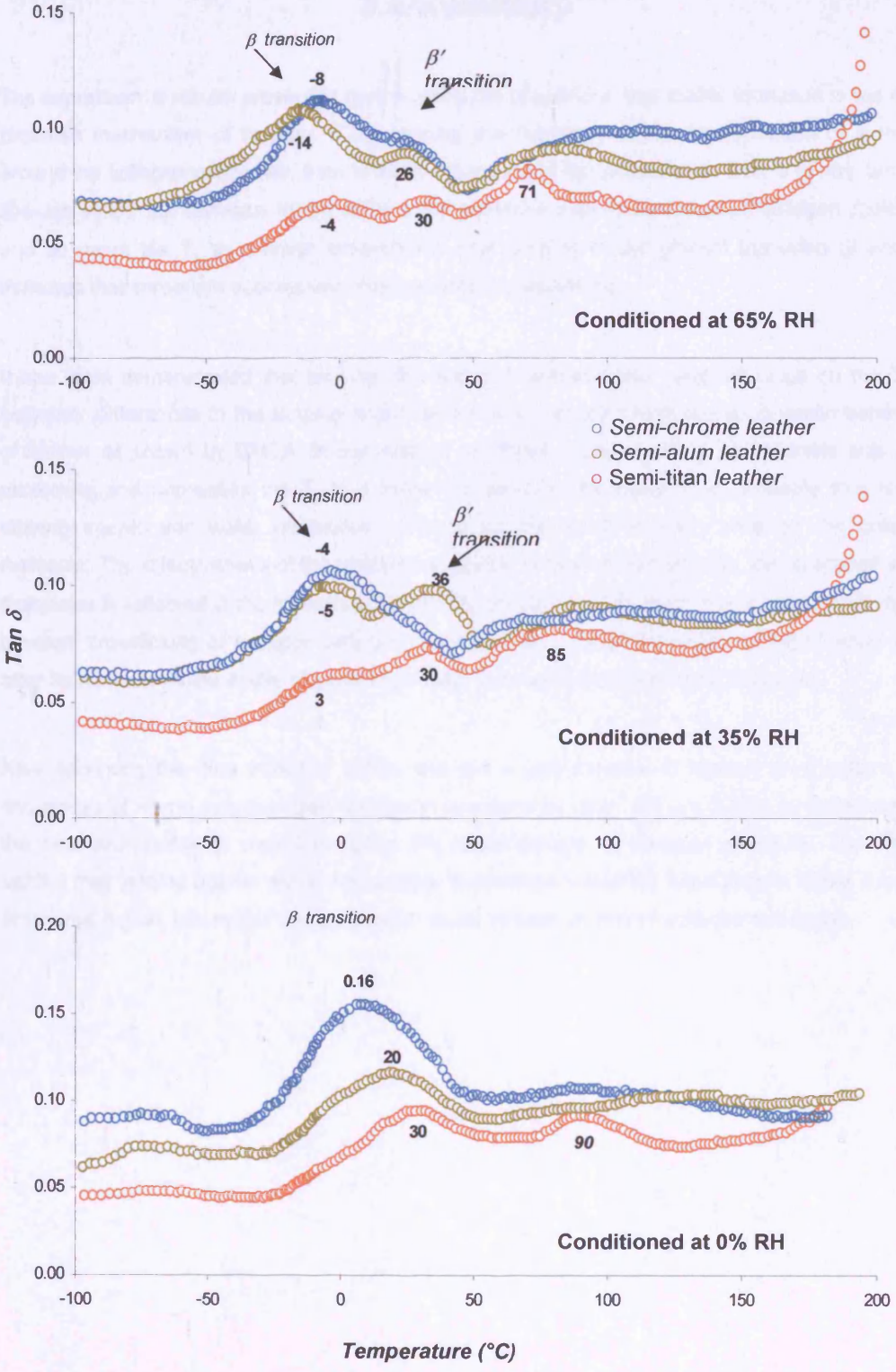

Figure 3.16: DMTA thermograms, showing tan δ as a function of temperature for semi-chrome (○), semi-alum (○) and semi-titan (○) leathers.

3.4 Summary

The experimental results presented here support the proposition that matrix formation is the most probable mechanism of tanning. If the tanning mechanism involves the formation of a matrix around the collagen molecules, then tanning agents are in fact plasticisers. That is to say, tanning species inside the collagen matrix reduce the attractive interaction between collagen molecule and so move the T_g to a lower temperature. The splitting of the glass/β transition (β and β') indicates that chromium species are also involved in crosslinking.

It has been demonstrated that tanning and water molecules have great influence on the T_g of collagen. Differences in the tanning chemistry are also apparent from the viscoelastic behaviour of leather as shown by DMTA. In the case of vegetable tanned leather, polyphenols acts as a plasticiser and depresses the T_g to a lower temperature. Moreover, it is probable that all the tanning agents and water molecules compete for the same reaction sites on the collagen molecule. The effectiveness of the tanning molecules to block these sites for the absorbed water molecules is reflected in the hydrothermal stability of collagen, assuming the β' transition is due to covalent crosslinking of collagen with tanning molecules. The plasticisation effect of water even after tanning shows the ability of water molecules to enter the tropocollagen molecule.

After analysing the data from the DMTA and the known theories of tanning mechanisms and sequences of amino acid residues, the model proposed by Bear[4] (Figure 3.5) is considered to be the best representative model to reflect the heterogeneity of collagen structure. This theory implies that tanning agents would accumulate themselves inside the band region. Since it is less structured region, this region can be viewed as amorphous portion of collagen molecules.

Chapter 4

INVESTIGATION OF LEATHER DRYING BY DYNAMIC MECHANICAL THERMAL ANALYSIS

4.1 Introduction

In recent years, the increasing demand for cheaper and speedier production of leather has placed a pressure on the leather industry to develop faster drying procedures that do not compromise product quality. There are several drying procedures, vacuum drying, toggle drying, microwave drying, drying tunnel etc., available to tanners today. However, often a lack of knowledge leads to the wrong drying procedure being used, which produces inferior quality leather. Leather tends to be a supple material, but over drying can introduce undesirable and irreversible stiffness. In order to understand the drying procedure, one should have not only well informed knowledge of general drying principles, but also good knowledge of the fibre structure of collagen molecule, especially, the interaction of water with collagen. Nuclear magnetic resonance studies show that the relaxation times of water protons are shorter in collagen tissue than in pure water and the rate of relaxation depends on the strength of the magnetic field[139]. The implication of this observation is that water molecules are present in different states, each of which has its own molecular dynamics and function within the collagen matrix.

Because leather is a viscoelastic material, and water acts as a plasticiser, introducing or removing this plasticiser will inevitably change the viscoelastic properties. It follows that, during drying, the viscoelastic properties of leather change continuously with the removal of water. Therefore, measurement of the dynamic mechanical behaviour of leather during drying can give useful information on changes occurring to the internal fibre structure. By studying these changes, a greater understanding of drying behaviour of leather can be gained. This Chapter is concerned with studies of the dynamic mechanical behaviour of leathers (chrome tanned and vegetable tanned) during drying. The effects of temperature on the mechanical performance of leather will be discussed and a new regime for drying leather will be proposed.

4.1.1 Interaction of water with leather

In order to understand the drying behaviour of leather, one must be aware of the relationship between moisture and leather fibres. There are several states of water known to be present in leather and they are divided into three main groups; structural water, bound water and bulk water. A detailed account of these stages of water molecules was discussed in Chapter 1 (Section 1.2.5). Bulk water has a liquid-like character and hence it is not restricted in forming ice crystals at 0°C upon cooling[63-65]. Bound water molecules, on the other hand, exhibit a transitional structure between solid and liquid, thus this state of water does not freeze at 0°C[63-66,140]. Structural water molecules are part of the fibre structure and behave like a solid. As this state of water is important for the structural function of leather, maintaining the relationship between these water molecules and leather fibres is therefore of critical importance, since removal of these water molecules may result in irreversible changes to the fibre structure of the leather[66-70].

4.1.2 The theory of drying

Drying can be defined[138] as the removal of a solvent or liquid from a solid and in the case of leather, most often the liquid is water. The most common method of drying is converting water into vapour, which is then removed from the system. During the drying of any solid, two processes are occurring simultaneously. They are;

- Transfer of heat
- Transfer of mass (vapour)

Factors determining both of these processes determine the effectiveness of the drying operation[140]. When tanned wet leather is exposed to dry air, water is evaporated from its surface and the rate of this evaporation process is influenced by various factors. It has been reported that drying of leathers occurs in three different phases, as indicated by Figure 4.1[140]. In the earliest stage of drying (α), there may be sufficient bulk water on the surface of a leather, thus it acts like a liquid water surface. Evaporation occurs at a constant rate, which is directly proportional to the surface area of leather and so the rate of drying is dependent on the temperature and the relative humidity of the air. In theory, harsh drying conditions can be used during this phase of drying, as long as the losses of the bound and structural water molecules are prevented. However, in practice, it is not easy to predict the precise end of this constant rate of drying period and prolonging these drying conditions into the next stage of drying may cause damage at the surface.

After this constant rate of drying period is completed, the rate of drying is controlled by the diffusion of moisture/vapour from the higher concentration in the centre of the leather to the lower concentration at the surface. During this period the rate of drying is entirely dependent on the ease of diffusion of water vapour through the structure. In the second phase, β, the evaporation proceeds from within the leather and is directly proportional to the amount of water inside the leather. It has been reported that during this phase of drying, only the weakly bound water molecules are removed[84]. This type of water migrates to the drying surface more easily than the structurally bound water.

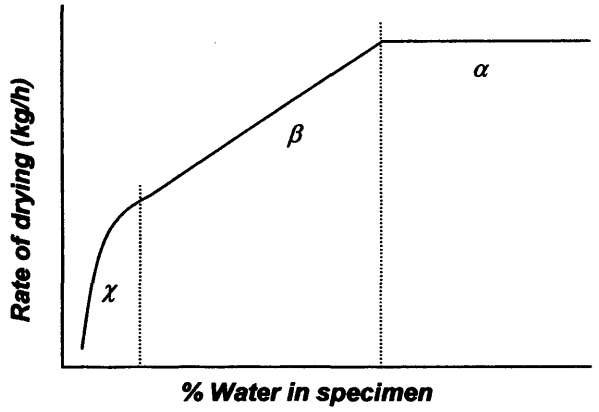

4.1: Diagrammatic representation of the rate of drying curve, indicating the constant period of rate of drying, α, and two periods of varying rate of drying, β and χ[140].

In the final stage, χ, structurally bound water is removed. During this period, the drying rate depends on the diffusion coefficient and on the rate of moisture flow or exchange between structurally bound water and water vapour. In order to mobilise and remove this state of water from collagen molecules, more energy is needed; hence it has a relatively high diffusion coefficient. This is reflected in the rate of drying of the final phase.

4.1.3 Literature review

Drying of leather has been intensively studied and reviewed over the past 20 years[84,63,84,140-152]. However, the theory does not fully explain many important phenomena encountered in practice, such as stiffness, shrinking of area etc. When reviewing the drying process, Komanowsky has tried to combine mathematical principles, surface chemistry and a structural knowledge of collagen to explain the different stages of drying[84]. He attributed each stage of drying to different states of water molecules within the leather. Like Komanowsky, some researchers have explained

different phases of drying in terms of different states of water molecules, which are found within leathers, while others explain the process purely on the basis of heat transfer[148-152].

Friedrich discussed the rate of drying of leather in terms of the different states of water[150]. He attributed the constant rate period (Figure 4.1) to the removal of water that is found between fibres, the first falling rate period to the water which is situated between the fibrils and the second falling rate period to the water located within the fibrils. He also pointed out that the constant drying rate and the first falling rate cease at the critical points of 50% and 30% moisture contents respectively. El Amir has also identified similar results for these critical moisture contents[151].

X-ray studies of tanned collagen by Heidemann and Keller also provide further support for the inflection point observed at 50% moisture content[70]. In this study, they demonstrated that the level of hydration (moisture content) not only affects the intensity, but also the position of side chain reflections (equatorial diffraction). The fact that water can influence the sharpness of X-ray patterns show that some water molecules are incorporated in the lattice of the fibril structure and influence the crystalline structure of collagen. They pointed out that collagen attains an optimum crystallinity when it contains approximately 50% moisture (on dry weight basis; refer to Figure 4.10).

The evidence for suggesting the removal of water from the intrafibril region, during the falling rate period, β (Figure 4.1), comes from X-ray diffraction studies. Several studies relate the water content of collagen tissue to equatorial diffraction spacing[68-69,120]. In all cases the diffraction spacing appears to converge to a single value for the dry state. The diffraction spacing increases with absorbed water content up to a characteristic limiting value, then it remains constant with further absorption of water. This suggests that the collagen molecules are forced apart with the accretion of water and when the water content exceeds some limit, there is no further expansion. Therefore, it can be presumed that the intermolecular crosslinks limit equatorial expansion and thereafter water fills other capillary spaces between fibres or fibrils. Rougvie and Bear have shown this limiting value is approximately 60% (dry weight basis) [120].

In its natural state, skin contains 150-200% of water by weight (dry weight basis). Beamhouse operations, tanning processes and fatliquoring change the fibre molecular structure and so the state of moisture in the pelt. However, when reviewing the leather–water relationship, Bienkiewicz stated that "with limitations, the basic features of the collagen remain unchanged by tanning and hence collagen in leather reacts with water in the same way as it does in hide" [63]. This author's remark may be only applicable to the closely bound water molecules that are associated with the molecular arrangement, because crosslinking is known to modify the dynamic water structure within a skin[64,152]. Moreover, it is well known that the physical structure of the fibres are modified

during the beamhouse operations and therefore the amounts of capillary and bulk water may differ from leather to leather, depending on process conditions.

The effect of drying on the D-period, can be observed by X-ray diffraction. In the hydrated state, collagen shows a fundamental axial periodicity of 67 nm and up to 140 meridional diffraction peaks, showing a high degree of crystallinity along the fibril axis[153]. However, the X-ray diffraction pattern of dry collagen shows a reduction of the D-period to 64 nm and 34 meridional diffraction peaks. The authors ascribed these changes to axial sliding of the molecules and an increase in the variability or disorder of molecular packing respectively. Moreover, on drying, the X-ray diffraction peaks are reported to broaden, which is expected if the radius of the fibril decreases[120,153].

4.2 Experimental procedure

4.2.1 Materials used and sampling position

(a) Materials

Unfatliquored chrome tanned and vegetable tanned bovine hides were prepared in-house by a typical process (Appendix 6), then they were sammed to obtain approximately 160% water content on a dry weight basis. All samples were sealed in a polyethylene bag and kept at 5°C, to prevent any loss of water.

(b) Sampling

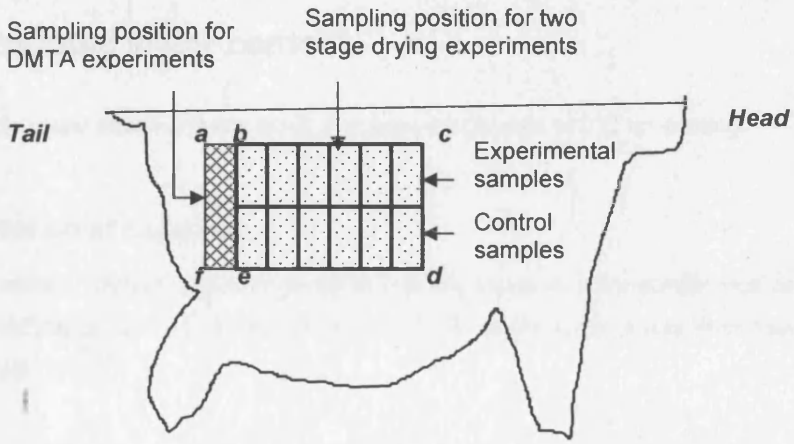

Figure 4.2: Sampling locations for DMTA and drying experiments.

The fibrils are aligned along the main lines of tension. This directional run profoundly affects the physical properties. In order to minimise the influence of structural variation, samples were taken from the official sampling position[95], as illustrated in Figure 4.2. For the individual experiments, all the samples were cut parallel to the backbone unless otherwise stated.

4.2.2 Dynamic mechanical properties of leather during drying

A dynamic mechanical thermal analyser, Mark II (Polymer Laboratories), was used in the dual-cantilever-bending mode, at frequencies of 1 and 10 Hz and an amplitude of 64 μm. The DMTA oven was heated to the preselected temperature of drying and then the weighed sample was placed inside the DMTA head and the dynamic mechanical properties were recorded against time. Samples were weighed before and after the run to determinate the moisture content; by

following the official leather method IUC 5[95]. Stiffness changes occurring during the drying of leather were followed by monitoring the storage modulus (E') and loss tangent (tan δ) as function of time.

4.2.3 Rate of drying

Weighed samples of leather were placed in a conditioning room at 65% RH and 20°C. The rate of drying was found by weighing the sample at constant time intervals, until a constant weight was achieved. Then, the leather was dried at 100°C until a constant dry weight, w(d), was attained. The rate of drying was calculated and expressed as indicated by equation 4.1, where, w(o) is the weight at start time 0, w(d) is the dry weight and t is time interval.

$$\text{Rate of drying} = \frac{w(o)-w(d)}{t} \qquad (4.1)$$

4.2.4 Freezable water content

The freezable water molecules are those that form ice crystals at 0°C on cooling.

(a) Preparation of samples

In order to obtain different moisture contents, leather samples were conditioned under different relative humidities at 25°C for a week (Appendix 7). Moisture content was then measured by the official method IUC 5[95].

(b) Determination of freezable water content

A Mettler TC10 Differential Scanning Calorimeter (DSC), equipped with a cooling device was used to characterise the solid-liquid phase transition of water in leather. Samples were placed inside a sealed aluminium sample pan, with an empty aluminium pan as reference. A standard experimental cycle was applied to all leathers. First, samples at different moisture contents were frozen by decreasing the temperature from room temperature to –50°C, at a rate of 5°C/min. After a pause of 5 min to stabilise the freezing, melting of ice was recorded by heating the samples from -50°C to +50°C at a of rate of 2°C/min. The heats of fusion due to the ice melting, Q, were calculated by integrating the corresponding enthalpy peaks (endothermic thermal transition centred at 0°C; refer to Appendix 9). The weight of freezable water (W(f)) was obtained as:

$$W(f) = Q/\Delta H \qquad (4.2)$$

Where ΔH is the melting enthalpy, assumed to be the same as that of bulk water (ΔH = 333.5 J/g), and Q is the heat absorbed during the melting process.

4.2.5 Determination of hydroxyproline

The collagen contents of wet blue and vegetable (tara) tanned leathers were determined by measuring the hydroxyproline contents as described by Heidemann[153]. A detail account of this process is given in Section 3.2.4.

4.2.6 Two stage drying process

Leather samples, taken from the area "bcde" as indicated by Figure 4.2, were subjected to a two stage drying process. During the first stage, leathers were dried at varying temperatures between 80 to 30°C. During the second stage, samples were conditioned at 65% RH and 20°C.

(a) Experimental set

Pieces of leather were dried under a controlled humidity of 80% RH at various temperatures for 48 hours, where a saturated salt solution was used to obtain 80% RH at a preselected temperature (refer to Appendix 7). Then the samples were conditioned to 65% RH at 20°C for 48 hours.

(b) Control set

Leather samples were dried at elevated temperature for 48 hours, when the relative humidity of the environment was not controlled. Then the samples were conditioned at 65% RH and 20°C for 48 hours, prior to physical testing.

4.2.7 Physical testing

(a) Bend modulus

As indicated in Figure 4.3, a rectangular shaped specimen was placed on the top of two supporting rollers, which sit in the semicircular slots on the supporting unit. The distance between the supporting rollers was set to 40 mm. A probe attached to the crosshead of an Instron 1122 tensometer was driven down at a speed of 50 mm/min to deform the specimen. The force exerted at a bending deformation of 4 mm was measured by a 1 N load cell. Elastic beam[155] theory, as indicated in equation 4.3, was used to calculate the bend modulus, E, as follows.

$$E = \frac{F \ell^3}{4 d w t^3} \qquad (4.3)$$

where F is the applied force to bend the sample to a depth d, ℓ is the distance between the two supporting points, w is the width of the sample, t is the thickness of the sample and E is the

modulus. It must be noted that calculation of bend modulus using this formula assumes uniformity across the thickness of the leather.

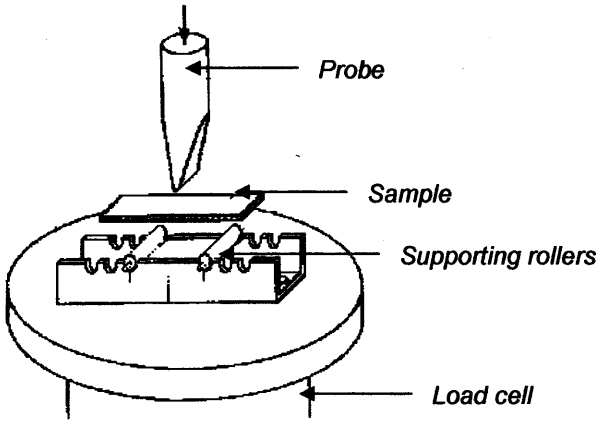

Figure 4.3: The instrumental set-up of the bending test[154].

(b) Softness

The procedure given in test protocol IUP 36 was used to determine softness[95].

(c) Tensile strength

The procedure given in test protocol IUP 6 was used to determine the tensile strength and elongation at break[95].

(d) Moisture content calculations (dry weight basis)

Samples of known weight were dried at 100 ± 2°C for 5 hours and then cooled to room temperature in a desiccator over silica gel. Samples were then reweighed. This heating and cooling cycle was continued until constant weight was obtained. The moisture content quoted throughout this thesis is calculated as indicated in equation 4.4 unless otherwise stated.

$$\text{Moisture content (\%)} = \frac{M_1 - M_2}{M_2} \times 100 \qquad (4.4)$$

where M_1 is the mass of the sample before drying and M_2 is the dry mass of the sample after drying.

3.3 Results and discussion

Figure 4.4 presents a DMTA drying curve for a constant air temperature of 70°C during the drying of partially processed leather tanned with chromium(III) salt, where modulus and tan δ are expressed as a function of time. Several isothermal DMTA drying curves of leathers are given also in Appendix 8. The bend modulus, E', indicating the stiffness of the leather, shows an overall increase as the leather changes from a wet state to the dry state. Such behaviour might be expected for any material as it dries. But the shape of the curve is far from reflecting a simple increase in stiffness as the leather dries. It is clear from Figure 4.4 that the initial increase in bend modulus is followed by a decrease to a minimum point, after which it continues to increase until a plateau is reached. The general shape of the curve is the same, regardless of the drying temperature (refer to Appendix 8): the only difference is the time at which infections are observed.

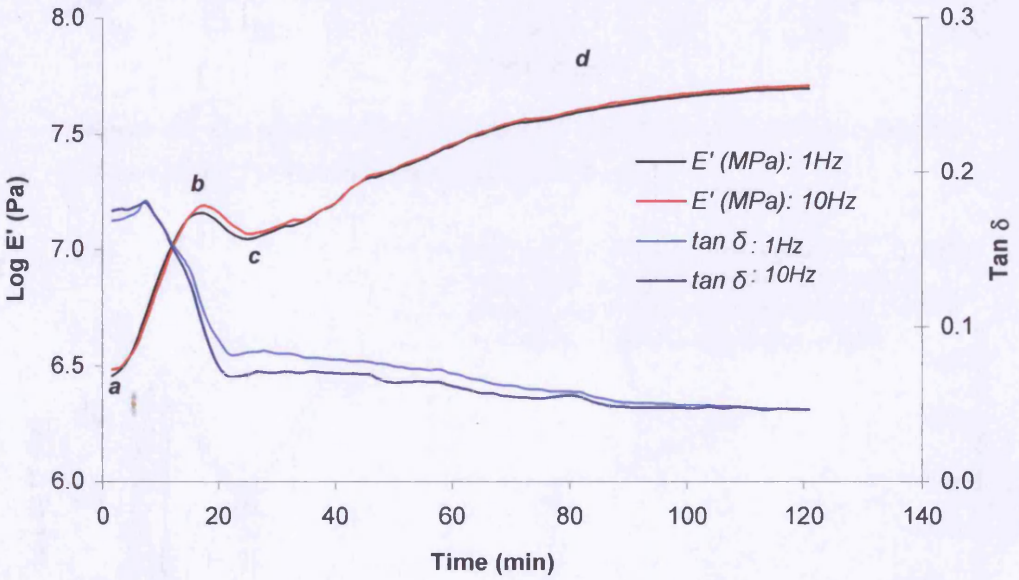

Figure 4.4: A typical DMTA drying trace of partially processed wet blue at 70°C. The initial and the final moisture contents of the sample were determined to be 162% and 7% (dry weight basis) respectively.

If the profile of the DMTA drying curve is related to the molecular motions associated with leather fibres, then at the second inflection point, ***c***, tan δ is expected to give rise to a peak. None of the results show such behaviour, hence suggest the changes observed in modulus must be related to the moisture content of the leather. In order to understand the relationship between moisture contents and modulus during drying, leather samples were subjected to isothermal DMTA scans for different time periods. Moisture content of the sample was determined immediately after the end of the experiment. The results are presented in Figures 4.5 to 4.7.

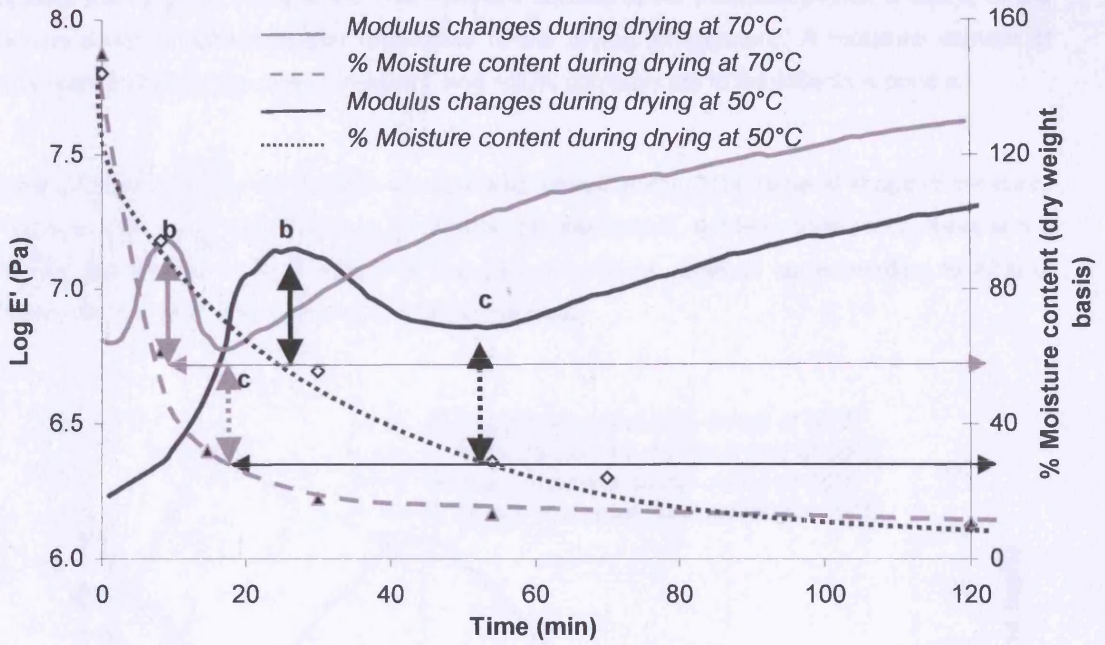

Figure 4.5: Changes in storage modulus (E') and moisture content as a function of time during drying of wet blue leather at 70°C and 50°C.

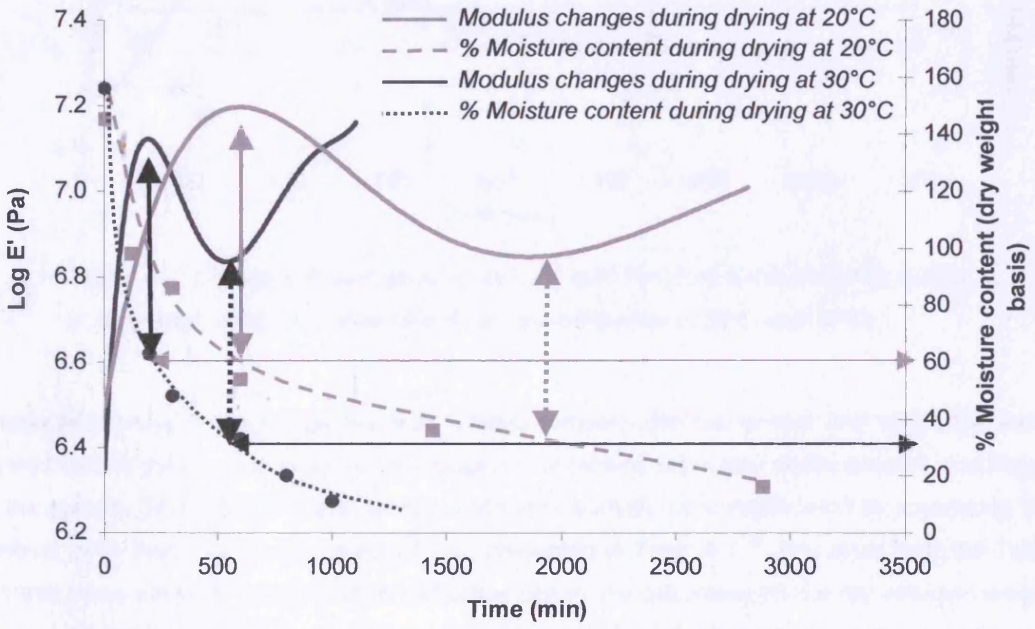

Figure 4.6: Changes in storage modulus (E') and moisture content as a function of time during drying of a wet blue at 20°C and 30°C.

It is clear from Figures 4.5 and 4.6, that moisture content at the inflection points, ***b*** and ***c***, of the modulus curve remains constant regardless of the drying temperature. A moisture content of ~60% corresponds to the inflection point b and ~30% corresponds to the inflection point ***c***.

Figure 4.7 indicates the drying profile of vegetable tanned leather. The general shape of the curve is same as that which was obtained for chrome tanned leather, but the moisture contents at the inflection points differ. It was found that the critical moisture contents corresponding to 42% at inflection point b and 27% moisture at inflection point ***c***.

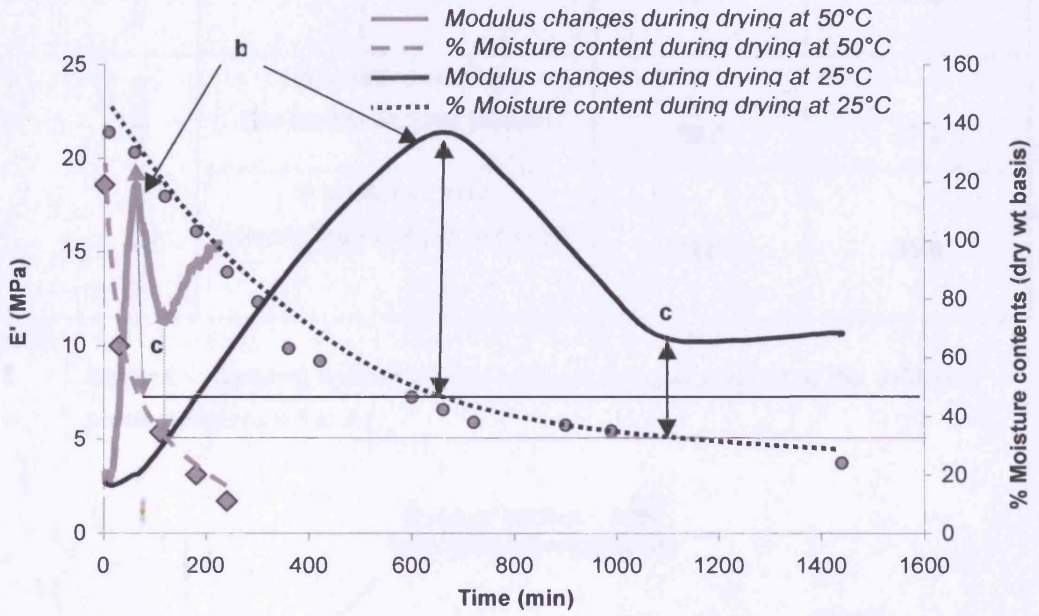

Figure 4.7: Changes in storage modulus (E') and moisture content during drying of a partially processed vegetable (tara) tanned leather at 25°C and 50°C.

These differences in the critical moisture content between chrome tanned and vegetable (tara) tanned leather may be due to either the interaction of tannins with water or the amount of collagen in the sample. Therefore, collagen contents of these leathers were determined by measuring the amount of hydroxyproline and the results are presented in Table 4.1[153]. It is clear from the Table 4.1 that when moisture contents at the inflection points are calculated on the dry collagen weight basis, both leathers show similar values. This suggests the inflection points on the drying curve are related to the collagen-water relationship, rather than leather type. After considering all the results presented, it was realised that changes in the modulus during the dehydration of a leather must be related to the different states of water[63-66]. From the results, a generic curve for drying of leather was compiled and presented in Figure 4.8.

Leather type		Chrome	Vegetable
% Collagen content		94.8	73.5
At inflection point *b*	% Moisture content (dry leather wt basis)	61.0	42.0
	% Moisture content (dry collagen wt basis)	**63.0**	**57.0**
At inflection point *c*	% Moisture content (dry leather wt basis (d.w.b))	30.0	27.0
	% Moisture content (dry collagen wt basis (d.c.w.b))	**32.0**	**36.0**

Table 4.1: Moisture content on the basis of collagen content at the inflection points in Figures 4.5 to 4.7.

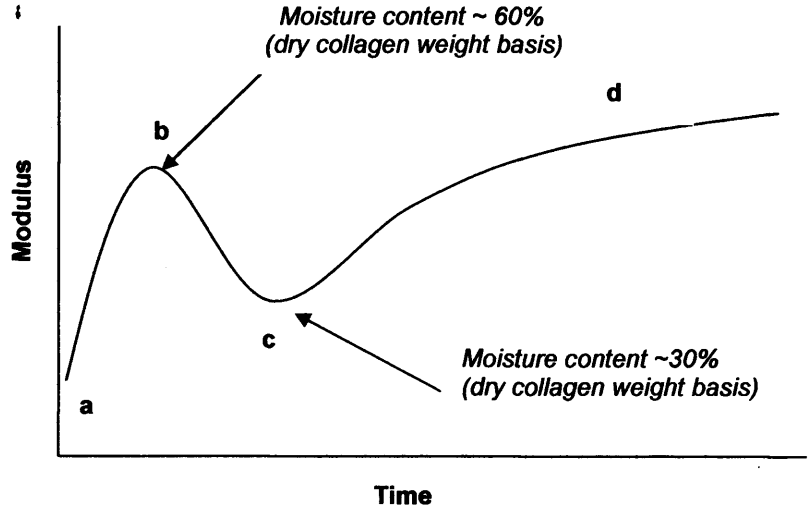

*Figure 4.8: Generic curve of changes in bend modulus during drying of a leather, showing the critical moisture contents, ~60% and ~30% (dry collagen weight basis), relating to the inflection points, **b** and **c**.*

Several researchers have studied the role of bulk water on the structural properties of collagen. From dynamic mechanical relaxation, Pineri and coworkers demonstrated that water molecules, which are present above 50% moisture content, can form clusters large enough to produce ice below 0°C[66]. This result is in agreement with calorimetry and NMR experiments, where freezable water was measured at water concentrations higher than 0.47 to 0.54 g water/g collagen[139]. The work of Kopp and coworkers[64] and Haly and Saith[65] supports this observation by providing further evidence for the presence of freezable water, which melts at 0°C.

To calculate the amount of freezable water in the leathers, DSC experiments were carried out on leather samples with different moisture contents. The endothermic transition peak at 0°C was integrated to obtain the amount of freezable water inside the leather sample. A few representative DSC thermograms are given in Appendix 9. It is apparent from Figure 4.9 that the non-freezable portions of water of leathers tanned with chrome and vegetable tannin are approximately 61% and 42% respectively. When these values are normalised to the weight of collagen in the leathers, as indicated by Table 4.1, both leathers contain approximately 60 ± 3% moisture on dry collagen weight basis. This value is in agreement with the limiting value quoted in the literature for the freezable water of collagen. Therefore, the initial increase in bend modulus (from **a** to **b** in Figure 4.8) is attributed to the removal of freezable water from the leather.

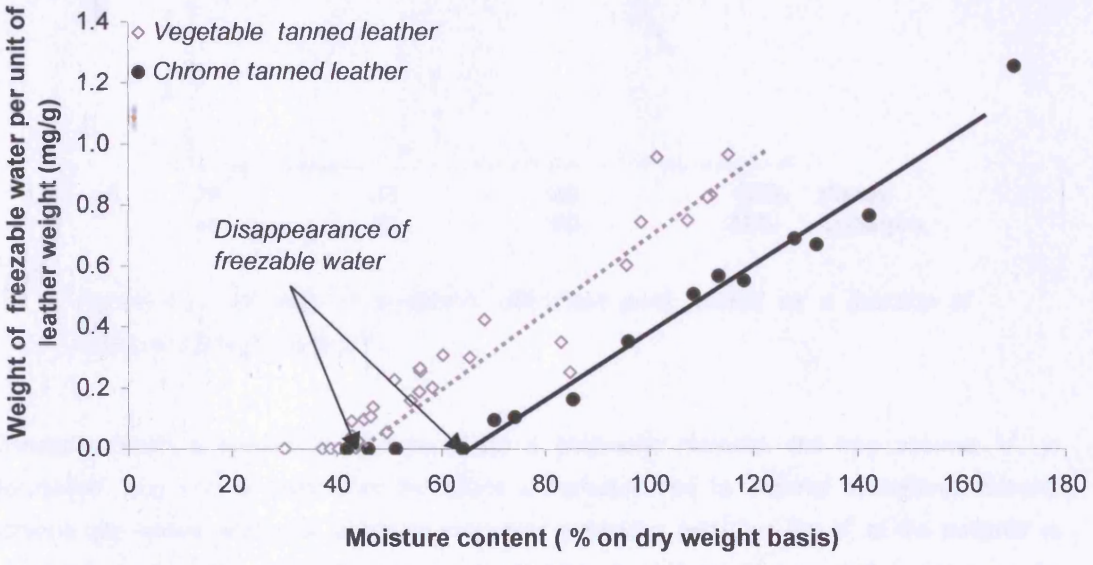

Figure 4.9: Freezable water detected by DSC plotted against total water content of the leather sample.

Heidemenn and Keller analysed the intensity of the equatorial diffraction peak of collagen at various moisture contents by X-ray diffraction, using a goniometer with impulse counting[70]. They

observed that the intensity of the diffraction goes through a maximum as water content is increased, as indicated by Figure 4.10. The implication of this observation is that the molecular packing of collagen is dependent on the moisture content and maximum order is achieved when the sample contains approximately 33% moisture on wet weight basis or 49% moisture on dry weight basis. Therefore, during the initial stage of drying, order within the molecular packing increases. Thus, storage modulus is expected to increase with decreasing moisture content until optimum molecular order is reached at 49% moisture content[12]. The initial increase in storage modulus from a to b (Figure 4.8) may also be attributed to an increase in the crystallinity of the collagen.

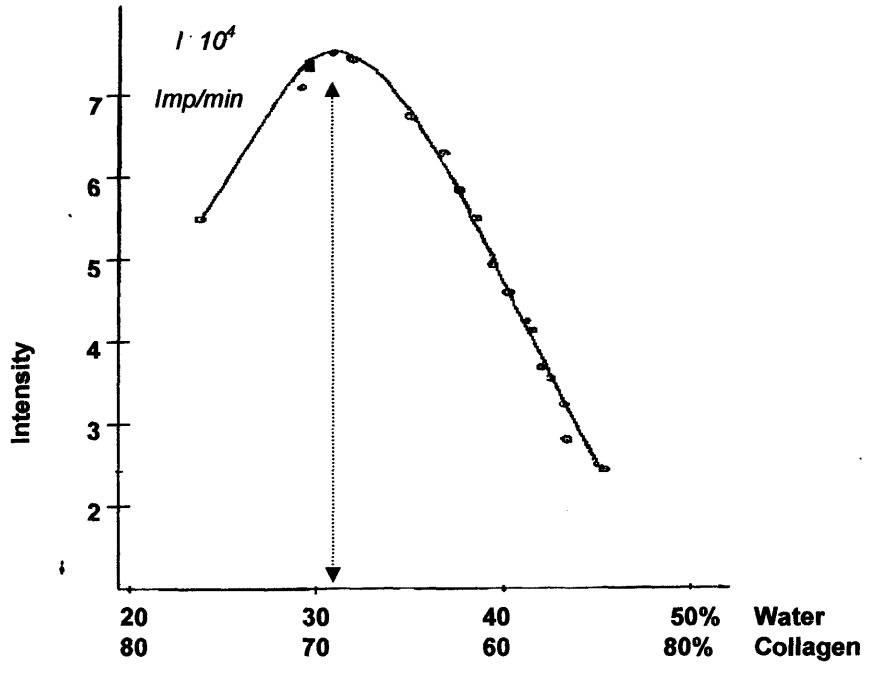

Figure 4.10: Intensity of equatorial diffraction peak plotted as a function of moisture content of a hide[70].

Generally, when a solvent is removed from a polymeric material, the free volume, V^f, is decreased, where V^f is defined as the space a molecule has for internal movement. Solvent screens any mutual attraction between polymeric molecules and thus the V^f of the polymer is increased. Hence, the removal of any solvent from a polymer is expected to increase its modulus[156].

The relative position of the collagen molecules within the ordered structure can be determined by analysing the X-ray diffraction pattern. The distance between the equatorial spacing gives a direct measurement of the spacing between collagen molecules. For rat-tail tendon, it is reported that

the diffraction spacing increases from 1.09 nm to a limiting value of 1.33 nm with the absorption of water[69]. Moreover, from this observation, the V^f of collagen molecules increases with absorbed water up to a limiting value. Figure 4.11 shows the effects of water content on the wide-angle equatorial spacing of collagen. Point b represents the limiting moisture content value, where side-chain distance is unaffected by further absorption of water. Below point b, the side-chain distance begins to decrease with decreasing moisture content, which indicates collagen molecules coming closer to each other. This figure also suggests that absorbed water will not impose an influence on the free volume of collagen molecules above 60% moisture content.

Theoretically, the modulus would be expected to increase continuously beyond the inflection point ***b*** of the DMTA trace (Figure 4.8). However, the result indicates otherwise, giving a strong indication that other structural changes must be responsible for the decrease in bend modulus between ***b*** to ***c***.

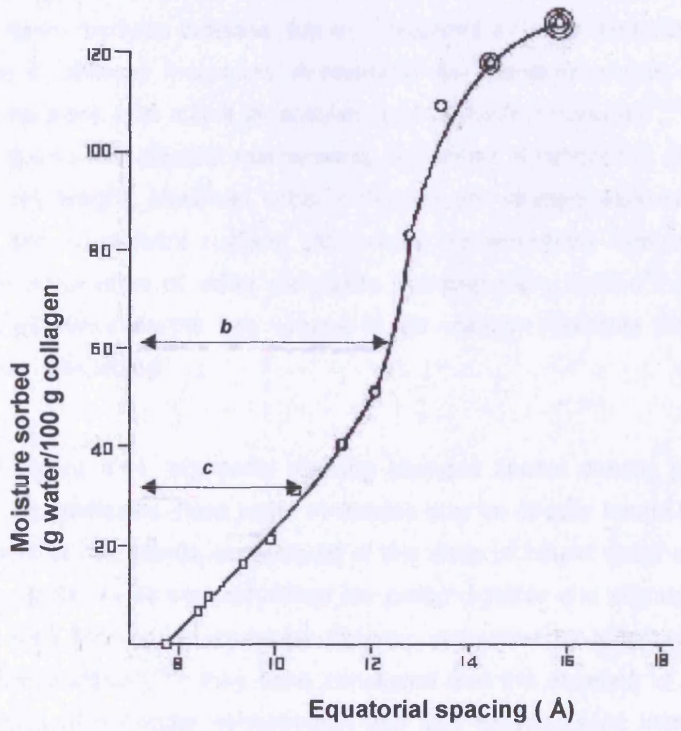

*Figure 4.11: Influence of moisture content on the major equatorial spacing, based on data of Figure 2, of Rougvie and Bear[120], points **b** and **c** represent the moisture contents of the inflection points in Figure 4.8.*

There are two possible explanations of the decrease in modulus from ***b*** to ***c*** (Figure 4.8). First, the decrease in modulus is in terms of decreasing crystallinity of the collagen molecules[12]. At the

critical moisture content of 60% (d.c.w.b), all the water molecules are associated with the molecular packing of the collagen molecules. When this associated water is removed, change to the molecular packing order is inevitable and hence as illustrated in Figure 4.10, crystallinity decreases with further removal of water. Thus, increasing disorder of the crystalline structure will be reflected in the reduction in the modulus values with decreasing moisture contents. The second possible explanation for the observed decrease in modulus might be due to the changes in fibril dimensions. Komanowsky has demonstrated that, as water is removed from the space between fibrils, rapid longitudinal and lateral shrinkage of fibrils takes place; this process occurs as the average moisture content drops from about 50% to about 27% (d.c.w.b) [84]. This moisture content range coincides with the decrease in modulus (from ***b*** to ***c*** in Figure 4.8). These dimensional changes are expected to allow more freedom of movement to the fibre network, so a decrease in bend modulus is expected with the decreased fibre size.

It is also noticeable from Figure 4.8 that, regardless of the drying temperature, the modulus begins to increase again after another critical point ***c*** is reached. This is probably the limiting moisture content, when modulus increase due to V^f changes exceeds modulus decrease due to structural changes in collagen molecules. A review of the literature reveals that the moisture content at the critical point, ***c***, is a limit for another state of water in collagen[63,66]. This increase in modulus may be due to two different mechanisms. A number of references suggest that below 23% on collagen dry weight, absorbed water molecules are strongly associated with collagen structure. Pineri and co-workers suggest that water concentrations between 11 and 23% correspond to the association of water molecules between triple helices[66]. Removal of such associated water will decrease the free volume of the collagen molecule further and thus an increase in modulus is expected.

Below point ***c*** of Figure 4.11, equatorial spacing changes almost directly proportionally with moisture content. This indicates these water molecules may be directly bound to the side chains of the collagen helix or microfibrils, so removal of this state of bound water molecules creates voids between the fibrils. To fill the void, fibres are pulled together and alignment of amino side chains may give fibre sticking. A molecular dynamic simulation by Mogilner and co-workers further illustrate this possibility[157]: they have concluded that the absence of associated water produces a distortion of molecular conformation and also introduces an increased number of hydrogen bonds. Therefore, it is possible that when bound structural water is removed, collagen molecules form crosslinks between them. This will restrict the molecular mobility of the collagen and will result in an increase in modulus. Hence, the storage modulus will increase. Once all the water that can be removed from the structure of collagen has been removed, the modulus will plateau. Furthermore, the DMTA drying profiles of leathers at various isothermal thermal conditions indicate only differences in the value of storage modulus are found between ***c*** to ***d***.

The implication of this observation is that the stiffness of leather is governed only by the final phase of drying.

Since leather contains a large concentration of hydrophilic groups, water absorption or removal depends not only on the physical fibre structure but also on the chemical composition of leather. From the argument presented here, the inflection points would be predicted at these critical moisture contents (60% and 30%) from the rate of drying curve. Figure 4.12 shows the rate of drying of wet blue in the controlled environment of 65% RH and 20°C.

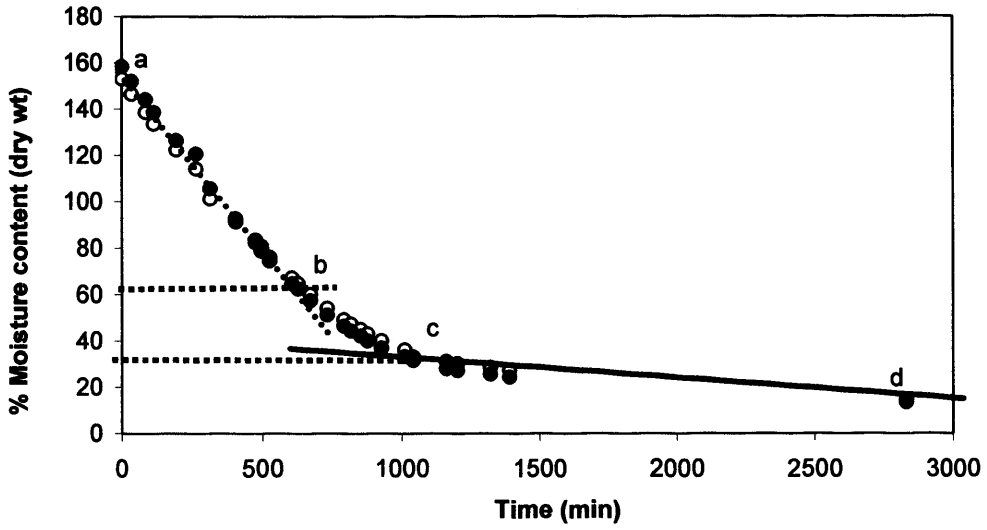

*Figure 4.12: Rate of drying curve; water content as a function of time of wet blue at 20°C and 65% RH. Segment **ab** is characterised by the constant rate of drying period, **bd** corresponding to the decreasing drying rate of drying period. Point **c**, where another inflection of rate of drying is observed.*

It is clear that constant rate of drying is replaced by a varying rate of drying at around 60-70% moisture. As predicted by the DMTA thermogram, the rate becomes inflected at point **c** (almost constant), when moisture content is approximately 30%.

From the DMTA experiments, the drying temperature does not control the molecular changes, which affect the leather during drying, rather they are controlled by residual moisture content. When a leather is dried at high temperature, this rate of drying is fast and hence structural water tends to be removed at a faster rate: this will introduce irreversible, intermolecular crosslinking between the collagen molecules. However, if the moisture content of the drying environment is controlled to maintain the moisture content of the leather above 30% (corresponding to point **c** in Figure 4.8), then an elevated temperature can be used for drying without any adverse affects.

To illustrate this point, a two stage drying process was performed, as described in section 4.3.6 and the resulting leather properties were assessed. Three point bending experiments were carried out to assess the stiffness of the leather. Tensile testing was also performed in order to assess if there had been any thermal degradation of the fibres.

Figure 4.13 shows how the bend modulus changes with drying temperature. The modulus of the experimental set of leather dried at controlled humidity is smaller (i.e. softer) than the control set. As expected, the difference diminishes when the drying temperature approaches ambient drying conditions (i.e. room temperature). Figure 4.13 demonstrates that the two stage drying process, when humidity is controlled, can confer softness to leathers, even when high temperatures are used. This confirms the observation from the DMTA thermogram, which suggests that the stiffness property of leather is only governed by the rate of removal of moisture below the inflection point c (refer Figure 4.8).

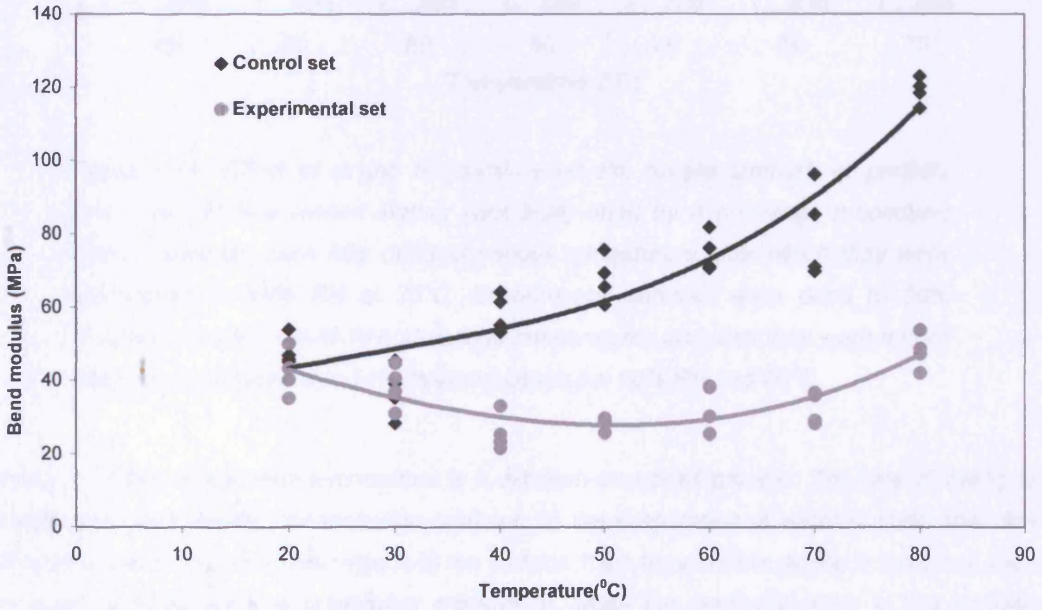

Figure 4.13: Effect of drying temperature on bend modulus, indicating stiffness (higher the value, the stiffer the sample). Control samples were fully dried at various temperatures after which they were conditioned to 65% RH at 20°C. Experimental samples were dried to 30% moisture content at various temperatures and then they were further dried by conditioning to 14% moisture content at 65% RH and 20°C.

In tannery drying procedures, when leather is dried at high temperature, the stiffness is generally found to be high. Therefore, it is typically believed that stiffness has a high dependency on the

drying temperature. However Figure 4.13 demonstrates that high degree of softness can be obtained, even with high temperature drying, if the water-leather relationship is controlled during the drying procedure. Figure 4.14 presents the tensile strength results of two stage drying process and the control set. It is seems that strength of the leather is not affected greatly by the drying temperature.

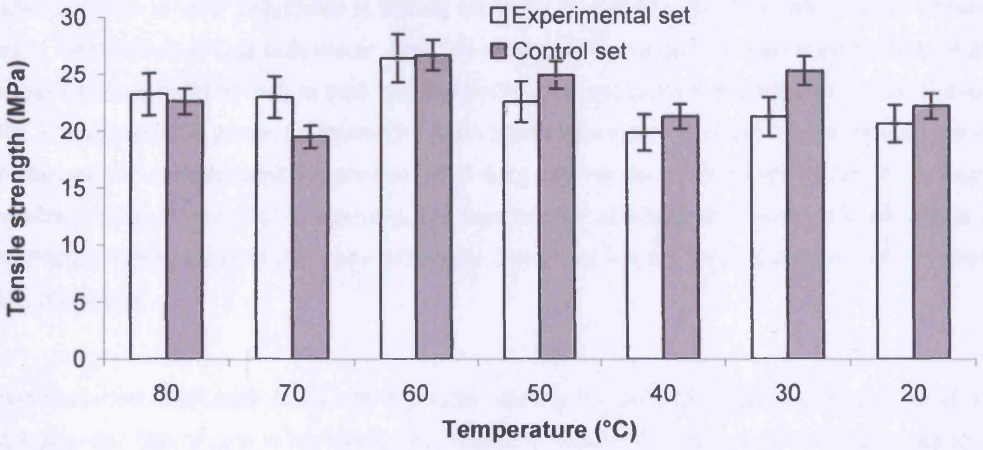

Figure 4.14: Effect of drying temperature on the tensile strength of partially processed chrome tanned leather (wet blue) dried by a two-stage procedure. Control samples were fully dried at various temperature after which they were conditioned to 65% RH at 20°C. Experimental samples were dried to 30% moisture content(~ 80% RH) at various temperatures and then they were further dried by conditioning d to 14% moisture content at 65% RH and 20°C.

Drying of leather at elevated temperature is a diffusion-controlled process. The rate of drying is entirely dependent on the concentration gradient, as the evaporation of water is faster than the diffusion of water from interfibril regions to the surface. If the temperature drying is too great, then the outer surfaces become irreversibly crosslinked, when the structural water is lost through evaporation. Once fibre sticking is introduced into the collagenous matrix, re-humidifying will not replace the lost structural water to the same extent as before, hence a high bend modulus was obtained (Figure 4.13) for the control leathers dried at high temperature.

When drying the leather at controlled humidity, the rate of drying is still a diffusion-controlled process at high temperature. When the equilibrium moisture content is approached, the rate of drying will slow down. This can lead to a slow rate of drying in the final stages of drying. If the relative humidity of the drying environment is high enough to stop any structural water being replaced, then drying the leather at high temperature will be faster, with no undesirable effect on stiffness.

If Komanowsky's arguments are included in this explanation, then greater insight into the critical moisture content at the inflection points ***b*** and ***c*** (Figure 4.7) can be attained[84]. He utilised the principles of surface chemistry to follow the events associated with different stages of water removal from leather during the drying procedure. He explained why a high degree of shrinkage of fibres occurs when moisture content drops from about 50% to 27%, based on the hydrostatic pressure inside the smaller and larger capillaries of leather. During the initial stage of drying, the water lost from smaller capillaries is quickly replaced by capillary "suction" from larger capillaries. Water freezable at 0°C is bulk water, possibly located in the larger capillaries (inter-fibre regions). Larger capillary regions vary in size and the hydrostatic pressure is reported to be lower than 3.5 atm. The hydrostatic pressure generated during the evaporation of water molecules will therefore not exceed the somatic swelling pressure (3.5 atm) and hence no shrinkage of fibre dimensions is expected. Thus, removal of freezable water from leather at elevated temperature will give a clear advantage with respect to time and efficiency, but there will be an undesirable consequence of fibre shrinkage.

After the larger capillaries have lost the water, during the second stage of drying (***b*** to ***c***), water from the inter fibril region is removed. This region is reported to have 1.55 nm capillaries and the hydrostatic pressure is reported to be –18.2 atm, which is greater than osmotic swelling pressure and hence a noticeable shrinkage of fibres is expected. A further shrinkage of fibrils occurs when water from the gap zone (hydrostatic pressure -78 atm) is removed. During this stage of drying, due to the fibre shrinkage as well as the decrease in crystallinity of the collagen molecules (Figure 4.8), modulus is decreased. Employing high temperature to remove moisture between 60% to 30% (dry weight basis) will not have an adverse effect on the fibre quality, since the collagen molecules are not expected to form crosslinks between each other.

During the final stage of drying, water molecules that are removed must be from the intra-fibril regions. Figure 4.11 (region below point ***c***) shows that the equatorial spacing between the collagen molecules is directly proportional to the moisture content. When water from the intra-fibril region is removed, for example at 20°C, the hydrostatic pressure (-27.7 atm) is greater than the swelling pressure and thus considerable fibre shrinkage is expected. If the leather is to be dried at elevated temperature during this phase of drying, the hydrostatic pressure, which is also temperature dependent, will be higher and hence the faster the shrinking process will be and hence will result in fibre sticking. High temperature also facilitates permanent crosslinking between collagen molecules by supplying the required activation energy. The DMTA trace of drying (Figure 4.7) has identified the second critical moisture content region (inflection point ***c***), when fibre sticking begins to affect fibre stiffness.

4.4 Summary

The process of dehydration or drying of leather is more complex than the mere removal of moisture. It affects not only the final physical and mechanical properties of leather, but also its aesthetic feel. From the results presented here, it can be concluded that leather may be dried at high temperatures to give softer product, as long as humidity is maintained at high enough values not to allow moisture content to fall below 30%. From a practical point of view, under carefully controlled humidity, leather can be initially dried at high temperature. Therefore a two stage drying is recommended.

Stage 1: Removal of moisture until 30% moisture by dry weight basis is achieved, when any type of drying method (utilising high temperatures) can be used.

Stage 2: Carefully controlled removal of associated water to achieve the required moisture (14%).

Wet leather undergoes a glass transition between 40-80°C, depending on the tannage. Therefore, if the leather is stretched and dried above its glass transition, the area gained will be stable, as observed for other polymers including wool, This phenomena will be investigated in the next chapter.

Chapter 5

EFFECT OF TEMPERATURE ON THE STRESS RELAXATION AND PLASTIC DEFORMATION/SET OF LEATHERS

5.1 Introduction

Leathers undergo mechanical stressing during processing, in operations such as samming, setting, toggle drying and staking. Some of these operations cause the leather to undergo stress relaxation and this will positively contribute to the permanent deformation of leather. For example, during the drying under a fixed strain, substantial stress relaxation occurs and is known to increase the area significantly, however the stiffness of the leather is also known to increase with applied strain[158]. This is reported to be due to the alignment of fibres in the direction of applied stress, which favours ordering within the leather fibres and hence higher elastic modulus and stiffness are obtained[158-160]. Leathers dried under tension also tend to have other undesirable physical properties, such as low extension at break[158]. Therefore, an industrially acceptable process that increases area must avoid any undesirable alteration in physical properties.

Amorphous polymeric materials show quite different mechanical properties depending on the temperature or time scale of the experiment[2]. Particularly at temperatures below the glass transition, behaviour is predominantly elastic, whilst above the glass transition it is predominantly viscous; in the transition region, both types of response make a significant contribution. These differences in the flow properties are often reflected in the temperature dependent physical properties of such materials[12]. Leather may be considered to be a semi-crystalline material (refer to Chapter 3) and its viscoelastic response will therefore be dependent on its T_g. However, the viscoelastic behaviour of leather not only arises from the molecular structure of collagen but also depends on the persistence of the entanglements of the long fibres; the presence of plasticisers and degree of crosslinking. Consequently, the ability of the molecules and fibres to move past one another is limited. Moreover, if the linkages (covalent, electrostatic, hydrophobic etc) between the fibres are broken, then this will result in the flow properties of the fibres being altered. Thus theoretically, at elevated temperature, collagenous materials should show different rheological properties.

Thermal energy is used to achieve permanent deformation/set in fibres such as wool and cotton and this process is widely known as heat setting [161-163]. Although such a principle is used in the lasting of shoes it is not applied in leather production. In order to understand the heat setting process, an understanding of the relaxation profile and the deformation properties of leather at various temperatures are needed. Therefore, in this chapter the stress relaxation and plastic deformation properties of leather at various temperatures were investigated and the results are presented in this Chapter.

5.1.1 Stress relaxation and plastic deformation/set

One important means of studying viscoelastic behaviour is to examine the relaxation of stress (force/area) of material held under tension. When an instantaneous stretch is applied to a material, the material responds by exerting an instantaneous stress followed by a time-dependent decrease in stress, when held under constant strain. A perfectly elastic material stores all of the energy created by the deforming force so that on removal of that force, it can return to its original dimensions. By definition therefore, a perfectly elastic material does not exhibit stress relaxation. In a perfectly viscous fluid, on the other hand, the stress created by deformation relaxes instantaneously to zero because of molecular flow. Viscoelastic materials however display the properties of both elastic solids and viscous fluids and hence exhibit time-dependent stress relaxation behaviour.

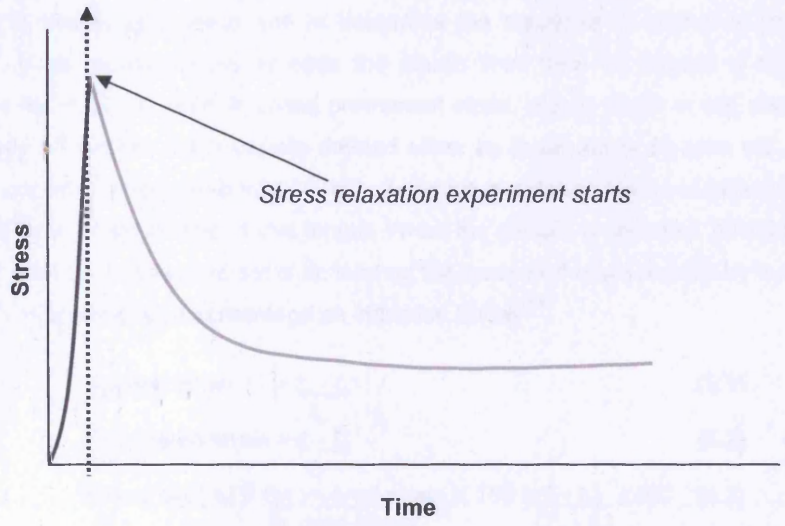

Figure 5.1: Schematic diagram of the curve obtained in a typical stress relaxation experiment. Leather is stretched at a predetermined strain rate, thus producing the stress-time curve shown to the left of the dashed line. The leather is then maintained at a defined strain and measurements of the stress is continued, resulting in the stress relaxation curve shown to the right of the dashed line.

In the stress relaxation test, a sample is quickly stretched to a set length and the decay of the stress exerted by the sample is measured. These are often difficult experiments, because the sample should ideally be strained quickly. In practice, a sample is initially stretched at constant rate of change rather than a sudden instantaneous stretch. A typical stress relaxation curve is presented in Figure 5.1.

This characteristic relaxation pattern is interpreted in terms of temperature activated molecular re-reorientation[2] (refer to Chapter 1, Section 1.1.1(a)). Over a short time range, the molecules react to applied force by stretching and slowly dissipate the energy by returning to their original length. In the case of tendon collagen, researchers have shown by X-ray diffraction that this phenomenon actually happens[165-167]. When a tendon is stretched while exposed to a beam of synchrotron radiation, its X-ray diffraction pattern shows that the strain induces an increase in the D-period, which disappears with stress relaxation. This result clearly indicates that applied stress induces deformation at the molecular level of collagen structure; the high potential energy results in high modulus values. As time proceeds reorganisation of molecules is possible and can occur. The molecular structure reconfigures to relieve local strains and a time dependent stress decay is observed. Theoretically, at longer times, molecules are expected to slide past each other to totally dissipate the stress of the system.

Another important property of leather is its ability to retain a degree of permanent strain following stretching. This viscoplastic property of leather is important, since it can be expected to influence area yield in leather production and to determine the response of leather in the shoe lasting process[163]. If an applied stress exceeds the elastic limit, then on release a residual strain is retained by the material which is called permanent strain, plastic strain or set, depending on the field of study. In leather, set is usually defined either by linear set or as area set. In the case of linear set, consider a sample of initial length, ℓ_o, which is extended to a predetermined length, ℓ_s, and is held for a period of time at that length. When the sample is released, it retracts to a length, ℓ_p (greater than ℓ_o). In this case set is defined as the recovered strain divided by the applied strain and usually expressed as a percentage as indicated below[164];

$$\text{Applied strain} = \frac{\ell_s - \ell_o}{\ell_o} \qquad (5.1)$$

$$\text{Recovered strain} = \frac{\ell_r - \ell_o}{\ell_o} \qquad (5.2)$$

$$\text{Linear set [\%]} = \frac{\text{Recovered strain}}{\text{Applied strain}} \times 100 = \frac{(\ell_r - \ell_o)}{(\ell_s - \ell_o)} \times 100 \qquad (5.3)$$

This definition is most used in the shoe industry. Another definition of set that has been used is simply to define set as the recovered strain, expressed as a percentage[164]. Unless otherwise stated, in this chapter, recovered strain is used for the characterisation of set. If a material is

subjected to multi-axial stresses, then set is characterised in terms of area changes using an approach similar to linear set.

5.1.2 Literature survey

Experimental and theoretical studies of the viscoelasticity of leather are limited. This is because the leather industry chooses the material on the basis of "fit for purpose" rather than for its thermo-mechanical behaviour. There are only a few papers, which deal with the relaxation properties of leather[16,84,164], but they fail to demonstrate a complete pattern of mechanical behaviour. Stress relaxation and creep experiments are often carried out in order to characterise the viscoelastic properties of a given material. An extensive study of the temperature dependence of the viscoelastic behaviour of leather will give the industry advantages in competing with synthetic polymers.

One approach to characterising these changes of stress and strain with time is to develop mathematical models. Researchers have used a generalised Maxwell model[16,168], a fractional Maxwell model[169], a linear combination of Kohlrausch-Williams-Watts models & a simple exponential decay function[170] and Burgers model[164] to calculate the relaxation profile of collagenous materials. To what extent such models can quantitatively describe the viscoelastic behaviour of leather remains to be investigated. Strictly speaking, such models can only be used to describe linear viscoelastic materials rather than non-linear materials like collagen. To have a universal mathematical model, which can be used to describe the viscoelastic behaviour of leather throughout a wide spectrum of temperature and strain is an impossible task, since the viscoelastic response depends highly on temperature and applied strain[171].

Komanowsky and his co-workers have studied the stress relaxation behaviour of dry, fat-liquored leathers[16]. They explained the complicated time dependent mechanical behaviour of leather using a generalised Maxwell model, consisting of three Maxwell units. They also described how both moisture and heat are necessary to cause leather to elongate permanently by a stress relaxation mechanism. Rigby and co-workers have examined the stress-strain and stress relaxation behaviour of rat tail tendon (RTT) with respect to strain, rate of strain and temperature[79]. They reported that elevating the temperature above 35°C caused a profound changes to the stress relaxation profile[172]. Their work suggests that permanent dimensional changes in leather can only be achieved by a thermal setting mechanism.

The effect of pH on the stress relaxation of RTT was studied by Usha and Ramasami and their results suggest that RTT relaxes faster as the pH decreases[173]. This can be explained in terms of molecular segmental motion. When collagen is in an acidic condition it behaves like a cation

(below its isoelectric point), when electrostatic crosslinks between the molecules are partially broken. The potential energy barrier for rotational and transitional motions of segments of the system is low. Collagen molecules can therefore dissipate mechanical energy through a sliding process faster at lower pH than at its isoelectric point.

Thermal setting processes have been used in the lasting of shoe-upper leather for a many years. Butlin has examined the plastic set of leather and reported that set increased with the amount of time the leather was held under applied strain[174]. He also demonstrated that this observed set was not permanent and decreased with time, after removal of the applied strain. Holmes and Ward studied the influence of dry heat setting and moist heat setting processes and pointed out that a moist heat setting process requires a lower applied force for setting than a dry heat setting process[175]. Dry heat setting produced area set as high as 60% as compared to steam heat setting which barely achieved an area set of about 40% after the same period of recovery. Their work also stated that set obtained through moist setting is a permanent deformation. The consequence of this observation is that there may be a temperature threshold, above which dissipation of applied energy is faster and hence permanent set.

When studying the mechanical properties of fully hydrated RTT, Rigby and Mason found that temperature has no effect upon the mechanical behaviour over the range 0 - 37°C, but above 37°C, they observed changes in the stress decay behaviour and permanent increase in set[86]. This suggests that permanent structural changes to hydrated collagen molecules are possible above this critical temperature of 37°C. The author has indicated that for this particular sample the shrinkage transition is 59°C and glass-like transition is 36°C (hydrated condition). Most possibly, the critical temperature above which a marked change in the set obtained, was a T_g.

Thermal setting is a well practised process in the fibre and textile industries and setting of wool has been studied extensively[161-163,176]. The literature states that in order to achieve a permanent set, the material needs to go through a phase transition (either T_g or melting). It also points out that the setting behaviour of a material is dependent on free volume. At and above a phase transition temperature, molecules can readjust their positions; due to the increased free volume on subsequent cooling they can establish new equilibrium positions. This is widely known as the molecular reorientation.

There are publications which indicate that stretching of wet native collagen creates an increase in the D-period, which stress relaxation causes to disappear over time[165-166,178]. This is an indication that changes in molecular rearrangement do occur and this contributes to stress relaxation in collagenous materials. These changes can be observed in the meridional small angle X-ray diffraction pattern. Mosler *et al.* have investigated tension-induced molecular rearrangements in wet native fibres of RTT and human finger flexor tendons (HFFT) by synchrotron radiation, in a

procedure known as time resolved diffraction[166]. They reported that the tension induces an increase in the D-period, but this is completely reversible on removal of the tension. They interpret the increase in D-period as partly due to a stretching of the triple helices themselves and partially due to a stretching of the crosslinked telopeptide regions. Folkhard et al. have reported that when a native fibre is held under stretch, the initial increase in D-period due to stretching decreases to its original value of 67nm[177]. Although the D-period relaxes back to the original value, 30% of the applied strain remains, indicating that deformation (set) has taken place. The decrease of the D-period occurring over time at constant elongation of the fibres indicates a mechanically retarded sliding and retraction of elastically lengthened units. The decrease in tension of the fibres is an indication of the dissipation of mechanical energy during the sliding process. They also concluded that there is a overwhelming evidence that in the wet state the triple helices stretch and slide past each other.

All the evidence so far points out that the set produced by stretching dry leather at room temperature is not permanent. In order to produce a permanent deformation of leather, elevated temperature and high moisture content are required. It is hypothesised that at elevated temperature and high moisture content, changes at the molecular level of leather are needed in order to cause the fibre structure to set in a new permanently stable form. Thus, it is further hypothesised that such changes are only expected to happen above a form of transition (helix-coil or T_g) in the leather.

5.2 Experimental procedure

5.2.1 Materials

Following the procedure given in Appendix 5, chrome tanned and vegetable tanned leathers were made with 8% offer of 25% basic chromium sulfate or 20% offer of tara (hydrolysable vegetable tannins) respectively. These leathers were not subjected to the fatliquoring process, in order to avoid the lubricating effect of fatliquor. From each, 160 x 10 mm strips were cut parallel to the backbone, then they were stored at low temperature (5°C).

5.2.2 Stress relaxation and set measurements

Experiments were carried out using uni-axial stretching to study the stress relaxation and set behaviour of leather. Figure 5.2 shows a schematic diagram of the custom-made tensometer (built by Avocet Engineering, Bristol, UK.), which was used for these experiments.

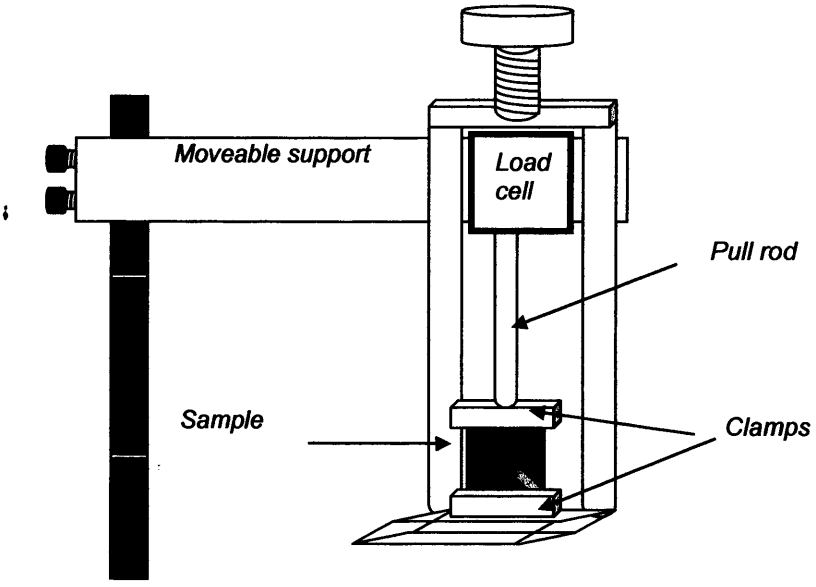

Figure 5.2: Diagrammatic representation of the stress relaxation apparatus (mini tensometer)

160x10 mm dumb-bell shaped samples were cut parallel to the backbone from fully hydrated samples. After measuring the thickness of the sample, two parallel lines were drawn 100 mm apart (Figure 5.3). The sample was then clamped between the jaws of the tensometer and immersed in a temperature controlled water bath (30-90°C) for 30 minutes. The sample was then stretched at a speed of 100 mm/min to give 5 to 30% strain, which was then maintained for 30

minutes while the force with time was recorded. After the 30 minute period, samples were removed from the tensometer and then their length measured both immediately, and after drying under standard conditions. In order to calculate the set after drying, a control sample was subjected to the same hydrothermal treatment, but with no stretching. Stress values, σ, were calculated by dividing the experimental load on each sample by its initial (unstretched) cross sectional area.

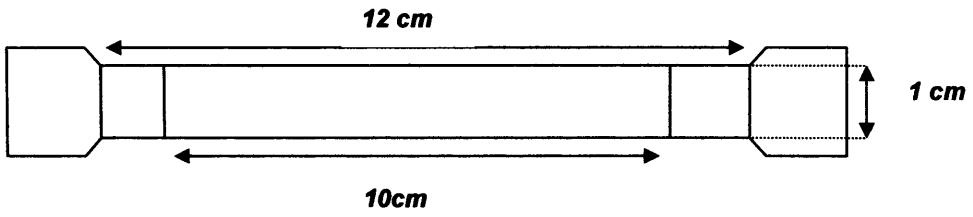

Figure 5.3: Sample dimension for stress relaxation studies

Immediate set (wet) and set after drying (dry) were calculated by equation 5.4 and 5.5 respectively.

$$\text{Immediate set [\%] (wet)} = \frac{(\ell_m - \ell_o)}{\ell_o} \times 100 \qquad (5.4)$$

$$\text{Set [\%] (dry)} = \frac{(\ell_d - \ell_c)}{\ell_c} \times 100 \qquad (5.5)$$

Where
- ℓ_o - original length (10 cm)
- ℓ_m - length immediately after removal of load.
- ℓ_d - length after drying
- ℓ_c - length after drying of unstretched control sample

5.2.3 Dynamic mechanical testing

The dynamic mechanical properties of wet leathers were obyained as described in section 2.2.2.

5.3 Results and discussions

The stress relaxation profile of fully hydrated vegetable (tara) tanned leather at 30°C is given in Figure 5.4. This shows the relationship between stress relaxation and applied strain. It is clear that, as expected, the initial (maximum) values of force increase with applied strain. When the initial force needed to stretch the leather is plotted against applied strain, as given in Figure 5.5, it is clear that, at an elevated temperature of 55°C, the force required to stretch the leather to any given strain is lower than that required at the lower temperature of 30°C. This indicates that at higher temperatures, either the fibres within leather exert lower frictional forces or they have greater tendency to flow; hence less force is needed for stretching them. One possible explanation for this observation might be the differences in the viscoelastic properties above and below the glass transition of leather. As discussed in Chapter 3, the amorphous portion of collagen is flexible above its glass transition and therefore dissipation of the applied stress is faster. Thus, faster relaxation occurs above the glass transition of the leather and lower force is required for stretching.

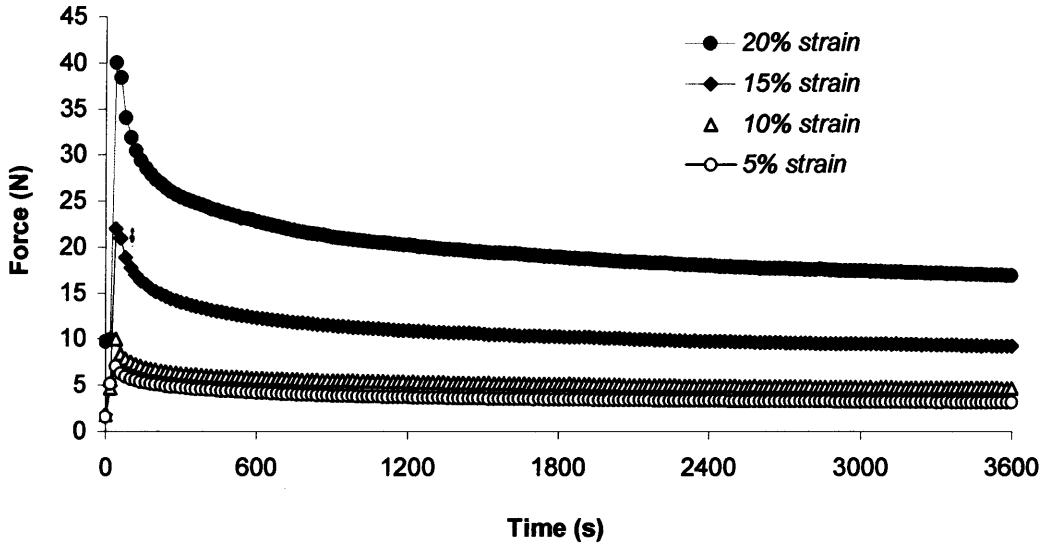

Figure 5.4: Relationship between stress relaxation and applied strain for a vegetable (tara) tanned leather at 30°C.

Fibrils in leather are held together by hydrophobic and electrostatic bonding. When leather is stretched, the fibrils may slip past each other breaking the cohesive forces between them. This requires activation energy. Such energy is readily available at elevated temperatures. Therefore, it is likely that breaking and reforming of bonding at elevated temperatures also allows structural relaxation to occur at a relatively faster rate within the leather fibrils. Therefore stretching the leather at elevated temperature requires lower force.

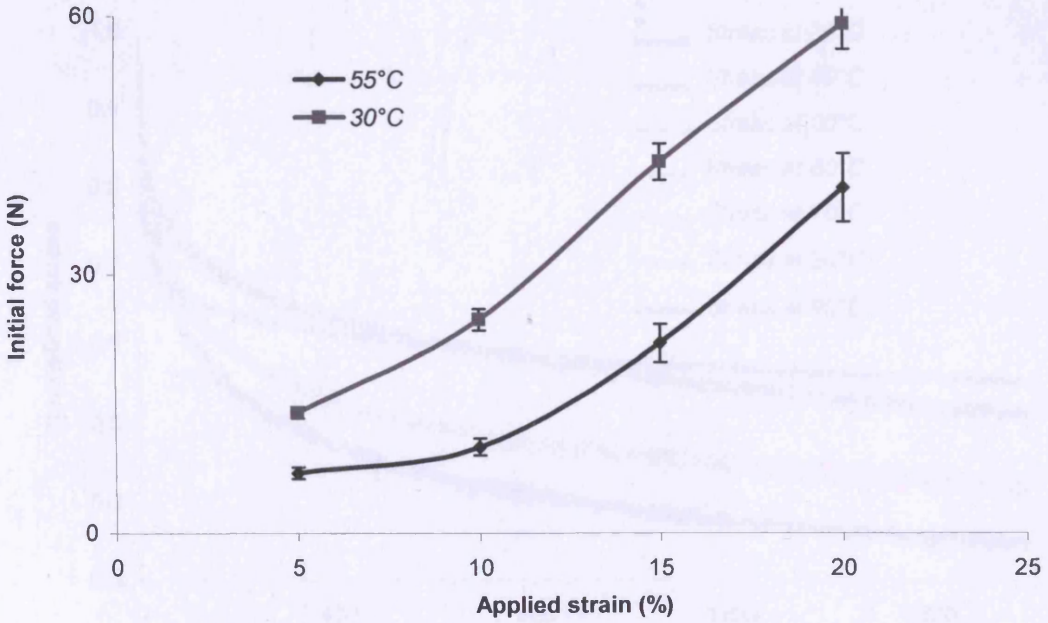

Figure 5.5: The effect of temperature upon the force needed to stretch vegetable (tara) tanned leather by 5, 10, 15 and 20%.

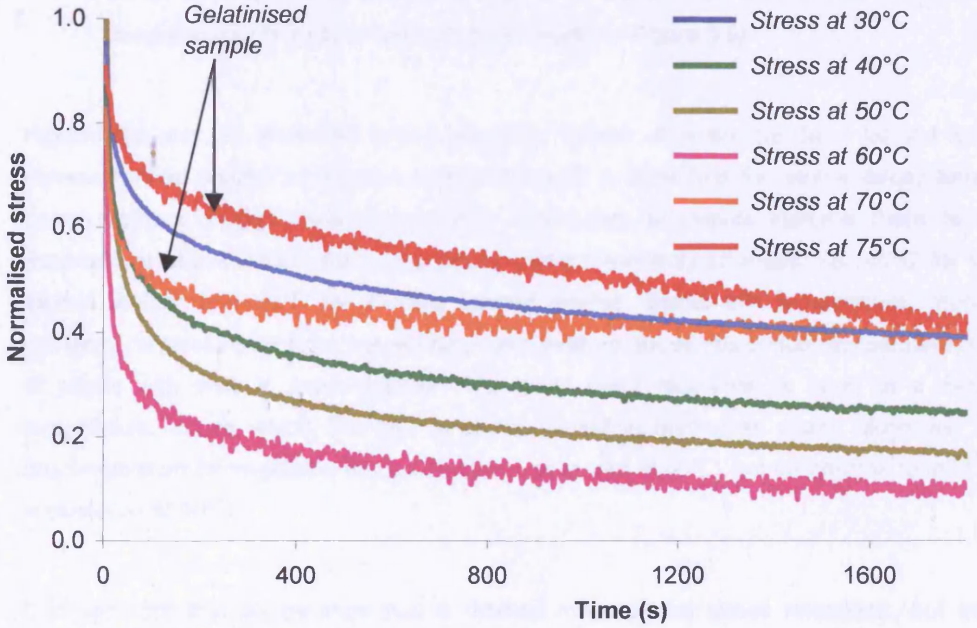

Figure 5.6: Normalised stress decay of vegetable (tara) tanned leather at various temperatures and when held at a strain of 20%: faster relaxation occurs above 40°C and optimum relaxation occurs at 60°C. The viscoelastic transition temperature (β) for this leather is 39°C (Refer to Figure 5.8).

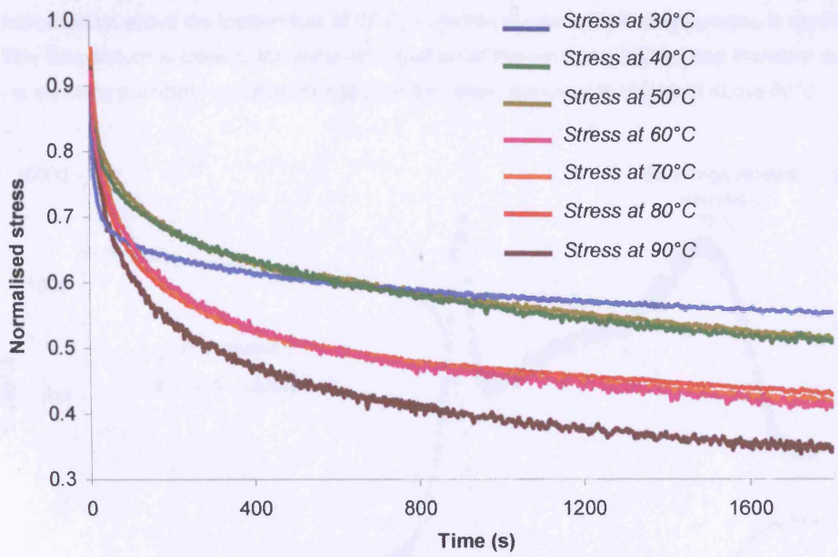

Figure 5.7: Normalised stress decay of chrome tanned leather at various temperatures and when held at a strain of 20%: faster relaxation occurs above 60°C and optimum relaxation occurs at 90°C. The viscoelastic transition temperature (β) for this leather is 52°C (Refer to Figure 5.9).

Figures 5.6 and 5.7 show the stress relaxation curves of vegetable (tara) tanned leather and chrome tanned leather at different temperatures. It is clear that the stress decay behaviour of these leathers changes with temperature. Both sets of results indicate there is a critical temperature above which the stress decay pattern suddenly changes; i.e. 40°C for vegetable tanned leather and 50°C for chrome tanned leather. Below this temperature, there is little relaxation of stress over time, but at higher temperature above this critical temperature, the decay of stress with time is much greater. The most rapid relaxation is seen at a certain high temperature, above which, the rate of stress relaxation decreases again. Moreover, the most rapid relaxation for vegetable tanned leather is observed at 60°C, but for chrome tanned leather it is observed at 90°C.

It is apparent that temperature has a marked influence on stress relaxation, but this is not straightforward, because the rate of stress relaxation at first increases then decreases with increasing temperature. The explanation of this observation is that leather displays glass transitions as indicated by Figures 5.8 and 5.9. At temperatures below the glass transition, the individual segments of the polymer chain are unable to move rapidly in response to applied stress and so the relaxation is slow. At temperatures above the glass transition, collagen molecules are

able to change conformation more easily and so faster relaxation is observed. Figure 5.6 indicates that above the temperature of 60°C, a marked decrease in stress relaxation is observed. This temperature is close to the shrinking transition of this particular leather and therefore due to the shrinking transition, a marked decrease in the stress relaxation is observed above 60°C.

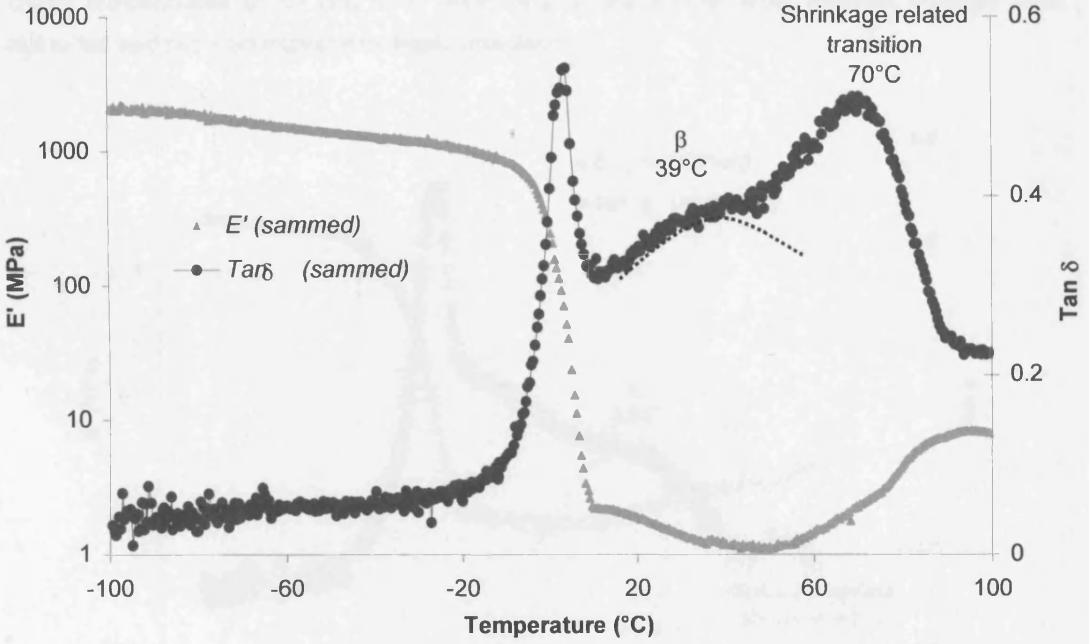

Figure 5.8: A DMTA thermogram of wet vegetable (tara) tanned leather, black filled circles (•) represent the loss tangent of the phase angle, tan δ, and filled triangles (▲)represent storage modulus, E', as a function of temperature. Note, the shrinking related transition, T_s, at around 70°C and the glass transition, T_β, at around 39°C. The transition at 0°C is due to melting of water.

Figures 5.8 and 5.9 show the DMTA traces of wet vegetable tanned leather and chrome tanned leather respectively. Wet leather also shows the liquid-solid phase transition of ice at 0°C. The DMTA trace for both leather types indicates a broad viscoelastic transition region stretching from 10 to 90°C. This region coincides with the temperatures range within which stress relaxation experiments which were performed and might be the reason why no distinct glassy region was observed (refer to Figure 5.10)

It has been shown in detail in Chapter 3 that glass transitions in leathers have dependency on moisture content. The DMTA experiments were performed in an open system, when moisture from the samples may evaporate during the course of the experiment. In the case of vegetable tanned leather, a pronounced shrinking related transition is observed at around 70°C, but in the case of chrome tanned leather only a small tan δ peak is observed at 95°C relating to the

shrinking related transition. Shrinkage temperature measured by DSC shows good agreement with results obtained from the dynamic mechanical experiments (refer to Table 5.1). The DMTA trace shows other broad viscoelastic transitions below the shrinkage transition. Therefore, it should also be appreciated that other structural relaxations (glass transition) take place in the wet leather at temperatures well below the shrinkage temperature. This is the reason why, above the critical temperatures of 40 and 60°C depending on the leather type, leathers undergo rapid relaxation and show an increase in stress relaxation.

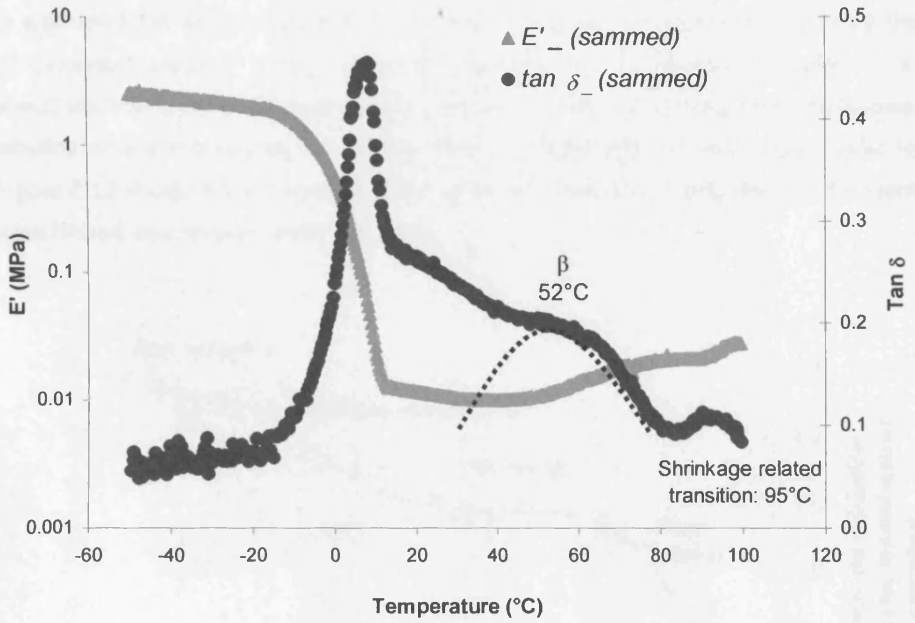

Figure 5.9: A DMTA thermogram of wet chrome tanned leather, filled circles (●) represent the loss tangent of the phase angle, tan δ, and filled triangles (▲) represent storage modulus, E' as a function of temperature. Note, the shrinking related transition, T_s, at around 95°C and the glass transition, T_g, at around 52°C.

Shrinking is a rate dependent phase transition and near the shrinkage temperature region quite different stress relaxation behaviour is expected. Above this transition, the collagen structure is completely altered and the resultant material, gelatin (partially or completely lacking the tertiary structure of collagen), shows a different stress relaxation profile.

Sample	***T_s (°C) determined by DSC***	***T_s (°C) determined by DMTA***

Chrome tanned leather	102 ± 2	95 ± 3
Vegetable tanned leather	79 ± 3	70 ± 5

Table 5.1: Shrinkage temperature of experimental leather samples.

Having examined the stress relaxation properties of leather, it is logical to compare them with specific behaviour patterns found with other polymers. As discussed in Chapter 1, a typical amorphous polymer shows four regions of viscoelastic behaviour and they are: the glassy region, the transition or leathery region, the rubbery plateau region and the flow region (refer to Figure 1.1). Figure 5.10 shows the ten-second stress relaxation modulus as a function of temperature for vegetable tanned and chrome tanned leathers.

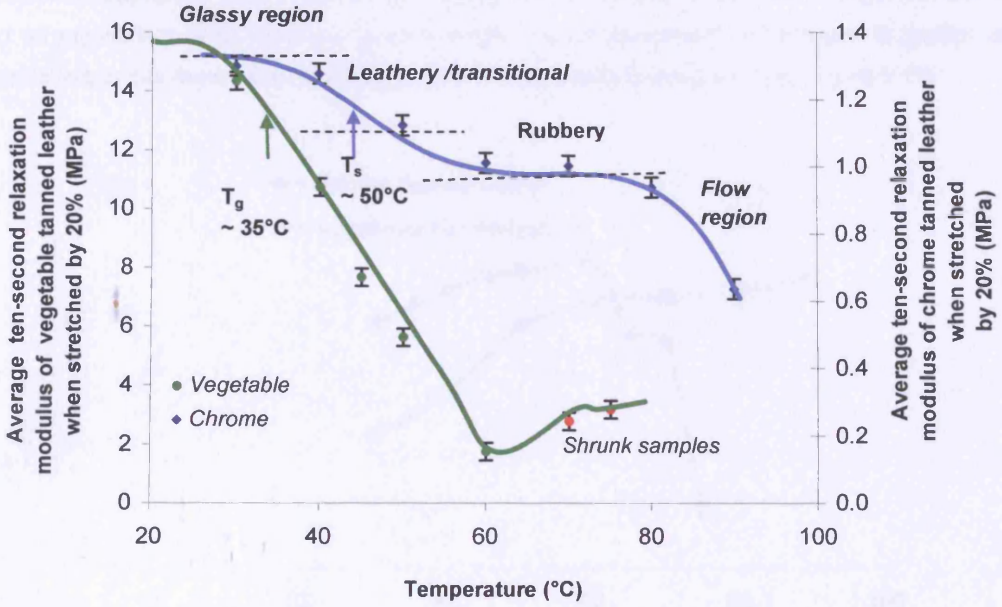

Figure 5.10: Ten-second relaxation modulus versus temperature curves showing various regions of viscoelastic behaviour for vegetable and chrome tanned leathers.

It is clear that they show different types of viscoelastic behaviour. Chrome tanned leather behaves in a similar way to the ideal polymer (refer to Figure 1.1), showing distinct viscoelastic regions, whereas vegetable tanned leather does not show any distinct regions. This may be explained by

the overlapping of glass transition and shrinking related molecular relaxation processes (refer to DMTA traces shown in Figure 5.8). Hence, vegetable tanned leather does not show a distinct rubbery region. It is therefore possible to conclude that the viscoelastic behaviours of vegetable tanned and chrome tanned leathers are different. These differences are reflected in the molecular relaxation and they show maximum stress relaxation at different temperatures, 60°C and 90°C respectively (refer to Figure 5.11).

Figure 5.11 shows set obtained after drying (equation 5.5) as a function of temperature. It is clear from these graphs that set increases with increasing temperature and reaches a maximum, beyond which set decreases for vegetable tanned leather, due to the low shrinkage temperature of that leather. When stress relaxation is applied close to the shrinkage temperature of leather the fibres will start to shrink, hence a decrease in set is observed.

For polymeric materials including leather, if a sample is stretched in the flow region, then the polymer molecules will slip by one another with ease, releasing the applied stress over time. When the applied strain is released, the sample will not recover to its former length but will relax to an equilibrium state having a greater length. Hence permanent deformation is greater after stretching in this region than stretching in other viscoelastic regions (refer to Figure 5.11).

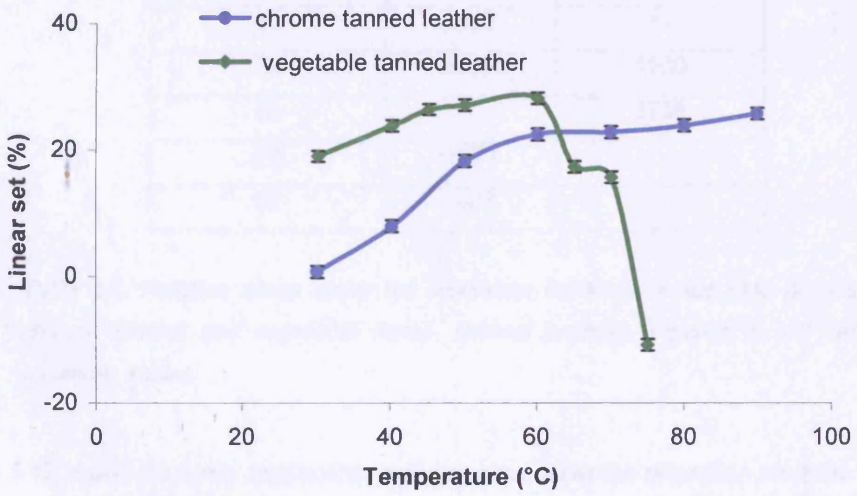

Figure 5.11: Relationship between set and thermal treatment temperature of vegetable tanned and chrome tanned leathers, stretched by 20%.

One interesting way to analyse the stress relaxation data is to consider the relationship between set and the area under the modulus vs. time curve, the apparent viscosity[12] (Appendix 10). Viscosity is defined as the resistance to flow, hence the lower the viscosity (as measured by the

area under the curve) then the higher the tendency to flow will be (i.e the lower the area under curve, then the greater the tendency to flow). Although leather is a solid material, it should be possible in principle to see how the temperature affects the flow properties. From the stress relaxation data, a time dependent relaxation modulus was calculated by dividing the time dependent stress by the applied strain (0.2). From the data, the modulus-time curves were plotted and the area under curve was calculated by integration (using the software package OriginPro 7). Table 5.2 gives the average relative area under the modulus-time curves of leathers stretched by 20% at various temperatures. It can be seen that as the thermal treatment temperature increases, the area under the curve decreases; hence the tendency of the leather to flow increases. It is also clear from the data that the tendency of leather to flow increases with temperature, reaching a maximum, where also maximum set was observed.

Temperature (°C)	Area under relaxation modulus vs. time curve (apparent viscosity) (MPa.s)	
	Chrome	Vegetable
30	2000	9400
40	1800	6500
50	1400	3000
60	1400	500
70	1300	1900
75		2700
80	1300	
90	1000	

Table 5.2: Relative areas under the relaxation modulus versus time graphs for chrome tanned and vegetable (tara) tanned leathers. Figures in red denote minimum values.

Figure 5.12 shows the linear relationship between area under the relaxation modulus versus time curve and the percentage linear set. It should be appreciated that, within experimental error, the values of the correlation coefficients (R) indicate that set has high dependency on the flow properties of leather. Both stress relaxation and set increase with increasing temperature, suggesting stress relaxation is directly related to plastic deformation. However, for leather, the shrinking transition ultimately determines the temperature at which optimum relaxation occurs.

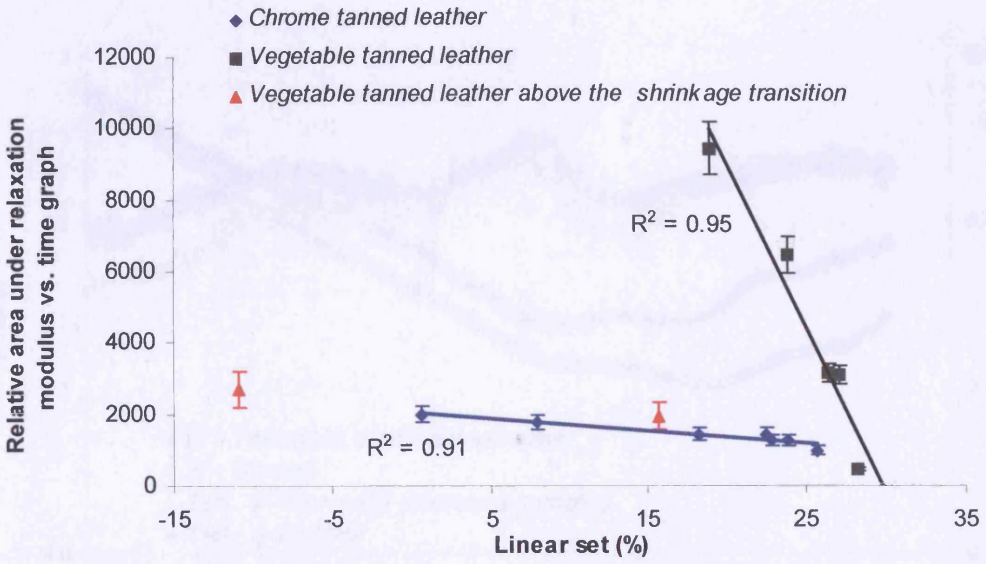

Figure 5.12: Linear relationships between relative area under relaxation modulus vs. time curves and experimentally measured linear set for vegetable tanned and chrome tanned leather. Gelatinised leather shows a different trend, which is indicated by the red triangles (▲).

Figure 5.13 shows the DMTA thermogram of chrome tanned leather, which had been subjected to thermal setting at 70°C, and an unstretched control. Both samples show the same transitions at the same temperature, indicating that no permanent structural modification has taken place. Therefore, it is expected that they will display the same physical properties. However, the thermally stretched leather exhibits a slightly higher shrinkage temperature (Control, 105 ± 2°C, thermally stretched sample, 107 ± 2°C) but it is not significantly different. One implication of these results is that a thermal setting procedure does not have adverse effects on the thermal properties of leather.

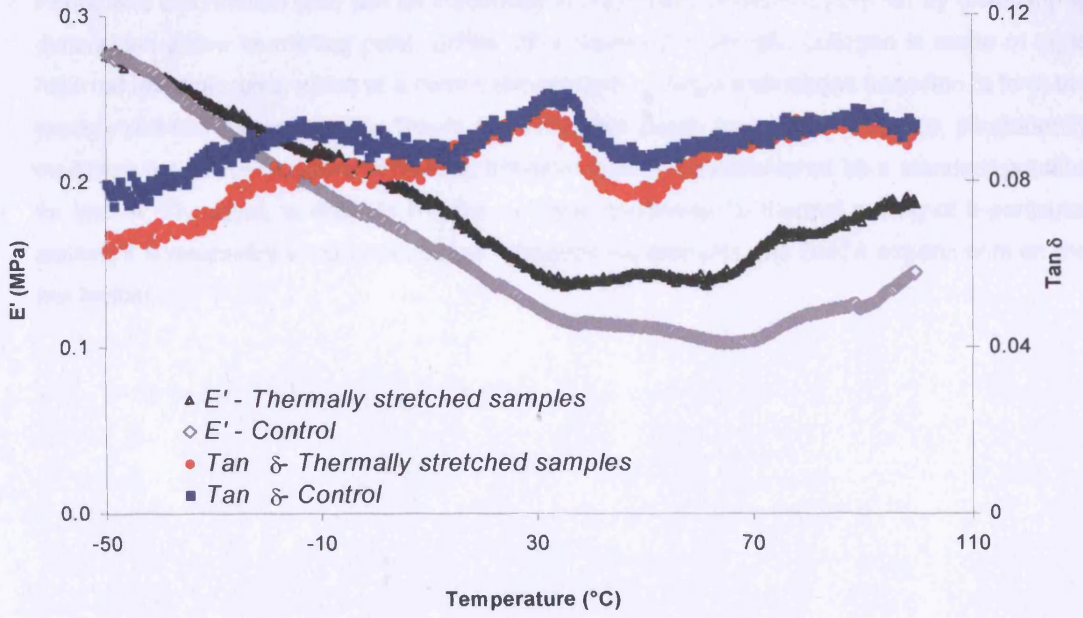

Figure 5.13: Comparison between the viscoelastic characteristics of chrome tanned leather thermally stretched at 70°C and control samples conditioned at 65% RH and 20°C for 48 hours.

One of the unique properties of leather is its ability to mould into a shape, which is retained over time. Because of this quality, leather is an ideal material for shoe manufacturing. From the DMTA trace, Figure 5.13, even dry leather shows a viscoelastic transition around body temperature. That means it is capable of undergoing permanent deformation when stretched. This could be the reason why leather shoes mould round one's feet and consequently give the "comfort feel".

All the evidence from previous literature as well as the results presented here, points to the stress relaxation behaviour of leather is due to its ability to dissipate energy through viscous sliding of fibrils. These flow properties are governed by the molecular structure, whose mobility has a high dependency on the position of its glass transition in relation to the working/ambient temperature.

The aim of any setting treatment to increase area is to make the material retain as much as possible of the initial deformation imposed on it. It has been demonstrated here that setting requires extensive re-arrangement of molecular/fibrous structure above the glass transition temperature. Collagen fibrils, including those in leather, are stabilised by hydrogen bonds. In order for the molecular segments of collagen to undergo rotational transitions with an associated re-arrangement of the relatively strong hydrogen bonds then the presence of water (or another hydrogen bond breaker) and heat are required.

Permanent deformation (set) can be introduced in a synthetic crystalline polymer by changing its dimensions above its melting point. Unlike other polymeric materials, collagen is made of triple helix rod like molecules, which at a certain temperature undergo a shrinkage transition to form the random coil structure of gelatin. This is an irreversible phase transition. Therefore, permanently modifying the structure above its melting transition cannot be considered as a standard practice for leather. Therefore, in order to find the optimum conditions for thermal setting of a particular leather, it is necessary to carry out stress relaxation experiments and DMTA experiments on the wet leather.

5.4 Summary

The stress relaxation property of leather is strongly related to its viscoelastic behaviour and has high dependency on temperature. The rate of stress relaxation is strain and temperature dependent. Wet leather has a broad viscoelastic transitional region, during which collagen molecules have freedom to move more readily. Hence under the right conditions, wet leathers can be stretched irreversibly to increase the area.

Two critical temperatures related to thermal stretch treatment were identified, which may be termed the critical and the optimum temperatures. Both of these temperatures are highly dependent on the leather type. The critical temperature is the temperature above which the set increases markedly and has been positively identified as being associated with a T_g of the leathers. Above the T_g segmental rotations of collagen molecules are probable and the molecules may dissipate mechanical energy more quickly and display profound relaxation. The optimum temperature is where maximum stress relaxation and set is obtained. The optimum condition for thermal setting condition for leather can be found experimentally either by DMTA or stress relaxation experiments or viscoelastic modelling (calculating the area under the curve of the relaxation modulus vs. time curve).

Chapter 6

CONCLUSIONS

The glass transition of leather has not previously been detected, however it has now been conclusively demonstrated that the Dynamic Mechanical Thermal Analyser is able to detect the glass and other viscoelastic transitions of leather quite clearly. It has also been established that the glass transition temperature of most leathers is located in the vicinity of room temperature. This means that at room temperature both side chain re-orientation and main-chain oscillation are taking place within the leather, which is part of the reason why leather exhibits flexible properties.

Tanning is a treatment, which causes a plasticisation of collagen, where an interpenetrating network of tanning molecules interposes itself between the collagen molecules and reduces the attractive forces holding the collagen molecules together. Thus the glass transition temperature of the amorphous portion of collagen is depressed to a lower temperature. However, the proposed theory does not rule out crosslinking between the interpenetrating network of the tanning agent and the reactive side-chains of the collagen molecules. In fact, DMTA thermograms of leathers indicate that selective clusters of amino acid residues are affected by some degree of crosslinking with chromium, semi-alum and semi-titan tanning agents. However, the plasticisation effect dominates over the crosslinking and the glass transition temperatures of tanned leathers at low moisture contents are lower than that of the untanned skin. Therefore, all tanning agents are effective plasticisers for the collagen molecules and hence are responsible for giving a supple feel to the leather. Different tanning agents impart differing degrees of plasticisation and so the glass transition temperature of leather depends on the type and amount of the tanning agent used. Taking all the evidence into account, tanning may be regarded as the plasticisation of collagen molecule. The transition temperatures of tanned and untanned skins have high dependency on the moisture content. Water molecules act as a typical plasticiser at a lower moisture content, however above a content of 14%, it acts as a both plasticiser and anti-plasticiser, possibly due to different degrees of hydration of the various amino acid residues.

Experimental evidence that is presented that in Chapter 4 indicates the final characteristics of leather depend highly on the way and which moisture-leather relationship is maintained during the drying procedure rather than drying temperature. Two critical moisture contents that accompanying the drying are identified. Therefore in practice, it is possible to speed up the drying

procedure by identifying such critical moisture contents and then utilise a high temperature to speed up the drying procedure whilst maintaining the moisture content of the drying environment to prevent fibre sticking.

It has been demonstrated that stress relaxation influences the setting properties of leather and it is highly temperature dependent. Overwhelming evidence is presented in Chapter 5 indicates that stretching the leather above its glass transition temperature produces stable set. However, it is also shown that the higher the temperature the faster the stress relaxation (dissipation of applied mechanical energy) and hence the greater the obtained set. Therefore the shrinking transition ultimately determines the optimum temperature to obtained maximum area set. In order to obtain maximum set from a given piece of leather, it is proposed that the leather be stretched 15 to 20°C below its shrinkage temperature.

The identification of the glass transition temperatures of leathers has several practical implications. This is especially so for post tanning, where it may be suggested that processing above the glass transition temperature will be beneficial. This is because fibres are much more flexible and hence the uptake and fixation of dyes, fatliquor and chemicals will be optimised. DMTA may also find use in quality control measurements, including determination of glass transition temperature and shrinkage temperature and stiffness. Modulus values, in the rubbery region, will give a direct measurement of the molecular stiffness of leather. It can even be used as a diagnostic tool in determining the type of leather, since, different types of tanning show different splitting/phase separation behaviour of the glass transition peaks.

Different leathers show different glass transition temperatures and thus their physical properties in ambient conditions differ greatly with respect to their molecular flexibility. Therefore, there is a need to elucidate the physical properties of leathers above and below their glass transition temperatures. At present, IUP protocol on physical testing specifies testing to be carried out at 20°C and 65% RH. Under these conditions, some leathers will be above the glass transition (e.g. leather tanned with vegetable tannins) whilst others will be the below glass transition (e.g. leather tanned with chromium).

Finally, it has been conclusively proved that DMTA is a highly effective technique for characterising the thermal transitions of collagen and leather. Whilst DSC is effective in determining the first-order transitions, such as shrinking and melting, DMTA is much more sensitive to molecular motions and detects higher-order thermal transitions, such as the glass transition and the pre-shrinking transition of collagen. The glass transition is the single most important thermal property to study because it is directly linked to the physical and mechanical properties of the material. The leather industry should embrace this new technique.

FUTURE WORK

All the DMTA experiments were carried out in an open system, where evaporation of water could not be prevented. However the water content of the sample has great influence on the transition temperatures of leathers regardless of tanning agents. In the later stages of this work humidity controlled DMTA became available and it is recommended that in future, such a system should be used to confirm the exact temperatures of transitions occurring at higher temperature. In such experiments, the precise plasticising effect of water and tannins can then also be measured. It is also recommended that ethylene glycol to be used to maintain a water like electrolytic medium. This will allow the phase transition related to ice formation to be eliminated from the DMTA thermal trace.

In order to quantify the contribution of molecular flexibility to the physical properties of leather, it is recommended that in future, the physical and mechanical testing to be investigated above and below the glass transition temperature of a leather. The results may explain why certain type of leathers shows different physio-mechanical properties than others.

Processing the skin above the glass transition temperature is recommended, where uptake and penetration of chemicals will be high. This is because the flexibility of the collagen can be altered without causing structural damage. Therefore future studies should also include the effect of different stages of leather processing in relation to the glass transition temperature of skin.

The use of DMTA as a quality control tool should also be investigated. In polymer science, the modulus values of the rubbery plateau region are often used as an indicator of the stiffness of a given material. Moreover, this region also reveals the crosslinking density of polymers. Therefore, there is a possibility that modulus values measured in the rubbery plateau region may be used as a more reproducible measurement of leather stiffness and also to gather information regarding the crosslinking density of a given tanning agent.

References

1. Silver, F.H., (Ed.), "Biological Materials: Structure, Mechanical properties, and modelling of soft tissues", (1987), NYU Press, New York and London.
2. Aklonis, J.J and MacKnight, W.J., (Ed.), "*Introduction to polymer viscoelasticity*", (1983), John Wiley and Sons, New York, Chichester, Brisbane, etc.
3. North, A. C. T., Cowan, P. M. and Randall, J. T., *Nature*, (1954), ***174***, 1142-1143.
4. Bear, R.S., *Adv. Protein Chem.*, (1952), ***7***, 69-155.
5. Wess, T.J., Hammersley, A. P., Wess L. and Miller A., *J. Mol. Biol.*, (1998), ***275***, 255-267.
6. Hulmes, D. J. S., Wess, T. J., Prockop, D. J. and Fratzl, P., Biophys. J., (1995), **68**, 1661-1670.
7. Miles, C. A. and Burjanadze, T. V., *Biophys J*, (2001), ***80***, 1480-1486.
8. Covington, A.D., Lampard, G.S., Hancock, R.A and Ioannidis, *J. Amer. Leather. Chem. Assoc.*, (1998), ***93***, 107-115.
9. Komanowsky, M., *J. Amer. Leather. Chem. Assoc.*, (1991), ***86***, 269-279.
10. Manich, M.A., Bosch, T., Carilla, J., Sala, J., Celma, P.J, Cot, J, Marsal, A., J. *Amer. Leather Chem. Assoc.*, (2002), ***97***, 441-450.
11. Manich, M.A., Bosch, T., Carilla, J., Sala, J., Celma, P.J, Cot, J, Marsal, A., *J. Amer. Leather Chem. Assoc.*, (2003), ***98***, 279-284.
12. Menard, K.P., (Ed.), "*Dynamic mechanical analysis*", (1999), CRC Press, Boca Raton, London, etc.
13. McCrum, N.G., Read, B.E. and Williams, G., (Ed.), "*Anelastic and dielectric effects in polymeric solids*", (1967), Wiley, New York.
14. Christensen, R.M., (Ed.), "*Theory of viscoelasticity, An introduction*", (1971), Academic Press, New York.
15. Flory, P., (Ed.), "*Principles of polymer chemistry*", (1987), Cornell University Press, Ithaca, New York.
16. Komanowsky, M., Cooke, P.H., Damert, W.C., Kronick, P.L. and McClintick, M.D., *J. Amer. Leather. Chem. Assoc.*, (1995), ***90***, 243-256.
17. Purslow, P.P., *J. Materials Sci.*, (1991), ***26***, 4468-4476.
18. Knonick, P.L. and Buechler, P.R., *J. Amer. Leather. Chem. Assoc.*, (1988), ***83***, 221-227.
19. Dunn, M.G. and Silver, F.H., Conn. Tiss. Res., (1983), 12, 59-65.
20. Elden, H.R., Collagen Currents, (1968), 7, 228-332.

21. Findley, W.N., Lai, J.S. and Onaran, K., (Ed.), "*Creep and relaxation of nonlinear viscoelastic materials*", (1989), Dover Publ., New York.

22. Boyd, R.H., *Polymer*, (1985), ***26***, 323-347.

23. Matsuoka, S., *J. Therm. Anal.*, (1996), ***46***, 985-1010.

24. Abe, A., Jernigan, R.L. and Flory, P.J., *J. Amer. Chem. Soc.*, (1966), ***88***, 631-639.

25. Ward I.M. and Healey, D.W, (Eds.), "*An introduction to the mechanical properties of solid polymers*" (1993), John Wiley & Sons Ltd., Chichester.

26. Williams, M.L., Landel, R.F. and Ferry, J.D., *J. Amer. Chem. Soc.*, (1955), ***77***, 3701-3782.

27. Wetton, R.E., (Ed., Brown, M.E.), "*Handbook of thermal analysis and calorimetry*", (1998), Elsevier, Amsterdam, Boston etc., ***Vol 1, Chap 6***.

28. Wetton, R.E, Marsh, R.D.L and Van-de-Velde, J.G., *Thermoch. Acta*, (1991), ***175***, 1-11.

29. Jones, D.J., *Int. J. Pharmaceutics*, (1998), ***179***, 167-178.

30. Barnes, H.A., Hutton, J.F. and Walters, K., "*An induction to rheology*", (1996), Elsevier, Amsterdam.

31. Craig, D.Q.M. and Johnson, F.A., *Thermoch. Acta*, (1995), ***248***, 97-115.

32. Turi, E., (Ed.), " *Thermal characterisation of polymeric materials*", (1981), Academic Press, Boston.

33. Bear, E., Cassidy, J., James, J. and Hiltner, A., " *Hierarchical structure of collagen composite systems: Lessons from biology*", (1991), ***Vol 7***.

34. Heidemann, E., (Ed.), "*Fundamentals of leather manufacturing*", (1993), Eduard Roether KG: Darmstadt.

35. Von Hippel, P.H., (Ed., Ramachandran G.N.,), "*Treatise on collagen*", (1967), Academic Press, London and New York, ***Ch. 6.***

36. Hannig, K. and Nordwig. A., (Ed., Ramachandran G.N.,)., "*Treatise on collagen*", (1967), Academic Press, London and New York, ***Ch. 2.***

37. Yannas, I.V., *J. Macromol. Sci. Revs. Macromol. Chem.*, (1972), ***7***, 49-105.

38. Bailey, A.J. and Paul, R.G., *J. Leather Tech. Chem.*, (1998), ***82***, 104-110.

39. Di Marzio, E.A., *Progress in Polym. Sci.*, (1999), ***24***, 329-377.

40. Bailey, A.J., *J. Leather Tech. Chem.*, (1992), ***76***, 111-127.

41. Rich, A. and Crick, F.H.C., *J. Mol. Biol.*, (1961), ***3***, 483-506.

42. Ramachandran, G.N. and Kartha, G., *Nature*, (1955), ***176***, 593-595.

43. Ramachandran, G.N., Bansal, M., Bhatnagar, R.S, *Biochim. Biophy. Acta*, (1973), ***322***, 166-171.

44. Lollar, *J. Am. Leather Chem. Assoc.*, (1958), ***53***, 2-9.

45. Kuhn, K., Hoffmann, H. and Grassmann, W., *Naturwissenschaften*, (1960), ***47***, 15-23.

46. Dolz, R. and Heidemann. E., *Biopolymer*, (1986), ***25***, 1069-1080.

47. Kadler, K.E., *Protein Profiles*, (1994), ***1***, 519-638.

48. Chen, J.M., Feairheller, S.H. and Brown, E.M., *J. Amer. Leather. Chem. Assoc.*, (1991), ,***86***, 487-497.

49. Hodge, A.J., and Schmitt, F.O, Proc. *Nat. Acad. Sci.*, (1960), ***46***, 186-197.

50. Bruns, R.R. and Cross J., *Biochemistry*, (1973), ***12***, 808-815.

51. Hulmes, D.J.S., Parry, D.A.D, et al. *J. Mol. Biol.*, (1973). ***79***, 127-144.

52. Fraser, R.D.B., MacRae, T.P. and Suzuki, E., *J. Mol. Biol.*, (1987), ***193***, 115-125.

53. Wess, T.J., Hammersley, A.P, Wess, L, and Miller, A., *J. Mol. Biol.*, (1995), **248**, 487-493.

54. Wess, T.J., Hammersley, A.P, Wess, L, and Miller, A., *J. Mol. Biol.*, (1998). ***122***, 92-100.

55. Gerngross, O. and Katz, J.R., *Kolloid-Z*, (1926), ***39***, 181-189.

56. Piez, K.A., (Ed., Ramachandran G.N.,)., "*Treatise on collagen*", 1967, Academic Press, London and New York, ***Ch. 5***.

57. Bear, R.S., Salo, T.P. and Bolduan, O.E.A., *J. Amer. Leather Chem. Assoc.*, (1951). ***46***, 107-117.

58. Fraga, A.N. and Williams, R.J.J., *Polymer*, (1985), ***26***, 113-118.

59. Dölz, R. and Heidemann, E., Biopolymer, (1986), ***25***, 1069-1080.

60. Kramer, R.Z. and Berman, H.M., *J. Biomolecular Structure & Dynamics*, (1998), ***16***, 367-380.

61. Bella, J., Brodsky, B. and Berman, H., *Structure*, (1995), ***3***, 893-906.

62. Kramer, P.Z. and Berman, H.M., *Structural Biology*, (1999), ***14***, 169-178.

63. Bienkiewicz, K.J., *J. Amer. Leather Chem. Assoc.*, (1990), ***85***, 305-325.

64. Kopp, J.,Bonnet, M. and Renou, *Matrix*, (1989), ***9***, 443-450.

65. Haly, A.R. and Snaith, J.W., *Biopolymers*, (1971), ***10***, 1681-1699.

66. Pineri, M.H., Escoubes, M. and Roche, G., *Bioploymers*, (1978), ***17***, 2799-2815.

67. Peto, S., Gillis, P. and Henri, V.P., *Biophys. J.*, (1990), ***57***, 71-84.

68. Lees, S., *Int. J. Biol. Macromol.*, (1986), ***8***, 66-72.

69. Lees, S., Pineri, M. and Escoubes, M., *Int. J. Biol. Macromol.*, (1984), ***6***, 133-136.

70. Heidemann, E. and Keller, H., *J. Amer. Leather Chem. Assoc.*, (1970), ***65***, 512-533.

71. Miles, C.A. and Bailey, A.J., *Micron*, (2001), ***32***, 325-332.

72. Rigby, B.J., *Biochim. Biophys. Acta*, (1967), ***133***, 272-277

73. McClain, P.E., Pearson, A.M., Miller, E.R. and. Dugan, L.R., *Biochim. Biophy. Acta - Protein Structure*, (1968), ***168***, 143-149.

74. Bigi, A., Roveri, N., Cojazzi, G., and Koch, M.H. J., *Int. J. Biol. Macromol.*, (1978), ***9***, 363-367.

75. Sionkowska, A., Kamińska, A., *Int. J. Biol. Macromol.*, (1999), ***24***, 337-340.

76. Haines, M.B., "*Parchment*", (1999), The Leather Conservation Centre, Northampton.

77. Hemminger, W. and Sarge, S.M., (Eds, Brown, M.E.), "*Handbook of Thermal Analysis and Calorimetry*", (1998), Elsevier, Amsterdam, Boston etc., ***Vol 1, Chap 2***.

78. Flory, P.J. and Garrett, R.R., *J. Amer. Chem. Soc.*, (1958), ***80***, 4836-4845.

79. Rigby, B.J. ,Harai, N., Spikes, J.D. and Eyring, H., *J. Gen. Physiol.*, (1959), ***43***, 265-283.

80. Weir, C.E., *J. Amer. Leather. Chem. Assoc.*, (1949), ***44***, 79-106 & 108-137.

81. Covington, A.D., *Soc. Leather Technol. Chem.*, (2001), ***85***, 24-34.

82. Flory, P.J., J. Chem. Phys., (1949), ***17***, 303-312, & Flory, P.J., *"Principles of polymer chemistry"*, (1953), Cornell, Ithaca.

83. Dorrington, K.L.,(eds, Vincent, J.F.V. and Currey, J.D.), "*The mechanical properties of biological materials*", Cambridge University Press, (1980) ***Ch.3***.

84. Komandwsky, M., *J. Amer. Leather Chem. Assoc.*, (1990), ***85***, 131-140.

85. Matveev, Y.I., Grinberg,V.Y. and Tolstoguzov, V.B., *Food Hydrocolloids*, (2000), ***14***, 425-437.

86. Rigby, B.J. and Manson, P., *Biochim. Biophys. Acta*, (1963), ***66***, 448-450

87. Baer, E., Kohn, R. and Papir, Y., *J. Mocromol. Sci. Phys.*, (1972), ***B6:4***, 761-774.

88. Nguyen, A., Vu, B.V. and Wilkes, G.L., *Biopolymers*, (1974), ***13***, 1023-1037.

89. Batzer, H. and Kreibich, T., *Polymer Bulletin*, (1981), ***5***, 585-590.

90. Kronick, P.L., Buechler, P, Scholnick, F. and Artymyshyn, B., *J. Appl. Polym. Sci.*, (1985), ***30***, 3095-3106.

91. Twombly, B., Cassel, B. and Miller, A.T., *NATAS Proceedings*, (1994), ***23***, 288-293.

92. Sarti, B. and Scandola, M., *Biomaterials*, (1995), ***16***, 785-792.

93. Odlyha, M., Foster, G.M., Cohen, N.S. and Larsen, R., *ICOM committee for conservation*, (1999), ***2***, 702-707.

94. Odlyha, M., Cohen, N.S., Foster, G.M., Aliev, A., Verdonck, E.V. and Grandy, D., J. *Therm. Anal. Cal.*, (2003), ***71***, 939-950.

95. IULTCS Official Method of Analysis, (1997).

96. Cohen, N.S., Odlyha, M. and Foster, G.M., *Thermochi. Acta.*, (2000), ***365***, 111-117.

97. Johari, G.P., Hallbrucker, A. and Mayer, E., *Nature*, (1987), ***330***, 552-553.

98. Koob, T.J. and Hernandez, D.J., *Biomaterials*, (2003), ***23***, 203-212.

99. Caballero J.A., Font R. and Esperanza, M.M., *J. Anal. Appl. Pyrol.,* (1998), 47, 165-181.

100. Reed, R., (Ed.), "*Ancient skins, parchments and leather*", (1972) Seminar Press, London, ***Ch 1***.

101. Collins, M.J., Covington, A.D., Menderes, O. and Waite, E., *J. Soc. Leather Technol. Chem.*, (1999), ***83***, 107-110.

102. Covington, A.D., *J. Amer. Leather Chem. Assoc.*, (1998), ***93***, 168-183.

103. Kallenberger, W.E. and Hernandez, J.F., *J. Amer. Leather Chem. Assoc.*, (1983), ***78***, 217-222.

104. Bienkiewicz, K J.,(Ed., Robert, E.), "*Physical chemistry of leather making*", (1983), Krieger Publishing Co., Malabar, Florida,

105. Heidemann, E., (Ed.), "*Fundamentals of leather manufacturing*", (1993), Eduard Roether KG: Darmstadt., ***Ch. 4***.

106. Dasgupta, S., *J. Soc. Leather Technol. Chem.,* (2004), ***88***, 116-120.

107. Covington, A.D., *J. Amer. Leather Chem. Assoc.*, (1982), ***96***, 467-480.

108. Sykes, R. L., *J. Amer. Leather Chem. Assoc.*, (1956), ***51***, 235-242.

109. Gustavson, K. H., *J. Amer. Leather Chem. Assoc.,* (1953), ***48***, 559-578.

110. Covington, A.D., *J. Amer. Leather Chem. Assoc.*, (1987), ***82***, 1-13.

111. Covington, A.D. and Sykes, R.D., *J. Amer. Leather Chem. Assoc.*, (1987), ***79***, 72-89.

112. Pojer, P.M., Chin, E.L.S. and Reddie, R.N., *J. Soc. Leather Technol. Chem.,* (1993), ***77***, 78-81.

113. Haslem, E, (Ed.), " *Practical polyphenolics: from structure to molecular recognition and physiological action*", (1998), Cambridge University Press, Cambridge.

114. Haslam, E., *J. Soc. Leather Technol. Chem.*, (1988), ***72***, 45-64.

115. Haslam, E., J. Soc. Leather Technol. Chem., (1997), ***81***, 45-51.

116. Bickley, J.C., *J. Soc. Leather Technol. Chem.*, (1992), ***76***, 1-5.

117. Levina, A. and Lay, P.A., *Coordination Chemistry Reviews*, In Press, Available online 9 April 2004,

118. Gustavson, K.H., *Adv. Protein Chem.*, (1949), ***5***, 354-421.

119. Gustavson, K.H., "*The Chemistry of tanning Processes*", (1956), Academic Press, New York.

120. Rougvie, M.A. and Bear, R., *J. Amer. Leather Chem. Assoc.*, (1953), ***48***, 735-751.

121. Covington, A.D. and Song, L., *IULTCS Congress*, (2003), Cancun, Mexico.

122. Larsen, R., (Ed.), " STEP leather project, évaluation of the correlation between natural and artificial ageing of vegetable tanned leather", (1994), " *ENVIRONMENT leather project, deterioration and conservation of vegetable tanned leather*" , (1997), Copenhagen, Royal Danish Academy of Fine Arts.

123. Covington, A.D., Lampard, G.S. and Pennington, M., *J. Soc. Leather Tech. Chem.*, (1997), ***82***, 78-80.

124. Compton, E., D., *J. Amer. Leather Chem. Assoc.*, (1949), ***44***, 140-151

125. Bienkiewicz, K. J., (Ed., Robert, E.), "*Physical chemistry of leather making*", Krieger Publishing Co., Malabar, Florida, (1983), ***Ch.14***.

126. Batzer, H., *Chemiker Z.*, (1952), 76, 397-404.

127. Ramasami, T., *J. Amer. Leather Chem. Assoc.*, (2001), ***96***, 290-304.

128. Heidemann, E., *J. Soc. Leather Trades' Chem.*, (1982), ***66***, 21-9.

129. Mousia, Z, Farhat, I.A., Blachot, J.F. and Mitchell, J.R, *Polymer*, (2000), ***41***,1841-1848.

130. Farhat, I.A., Mitchell, J.R., Blanshard, J.M.V. and Derbyshire, W.A., *Carbohydrate Polymer*, (1996), ***30***, 219-127.

131. Kalichevsky, M.T., Blanshard, J.M.V, *Carbohydrate Polymer*, (1992), ***19***, 271-278.

132. Covington, A.D., Lampard, G.S., Menderes, O, Chadwick, A.V, Rafeletos, G. and O'Brien, P., *Polyhedron*, (2001), ***20***, 461-466.

133. Traore, A., Foucat, L. and Renou, J.P., *Europ. Biophy. J. with Biophy. Letters*, (2000), ***29***, 159-164.

134. Bella, J., Brodsky, B., and Berman, H.M., *Connect. Tissue Res.*, (1996), ***35***, 455-460.

135. Mrevlishvili G.M., *Thermoch. Acta*, (1998), ***308***, 49-54.

136. Stefonou, H., Woodward, A.E. and Morrow, D, *Biophysical J.*, (1973), ***13***, 772-779.

137. Dong, R., Yan, X, Pang, X. and Liu, S, *Spectrochimica Acta*, (2004), ***60***, 557–561.

138. Keey, R.B., (Ed.,), "*Drying principles and practice*", Pergamon press, Oxford (1972), ***Ch 1***.

139. Fung, B.M. and Trautmann, P., *Biopolymers*, (1971),***10***, 391-397.

140. Bienkiewicz, K. J., (Ed., Robert, E.), "*Physical chemistry of leather making*", Krieger Publishing Co., Malabar, Florida, (1983), ***Ch.22***.

141. Lamb, J., *J. Soc. Leather Tech. Chem.*, (1982), ***66***, 8-10.

142. Buck, L., (Ed., O'Flaherty, et al.), " *The chemistry and technology of leather*", Reinhold Publ.Corp. New York, (1962), ***Vol.3***.

143. Alexander, K. T. W., Corning, D.R. and Covington, A.D., *J. Amer. Leather Chem. Assoc.*, (1993), ***88***, 254-268.

144. Heidemann,E., "*Fundamentals of leather manufacturing*", (editor, Heidemann, E.), Darmstadt, Eduard Roether KG, (1993) ***Ch 17***.

145. Landmann, A. W., *J. Soc. Leather Tech. Chem.*, (1994), ***78***, 44-45.

146. Shivas, S. A. J., and Choquette, A., *J. Amer. Leather Chem. Assoc.*, (1985), ***80***, 129-136.

147. Abuelhassan, I.B., Ward, A.G. and Wolstenholme, S., *J. Soc. Leather Tech. Chem.*, (1984), ***68***, 159-177.

148. Monzo-Cabrera, *et al.*, *J. Soc. Leather Tech. Chem.*, (2000), ***84***, 38-44.

149. Lhuede, E.P., *J. Amer. Leather Chem. Assoc.*, (1969), ***64***, 375-387.

150. Friedrich, E., (editor, Grassmann, W.), " Handbuch der Gerbereichemie und lederfabrikation, ***Vol III, Part 1.***

151. El Amir, Ph.D thesis, University of Leeds, (1975).

152. Lee, G. and Friess, W., *Biomaterials*, (1996), ***17(23)***, 2289-2294.

153. Wess, T.J. and Orgel, J.P., *Thermochim. Acta*, (2000), ***365***, 119-128.

154. Wenge, Y., PhD Thesis, British School of Leather Technology (Leicester University), (1999).

155. William, J. G., (Ed.), "Stress analysis of polymers", (1980), Halsted Press, Chichester, New York, 2nd edition.

156. Vrentas, J. S., Duda, J.L. and Huang, W.J., *Macromolecules*, (1986), ***19***, 1718-1724.

157. Mogilner, G. I., Ruderman, G. and Grigera, R., *J. Molecular Graphic and Modelling*, (2002). ***21(3),*** 209-213.

158. Wright, D.M. and Attenburrow, G.E., *J. Mater. Sci.*, (2000), ***35***, 1353 – 1357.

159. Boote, C., Sturrock, E.J., Attenburrow, G.E. and Meek, K.M., *J. Mater. Sci.*, (2002), ***37***, 3651-3656.

160. Boote, C., Sturrock, E.J., Attenburrow, G.E. and Meek, K.M., *J. Soc. Leather Tech. Chem.*, (2002), ***86***, 6-11.

161. Hearle, J. W.S., (Eds., Hearle, J.W.S. and Miles, L.W.C.), "*The setting of fibres and fabrics*", (1971), Merrow Publ.Co. Watford, England, ***Ch.1***.

162. Farnworth, A.J. and Delmenico, J., (Ed., Cook, J.G.), "*Permanent setting of wool*", (1971), Merrow Publ.Co. Watford, England, ***Ch.1.***

163. Mukhopadhyay, S.K., (Ed., Mukhopadhyay, S.K.), " *Advances in fibre science*", (1992), The Textile Institute, Manchester. ***Ch 6***.

164. Attenburrow, G.E., J. Soc. Leather Tech. Chem., (1993), ***77***, 107-114.

165. Gathercole, L.J., Shah, J.S. and Nave,C, Int. J. Biol. Macromol., (1887), 9, 181-183.

166. Mosler, E., Folkhard, W., Knorzer, E., Memetschek, N.T. and Koch, M.H.J., *J. Mol. Biol.*, (1985), ***182***, 589-596.

167. Sasaki, N., Shukunami, N., Matsushima, N. and Izumi, Y., J. Biomechanics, (1999), ***32***, 285-292.

168. Bonet, J., *Int. J. Solids and Structures*, (2001), ***38***, 2953-2968.

169. Hernández-Jiménez, A., Hernández-Santiago, J., Macias-García, A. and Sánchez-González, J, *Polymer Testing*, (2002), ***21(3)***, 325-331.

170. Sasaki, N. and Enyo, A., J. *Biomechanics*, (1995), ***28(7)***, 809-815.

171. Elden, H.R., "*Biophysical properties of the skin*", (1971), Wiley & Sons, New York, ***Ch 3***.

172. Rigby, P, J., *Biochim. Biophys. Acta*, (1963), ***66***, 448-450.

173. Usha, R. and Ramasami, T., *J. Appl. Poly. Sci.,* (2000), ***75***, 1577-1584.

174. Butlin, J.G., J. Soc. Leather Technol. Chem., (1963), ***47***, 3-38.

175. Holmes, C.M. and Ward, A.G., *J. Soc. Leather Technol. Chem.*, (1971), ***55***, 242-262.

176. Astbury, W.T. and Woods, H.J., *Phil. Trans.*, (1933), ***232***, 333-396.

177. Folkhard, W., Mosler, E., Greercken, W., Nemetschek-Gansler, H. and Nemetschek, T., *Int. J. Biol. Macromol*, (1987), ***9***, 169-173.

178. Weast, R.C., Astle, M.J. and William, H.B., (Eds.), "*Hand book of Chemistry and Physics*", (1987), 68th edition, CRC Press Inc, Boca Raton, Florida.

APPENDIX 1:

Stress relaxation

One of the simplest methods of characterising the viscoelasticity of a material is the stress relaxation test, in which the test specimen is quickly strained by a fixed amount and then the stress needed to maintain this strain is measured as a function of time. A typical result is given in Figure 1. Initially, the stress rises with applied strain and then decays with time, as the elastically stored energy diminishes as a consequence of the fluid-like energy dissipation mechanism[2].

When a linear viscoelastic solid is subjected to an instantaneous tensile strain, the stress will decrease with time (t). The time dependent stress divided by the imposed strain is the time dependent relaxation modulus, E(t), and is mathematically defined by equation 1, where $\sigma(t)$ is the relaxation true stress and ε_0 is the tensile strain applied at t = 0.

$$E(t) = \frac{\sigma(t)}{\varepsilon_0} \qquad (1)$$

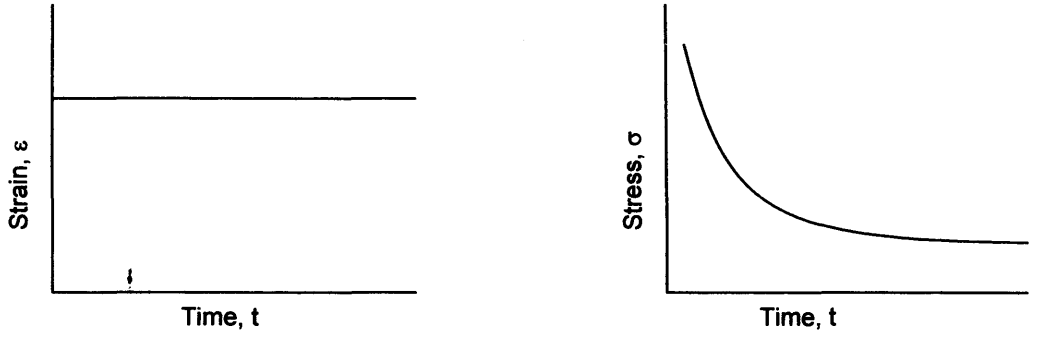

Figure 1: Stress Relaxation at constant strain[21].

To permit a mathematical analysis of the stress relaxation phenomenon, models combining massless Hookean springs and dashpots filled with Newtonian fluid, are frequently used. The springs and dashpots correspond to the elastic and energy dissipative responses respectively. If these units are connected in series, then they form the Maxwell model (Figure 2(a)). If the units are connected in parallel, then they form the Voigt model (Figure 2(b)). Analysis of these models allows definition of complex viscosity in terms of the dashpot viscosity constant and the spring constant. The relaxation time, τ, is a measure of the time required for the energy stored in the spring to shift to the dashpot and dissipate[21].

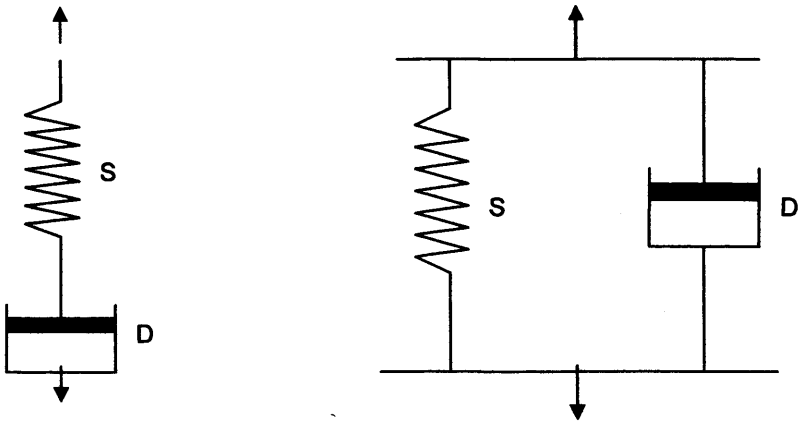

Figure 2: Viscoelastic models, represented by the combination of spring (S) and dashpot (D).

$$\sigma(t) = \sigma_0 e^{-t/\tau} \qquad (2)$$

$$\sigma = E\varepsilon \qquad (3)$$

Equation 2 shows that a single Maxwell model gives a much more reasonable prediction for the stress relaxation experiment than a Voigt model. It is clear from equation 3 that the Voigt model fails to predict a decaying relationship of the stress with respect to time.

Real experimental data do not fit the prediction of the single Maxwell model. Instead, the stress relaxes at a rate that cannot be described by a single relaxation time. One way of understanding this type of behaviour is to assume that there is not one but many relaxation mechanisms with varying relaxation times. Such an assumption has been demonstrated to predict experimental data closely. Thus the overall time dependent relaxation modulus, E(t), can now be expressed in terms of a set of discrete relaxation times, τ_i, as indicated in equation 4. In this equation, the relaxation modulus is assumed to consist of the sum of individually relaxing elements, each with a characteristic relaxation time.

$$E(t) = \sum_i E_i \exp(-t/\tau_i) \qquad (4)$$

APPENDIX 2:

Creep and Recovery

In a creep experiment, the stress is maintained at constant whilst the strain increases with time. Figure 3 shows the result of a typical creep experiment. Creep is a slow continuous deformation of a material under constant stress, some recovery is expected when the load is removed. This strain recovery is also called delayed elasticity.

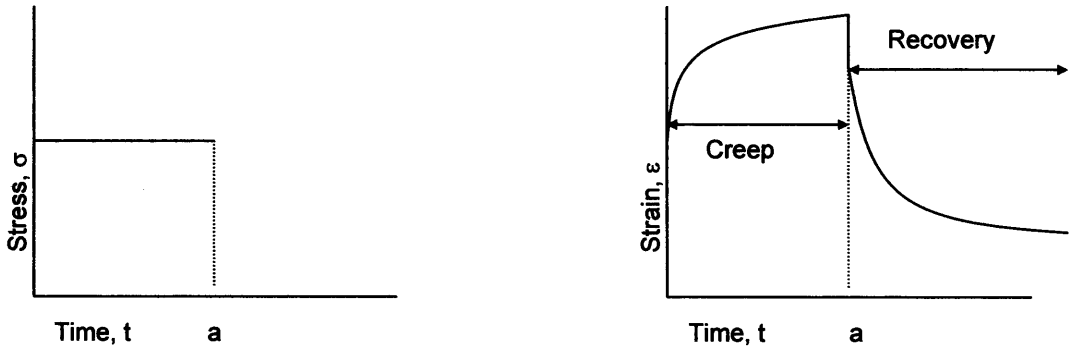

Figure 3: Creep and recovery[21].

$$d\varepsilon/dt=\sigma/\eta \qquad (5)$$

Equation 5 indicates that the Maxwell model behaves as a viscous fluid under a constant stress and hence this model fails to predict creep relaxation behaviour.

$$d\varepsilon/dt=\sigma_0/\eta e^{-Rt/\eta} \qquad (6)$$

The Voigt model predicts the time dependent creep relaxation behaviour quite well, as indicated in equation 6, where $d\varepsilon/dt$ is the strain rate, η is the coefficient of viscosity and R is the spring constant. Therefore, this model gives reasonable predictions for creep experiments.

APPENDIX 3:

Procedure for processing the skin to the pickled state

Process	Offer (%)	Product	Running Time (min)	Remarks
Dirt soak				
	400	Water @ 20°C	60	pH=6.85, *B_e=4.2, T=15°C
Drain				
	400	Water @ 20°C		
Main Soak	1	Remcoil KTU		Non-ionic wetting Agent
	1	Ecopel PDL		Anti-wrinkling agent
	1	Sodium carbonate		
	1	Soaking enzyme		
	0.1	Tolcide C30	240	Bactericide
		Leave overnight		pH=9.3, B_e=3.8,T=22°C
Drain				
	80	Water @ 25°C		
Unhairing	1	Sodium sulfide	60	
	1	Sodium sulfide		
	1	Ecopel PDL (DMA)	60	
	50	Water @ 25°C		
Swelling	0.5	Sodium sulfide	60	
	2	Lime		
	50	Water @ 25°C	60	Static
	50	Water @ 25°C	60	
		Leave overnight		
Wash	200	Water @ 30°C	30	
Drain				
Wash	200	Water @ 30°C	15	
Drain				
	200	Water @ 35°C		
Deliming	2	Ammonium sulfate		pH=8.3
	0.5	Sodium metabisulfate	45-60	
Bating	1	Pancreol PBW1	45	Bating enzyme
Drain				
Wash	300	Water @ 20°C	15	
Drain				pH=8.5
Wash	300	Water @ 20°C	15	
Drain				
	80	Water @ 20°C		
	8	Sodium chloride	10	(B_e should be > 5) B_e=6.8
	0.8	Sulfuric acid 1:5 water		
Pickle	0.4	Formic acid 1:5 water	120	
		Leave overnight		pH=2, B_e=5.7,

* Measurement of density.

APPENDIX 4:

Saturated salt solutions for controlling relative humidity

Relative humidity is defined as the ratio of the water vapour pressure (P_w) to the saturation vapour pressure, P_{ws}, (over water) at the temperature of the gas, as indicated by equation 7.

$$RH = P_w/P_{ws} \times 100 \qquad (7)$$

Water vapour can be treated as a gas. At a particular temperature air can only hold so much water vapour. When air is saturated the relative humidity would be 100% RH; the relative humidity describes how close to saturation the air is. The water vapour concentration and therefore the relative humidity over a salt solution is less than that over the pure water. This is because water is present in both the gas and the liquid phase, whereas the salt molecules are only present in the liquid; they dilute the water and hinder escape of water molecules into the air. The rate of return of water molecules to the liquid surface is proportional to their concentration in the gas, where there are no salt ions to interfere. The system therefore adjusts to equilibrium, when there are fewer water molecules in the air than there would be over a pure water surface[178]. The RH is therefore lower than 100%. The following table shows % humidity at room temperature within a closed space when an excess of the salt is in contact with saturated aqueous solution at 20°C.

Substance	Relative humidity at 20°C (%)
H_2O	100
$CuSO_4.5H_2O$	98
$ZnSO_4.7H_2O$	90
NH_4Cl	80
$NaNO_2$	65
$CaCl_2.6H_2O$	32
$H_3PO_4.2H_2O$	9
P_2O_5 (desiccant)	0

APPENDIX 5:

Procedure for tanning with chrome sulfate

Starting material: Pickled pelt (obtained from Hewit and Sons, Scotland, UK)

Process	Offer (%)	Product	Running Time (min)	Remarks
Re-pickle	80	Water @ 20°C		
	8	Sodium chloride	10	(B_e should be > 5) B_e=6.8
	0.8	Sulfuric acid 1:5 water		
	0.4	Formic acid 1:5 water	120	
		Leave overnight		pH=2, B_e=5.7,
Chrome Tannage Basifying	8	Chrome Powder 33% Basic		
	0.4	Tanbase (magnesium oxide)	60	
		Raise temperature to 40°C	90	
Neutralise	200	Water @ 35°C		
	1.5	Ammonium bicarbonate		
	0.4	Sodium formate	45	pH=4.5,
Drain				
Wash	200	Water @ 45°C	15	
Drain				
Wash	200	Water @ 45°C	15	
Drain				

Procedure for tanning with vegetable tannins

Starting material: Pickled pelt (obtained from Hewit and Sons, Scotland, UK)

Process	Offer (%)	Product	Running Time (min)	Remarks
Tanning	10	Tara Powder 60% tannins content	60	
	5	Tara	60	
	5	Tara	180	
Neutralise	200	Water @ 35°C		
	1.5	Ammonium Bicarbonate		
	0.4	Sodium Formate	45	pH=4.5,
Drain				
Wash	200	Water @ 45°C	15	
Drain				

Procedure for re-tanning with metal tanning agents

Starting material: Vegetable tanned leather prepared by the method described above.

Process	Offer (%)	Product	Running Time (min)	Remarks
Metal re-tan	100	H_2O	5	
	0.1	EDTA	5	
	2.0	*Metal (A(III) or Ti(III) or Cr(III))	180	2% equivalent of metal oxide
Neutralise	200	Water @ 35°C		
	x	Ammonium bicarbonate		
	x	Sodium formate	45	pH=4.5,
Drain				
Wash	200	Water @ 45°C	15	
Drain				

* *Aluminium(III) sulfate, 2% Al_2O_3*

Titanium(III) sulfate, 2% Ti_2O_3

Chromium(III) sulfate, 2% Cr_2O_3

APPENDIX 6:

Procedure for chrome tanning

Process	Offer (%)	Product	Running Time (min)	Remarks
Dirt soak	*400*	*Water @ 20°C*	*60*	*pH=6.85, *B_e=4.2, T=15°C*
Drain				
Main Soak	*400*	*Water @ 20°C*		
	1	*Remcoil KTU*		*Non-ionic wetting agent*
	1	*Ecopel PDL (DMA)*		*Anti-wrinkling agent*
	1	*Sodium carbonate*		
	1	*Soaking enzyme*		
	0.1	*Tolcide C30*	*240*	*Bactericide*
		Leave overnight		*pH=9.3, B_e=3.8, T=22°C*
Drain				
Unhairing	*80*	*Water @ 25°C*		
	1	*Sodium sulfide*	*60*	
	1	*Sodium sulfide*		
	1	*Ecopel PDL (DMA)*	*60*	
Swelling	*50*	*Water @ 25°C*		
	0.5	*Sodium sulfide*	*60*	
	2	*Lime*		
	50	*Water @ 25°C*	*60*	
	50	*Water @ 25°C*	*60*	
		Leave overnight		*Static*
Wash	*200*	*Water @ 30°C*	*30*	
Drain				
Wash	*200*	*Water @ 30°C*	*15*	
Drain				
Deliming	*200*	*Water @ 35°C*		
	2	*Ammonium sulfate*		
	0.5	*Sodium metabisulfate*	*45-60*	*pH=8.3*
Bating	*1*	*Pancreol PBW1*	*45*	*Bating Enzyme*
Drain				*pH=8.5*
Wash	*300*	*Water @ 20°C*	*15*	
Drain				
Wash	*300*	*Water @ 20°C*	*15*	
Drain				
Pickle	*80*	*Water @ 20°C*		
	8	*Sodium chloride*	*10*	*(B_e should be > 5) B_e=6.8*
	0.8	*Sulfuric acid 1:5 water*		
	0.4	*Formic acid 1:5 water*	*120*	
		Leave overnight		*pH=2, B_e=5.7,*
Chrome Tannage	*10*	*Chrome Powder 33% Basic*		
	0.4	*Tanbase (magnesium oxide)*	*60*	
Basifying		*Raise temperature to 40°C*	*90*	
	1.5	*Ammonium Bicarbonate*		
	0.4	*Sodium formate*		*pH=4.0*
Neutralisation	*200*	*Water @ 35°C*		
	1.0	*Ammonium bicarbonate*		
	0.4	*Sodium formate*	*45*	*pH=5,*

* Measurement of density

Procedure for vegetable tanning

Process	Offer (%)	Product	Running Time (min)	Remarks
Dirt soak	400	Water @ 20°C	60	pH=6.85, *B_e=4.2, T=15°C
Drain				
Main Soak	400	Water @ 20°C		
	1	Remcoil KTU		Non-ionic wetting agent
	1	Ecopel PDL		Anti-wrinkling agent
	1	Sodium carbonate		
	1	Soaking enzyme		
	0.1	Tolcide C30)	240	Bactericide
		Leave overnight		pH=9.3, B_e=3.8,T=22°C
Drain				
Unhairing	80	Water @ 25°C		
	1	Sodium sulfide	60	
	1	Sodium sulfide		
	1	Ecopel PDL (DMA)	60	
Swelling	50	Water @ 25°C		
	0.5	Sodium sulfide	60	
	2	Lime		
	50	Water @ 25°C	60	
	50	Water @ 25°C	60	
		Leave overnight		Static
Wash	200	Water @ 30°C	30	
Drain				
Wash	200	Water @ 30°C	15	
Drain				
Deliming	200	Water @ 35°C		
	2	Ammonium sulfate		
	0.5	Sodium metabisulfate	45-60	pH=8.3
Bating	1	Pancreol PBW1	45	Bating enzyme
Drain				
Wash	300	Water @ 20°C	15	
Drain				
Wash	300	Water @ 20°C	15	
Drain				
Pickle	80	Water @ 20°C		
	8	Sodium chloride	10	(B_e should be > 5)
	0.8	Sulfuric acid 1:5 water		
	0.4	Formic acid 1:5 water	120	pH=2, B_e=5.7,
		Drain		
Tannage	25	Water @ 25°C		
	x	Sodium chloride	10	
	x	Sodium bicarbonate	30-60	
	5	Tara	60	pH = 4 to 4.5
	5	Tara	60	
	10	Tara	480	
	100	Water @ 25°C	5	
		Drain and horse up		

* Measurement of density

APPENDIX 7

Saturated salt solution to obtain constant humidity of approximately 80% RH

Substance	Relative humidity (%)	Temperature (°C)
KBr	81	20
NH_4Cl	79	30
$(NH_4)_2SO_4$	84	40
*KCl	80	50
*KCl	80	60
K_2SO_4	80	70
KNO_3	85	80

* Saturated solution of KCl gives 80% RH at temperatures between 50 to 75°C

APPENDIX 8:

DMTA drying traces of partially processed wet blue at various temperatures, showing inflection points at 60 and 30% moisture contents.

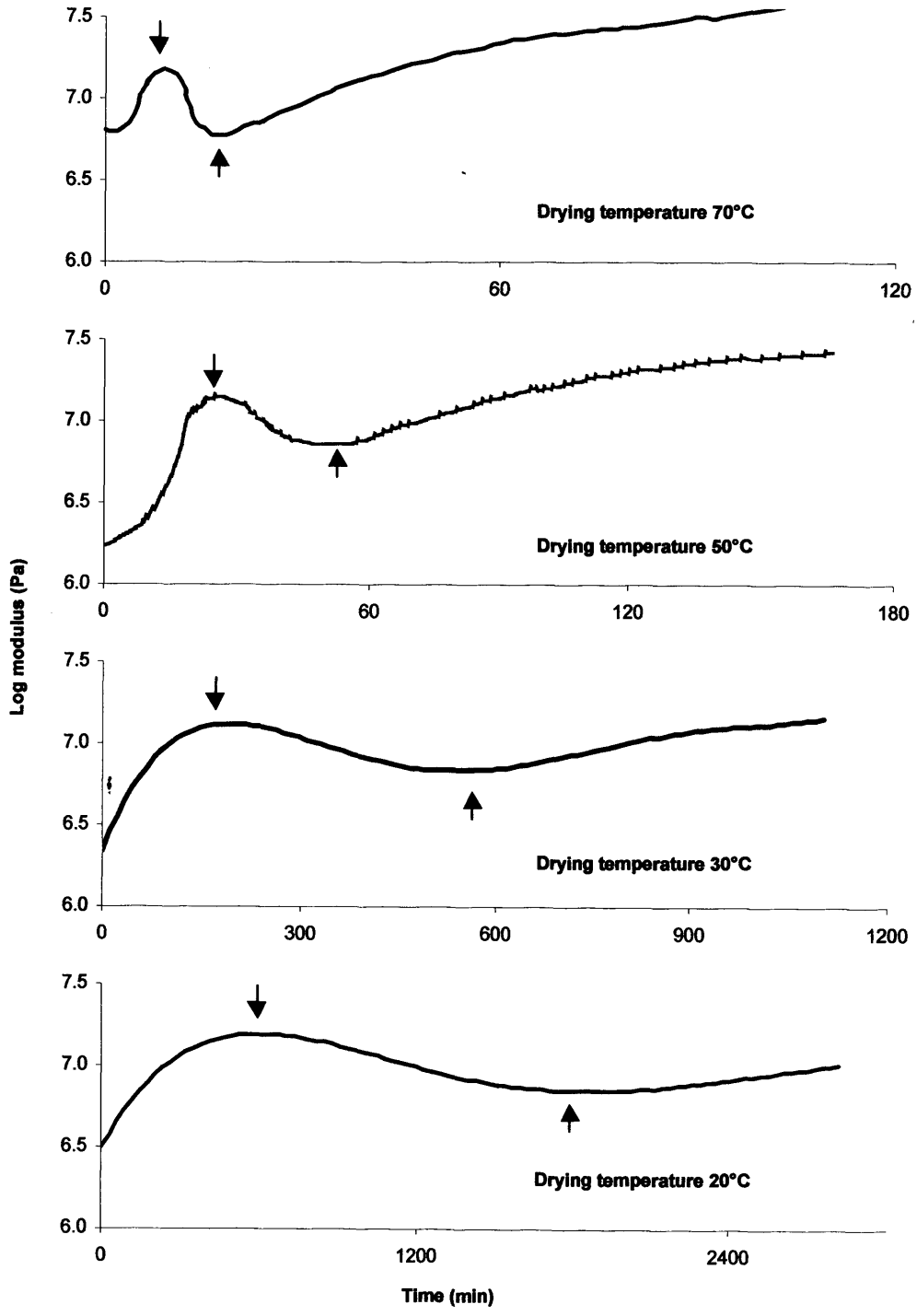

DMTA drying traces of partially processed vegetable tanned leather at various temperatures, showing inflection points at 60 and 30% moisture contents.

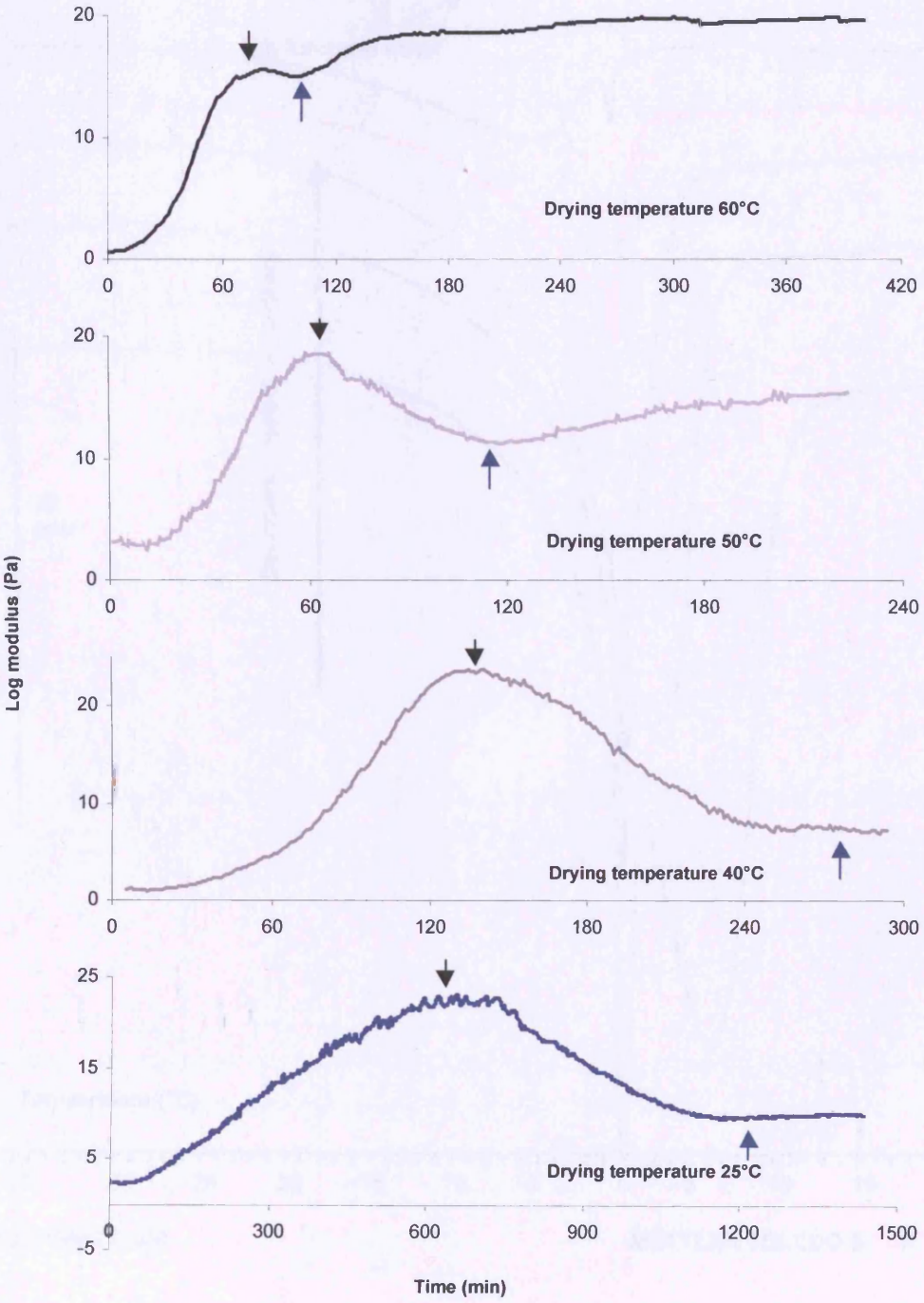

APPENDIX 9:

DSC thermograms showing endothermic ice melting peaks

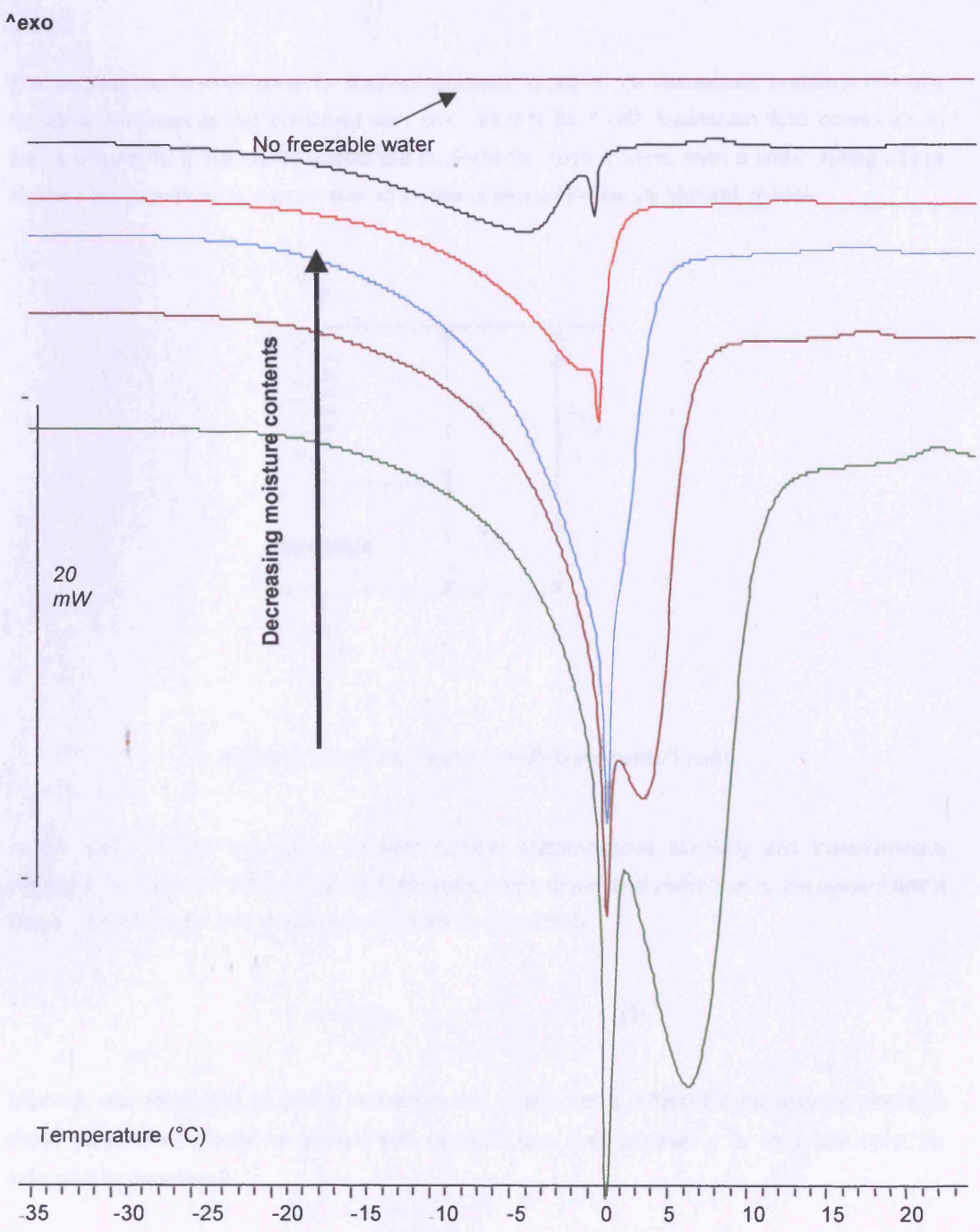

BSLT: METTLER

METTLER TOLEDO S TAR[e] System

APPENDIX 10:

Viscoelastic modelling: Area under the relaxation modulus vs. time curve

Theory

The simplest mechanical model for a stress relaxation process in a viscoelastic system is one of a massless Hookean spring combined with one dashpot filled with Newtonian fluid connected in series (Figure 4). If the inertia effects are neglected in such models, then a linear spring obeys Hooke's law (equation 1). As we have seen, this is termed the single Maxwell model.

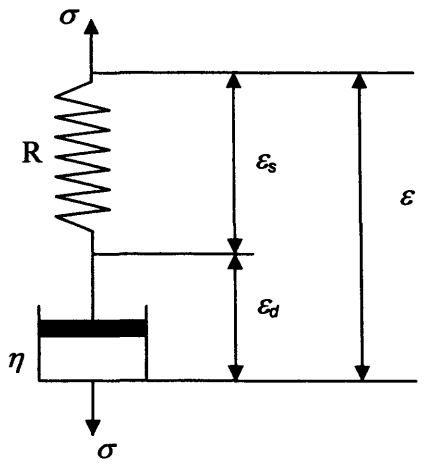

Figure 4: Single Maxwell model (two elements/1 unit).

In the above model, the spring element exhibits instantaneous elasticity and instantaneous recovery, whereas the viscous dashpot introduces time dependent behaviour to the system and it obeys Newton's law. This relationship is given by equation 8.

$$\sigma = \eta \frac{d\varepsilon_d}{dt} \qquad (8)$$

Maxwell was interested in stress relaxation and developed a differential equation to describe these properties. Initially he started with Hooke's law, then allowed σ to vary with time, as indicated by equation 9.

$$\frac{d\sigma}{dt} = R \frac{d\varepsilon}{dt} \qquad (9)$$

Assuming that the rate of strain is simply a sum of these two contributions for viscoelastic materials, then equation 10 can be obtained.

$$\frac{d\varepsilon}{dt} = \frac{\sigma}{\eta} + \frac{1}{R}\frac{d\sigma}{dt} \qquad (10)$$

In the case of stress relaxation, $d\varepsilon/dt = 0$; therefore equation 10 can be written as follows,

$$d\sigma/dt = -(R/\eta)\,\sigma \qquad (11)$$

This can be readily integrated: at t=0, then $\sigma = \sigma_0$, leading to equation 12.

$$\sigma(t)/\varepsilon_0 = E(t) = R \exp(-tR/\eta) \qquad (12)$$

where E(t) is the time dependent relaxation modulus. Further integration of both sides of equation 12 with respect to time will give equation 13. The left hand side of this equation can be calculated from the area under the relaxation modulus time curve.

$$\int_{t=0}^{t=\infty} E(t)\,dt = -\eta \exp(-tR/\eta) \qquad (13)$$

Equation 13 defines the relationship between the area under a relaxation modulus-time curve and the internal viscosity. It can be deduced from this equation that the area under the stress relaxation curve is in principle directly proportional to the internal viscosity of the system. Strictly speaking, viscosity is not a term that can be applicable to solid materials (such as leather), so it is assumed that the area under the curve is related to the material's tendency to flow rather than its viscosity.